Synthetic lethality of TNK2 inhibition in PTPN11-mutant leukemia

By

Chelsea Jenkins

A DISSERTATION

Presented to the Cancer Biology graduate program
and the Oregon Health & Science University
School of Medicine

in partial fulfillment of
the requirements for the degree of

Doctor of Philosophy

October 2017

School of Medicine

Oregon Health & Science University

CERTIFICATE OF APPROVAL

This is to certify that the PhD dissertation of

Chelsea Jenkins

has been approved

_____
Jeffrey Tyner (Mentor)

_____
Philip Stork (Committee Chair)

_____
Maureen Hoatlin (Committee Member)

_____
R. Stephen Lloyd (Committee Member)

_____
Xiaolin Nan (Committee Member)

_____
(Examination Member)

Contents

Figures and Tables

Abbreviations

ABL1	Abelson kinase 1
ACK1	Activated CDC-42 kinase 1, TNK2
ACK2	Activated CDC-42 kinase 2
AML	Acute Myelogenous Leukemia
ANOVA	Analysis of Variance statistical test
ARK-1	ACK-related tyrosine kinase 1
ATP	Adenosine triphosphate
BCR	Breakpoint cluster region
BRF	RNA polymerase III transcription factor initiation factor subunit
c-FOS	Finkel–Biskis–Jinkins murine osteogenic sarcoma oncogene
c-Myc	Myelocytomatosis oncogene
c-PLA2	Phospholipase A2
C-SH2	SH2 domain closer to the C-terminus of PTPN11
CBL	*Cbl* (named after Casitas B-lineage Lymphoma), an Ubiquitin E3 ligase
CCL3	Chemokine (C-C motif) ligand 3 (CCL3) also known as macrophage inflammatory protein 1-alpha (MIP-1-alpha)
CDC42	Cell division control protein 42 homolog
CL	Clathrin binding domain of TNK2
CML	Chronic Myelogenous Leukemia
Co-IP	Co-Immunoprecipitation
CRIB	CDC-42/RAC-interactive domain of TNK2
CSF3R	granulocyte colony-stimulating factor receptor (G-CSF-R) also known as CD114 (Cluster of Differentiation 114)
DACK	Drosophila ACK

DMSO	Dimethyl sulfoxide
DPR2	DACT2, Dishevelled Binding Antagonist Of Beta Catenin 2
EBD	EGFR-binding domain of TNK2
EGF/EGFR	Epidermal growth factor ligand/receptor
EIF4E	Eukaryotic translation initiation factor 4E
ELK1	ETS transcription factor
ERK	Extracellular signal-related kinase
FACS	Fluorescence-activated cell sorting
FBS	Fetal Bovine Serum
FGFR	Fibroblast growth factor receptor
FLAG	FLAG-tag, or FLAG octapeptide, or FLAG epitope, is a polypeptide protein tag that can be added to a protein using recombinant DNA technology, having the sequence motif DYKDDDDK
FLT3	Cluster of differentiation antigen 135 (CD135) also known as fms like tyrosine kinase 3 (FLT-3), receptor-type tyrosine-protein kinase FLT3, or fetal liver kinase-2 (Flk2)
Gab2	GRB2-associated-binding protein 2
Gas6	Growth arrest 6, ligand for MERTK
GDP	Guanosine diphosphate
GM-CSF	Granulocyte-macrophage colony stimulating factor
Grb2	Growth factor receptor-bound protein 2
GTP	Guanosine triphosphate
HEK293/293T17	Human endothelial kidney cell line 293 T17
HEPES	4-(2-hydroxyethyl)-1-piperazineethanesulfonic acid
HER2	Receptor tyrosine-protein kinase erbB-2, also known as CD340 (cluster of differentiation 340), proto-oncogene Neu, Erbb2 (rodent), or ERBB2 (human)
IC_{50}	half maximal inhibitory concentration

IL-3	Interleukin 3, a cytokine
IL-6	Interleukin 6, a cytokine
IP	Immunoprecipitation
JAK/Stat	The JAK-STAT signalling cascade consists of three main components: a cell surface receptor, a Janus kinase (JAK) and two Signal Transducer and Activator of Transcription (STAT) proteins.
JMML	Juvenile Myelomonocytic Leukemia
Kos-1	Kinase of embryonic stem cells
LEOPARD	Lentigenes, electrocardiograph conduction defects, ocular hypotelorism, pulmonary stenosis, abnormalities of genitals, retarded growth, and deafness. A germline Rasopathy.
m-SCF	Mouse stem cell factor
MAPK	Mitogen activated protein kinase
MCF-10a	Non-tumorigenic human epithelial breast cell line
MERTK	Proto-oncogene tyrosine-protein kinase MER
MH/MHR	Mig-6 homology region of TNK2
mRNA	messenger RNA
Nedd4-2	Neural precursor cell expressed and developmentally down-regulated, an E3-Ubiquitin ligase
N-SH2	SH2 domain closer to the N-terminus of PTPN11
NF1	Neurofibromin 1, a Ras-GAP
NS	Noonan syndrome, a germline Rasopathy
PAK	p21-activated kinase
PDGFR	Platelet-derived growth factor receptor
PDGFRB	Platelet-derived growth factor receptor B
PI3K/Akt	PI3K/AKT/mTOR pathway is an intracellular signaling pathway important in regulating the cell cycle

PTP	Protein tyrosine phosphatase
PTPN11	SRC homology 2 domain-containing phosphatase 2
PZR	Protein zero-related
RSK	Ribosomal S6 Kinase
RTK	Receptor tyrosine kinase
SAM	Sterile alpha motif domain
SEM	Standard error of the mean
SIAH	Seven in absentia homolog: an E3 Ubiquitin Ligase
SFK	Src-family kinase
SH2	Src homology 2 domain: binds phospho-tyrosines
SH3	Src-homology domain 3
SHP2	SRC homology 2 domain-containing phosphatase 2, PTPN11
siRNA/RNA1	Small interfering RNA
SOS1	Son of Sevenless 1, a Ras GNEF
SRC	Proto-oncogene tyrosine-protein kinase Src
TNK1	Tyrosine kinase non-receptor 1
TNK2	Tyrosine kinase non-receptor 2
Tyr	Tyrosine
UBA	Ubiquitin associated domain of TNK2
UBF	Nuclear transcription factor 1 encoding gene
WBC	White blood cell count
WT	Wild-type
WWOX	WW domain-containing oxidoreductase, a tumor-suppressor

Acknowledgements

I feel that I am fortunate to finish this journey with my love for science intact. That would not be true without the support of a whole community of people. I would like to thank my family for their love and support. Thanks to my husband Paul, for being a wonderful partner and father. I'm not sure you suffered on all those trips to the park while I wrote this dissertation, but I am forever grateful.

I am grateful to the mentors that provided experience and guidance for me to join the program and especially through the first year: Maureen Hoatlin, Matt Thayer, Leslie Smith, and Stephen Lloyd.

I would like to thank the members of the Druker lab for providing a productive and supportive home for me for the last five years. Thanks to Sarah Bowden Zoe Schmidt, Kara Johnson, Christina Tognon, Olga Ryabinina and Rebecca Smith for making the lab run smoothly. I am grateful for having received so much practical and scientific advice from everyone, especially Anupriya Agarwal, Jamie Keck, Monika Davare, Kara Johnson, Christina Tognon, Rebecca Smith, Steve Kurtz, Kim-Hien Dao, Michael Garbati, Jessica Leonard, Tamilla Nechiporuk, Elie Traer, Michie Degnin, Jakki Martinez, Aashis Thapa, and Christopher Eide. Lastly I would like to thank the members of the lab for their incredible outpouring of support in my times of celebration and times of grief.

My sincere thanks my fellow PMCB students, from whom I learned how to be a successful graduate student. The Druker and Tyner labs have been especially wonderful because I have been befriended and assisted by Kevin Watanabe-Smith, Marilynn Chow, Nathalie Javidi-Sharifi, and David K. Edwards. I would also like to thank Lilly Klug, Eleanora Juarez, Sarah Wicher, Shannon Liudahl, Lizzy Sunderhaus, and Spencer Watson for their advice and collaboration.

The work in this dissertation would not exist if I did not have the assistance of others to do the work itself. I would like to thank Julia Maxson for close supervision during my rotation through the lab and in my early days as a lab member. I would like to thank Samuel Luty for the enormous amount of work he put into assisting me with my research, especially with mouse bone marrow colony formation assays. My sincere thanks to Joelle Rowley for her efforts to establish xenograft models for this project. She put in an

enormous(e) amount of time and it is greatly appreciated. I would like to thank technicians of the Flow Core: Pamela Canaday, Dorian LaTocha, and Brianna Garcia. They have always been more than helpful and willing to work with whatever I throw at them. I am indebted to our collaborators in the bioinformatics program: Beth Wilmot, Daniel Bottomly, and Shannon McWeeney. Thanks to Eneida Nemecek and Bill Chang, who treated the patient from whom this entire project arose.

Thanks to the members of my Dissertation Advisory Committee for providing encouragement, critical thinking, and focus for my research: Philip Stork, Stephen Lloyd, Maureen Hoatlin, Xiaolin Nan, and Evan Lind.

I am grateful for the external funding sources during my time here, especially: the PMCB T32 training grant program led by Cheryl Maslen, the OCTRI OSLER TL1 training grant, and the Friends of Doernbecher grant.

And another thing…I would like to thank Bill Chang for allowing me to adopt him as a collaborator and additional mentor. His expertise and sense of humor have helped immensely with my research.

Finally, I would like to give a special thanks to Jeffrey Tyner for taking on two students in one year. I did not enter the program with the intention to study cancer cell signaling, but I am truly grateful that I ended up in the Tyner Lab. Jeff has given me the time and room to grow into this profession, while providing steady support whenever I needed it. Thank you.

Academic Curriculum Vitae

Chelsea Jenkins
jenkins@ohsu.edu
cjenkinsphd@gmail.com

EDUCATION

Oregon Health & Science University
Molecular and Cellular Biosciences
Ph.D. Cancer Biology expected 2017
Advisor: Jeffrey Tyner
Dissertation: Synthetic lethality of TNK2 in PTPN11-mutant leukemia

Portland State University
Post-Baccalaureate Studies 2009

University of Oregon
B.S. Biology, 2006

RESEARCH EXPERIENCE

Oregon Health and Science University 2012-2017
Graduate Researcher
Tyner Lab
My work in the Tyner lab has centered on developing new cancer therapies based on identifying drug sensitivities in primary patient cells. These sensitivities arise from weak links in molecular signaling pathways that can be targeted by enzyme-specific inhibitors. My research has determined the mechanism whereby leukemia cells with activating mutations in the phosphatase PTPN11 are sensitive to inhibition of an upstream kinase, TNK2. This work has enabled me to hone my molecular biology skillset including sequencing, PCR, cell culture, Western blots, and cloning as well as the use of a mouse model of leukemia. As an independent researcher I have gained the ability to research and formulate hypotheses, communicate my research through oral presentations and written manuscripts, and to prioritize multiple tasks at one time.

Hoatlin Lab 2010-2012
Research Assistant
Identified small molecule inhibitors of the Fanconi Anemia pathway for potential synthetic lethal cancer therapeutics. Contributed to an effort started by a former lab member to develop a high-throughput BRET assay.

Sol-gel Solutions, Gainesville, FL, 2009-2010
Lab Technician
Performed experiments associated with the development of new technology for removal of mercury from water and air.

Oregon Health & Science University, 2009
Thayer Lab
Lab Aide
Cleaned and sterilized glassware, prepared lab stock solutions and tissue culture media, plasmid and BAC preps.
Kabat Lab 2009
Lab Aide
Cleaned and sterilized glassware, prepared lab stock solutions and tissue culture media.

Wood Kote Products, Inc. Portland, Oregon 2007-2008
Laboratory Assistant, MSDS Manager, Office Manager
Responsible for quality control and new product formulation in the chemical laboratory. Author and maintaining MSDS materials for manufactured products and the workplace. Clerical tasks such as answering the phone, order processing, data entry, and office tasks. Also served as Safety Committee Secretary, writing and maintaining company's Safety Plan.

University of Oregon Chemistry Department Eugene, Oregon 2003-2006
Laboratory Assistant
Prepared and performed chemistry demos for courses in Chemistry and University outreach programs. General laboratory cleanup and organization.

PUBLICATIONS

Jenkins, C, Samuel Luty, Julia Maxson , Christopher Eide, Melissa Abel, Corinne Togiai, Eneida Nemecek, Daniel Bottomly, Shannon McWeeney , Beth Wilmot, Marc Loriaux, Bill Chang & Jeffrey Tyner. Synthetic lethality of TNK2 in PTPN11-mutant leukemia. 2017. In review.

Uchida, Kimberly A, Christopher A. Eide, Samantha L. Savage, Beth Wilmot, Daniel Bottomly, Shannon K. McWeeney, Anupriya Agarwal **Chelsea Jenkins**, Jeffrey W. Tyner, Cristina E. Tognon, Brian J. Druker. Mutational activation of the MEK/ERK signaling pathway in BCR-ABL kinase-independent tyrosine kinase inhibitor-refractory chronic myeloid leukemia. 2017. In preparation.

Jenkins C, Kan J, Hoatlin ME. Targeting the Fanconi Anemia pathway to identify tailored anticancer therapeutics. Anemia. 012;2012:481583. Epub 2012 May 24.

POSTERS AND ABSTRACTS

Savage, Samantha L., Julia E. Maxson, Christopher A. Eide, **Chelsea Jenkins**, Melissa L. Abel, Anna M. Reister Schultz, Daniel Bottomly, Beth Wilmot, Shannon K. McWeeney, Cristina E. Tognon, Jeffrey W. Tyner, Brian J. Druker. Therapeutically targetable activating c-ABL1 mutations in Philadelphia chromosome-negative leukemias. ASH Conference Poster Abstract. Dec. 2017.

Jenkins, Chelsea, Samuel Luty, Julia Maxson, Chris Eide, BH Chang, Jeffrey Tyner. PTPN11 mutations in JMML confer dasatinib sensitivity in a TNK2-dependent manner. ASH Conference Poster Abstract Dec. 2016

Highlighted in an ASH Educational Presentation

Jenkins, Chelsea, Samuel Luty, Julia Maxson, Chris Eide, BH Chang, Jeffrey Tyner. Defining the functional role of TNK2 in PTPN11-mutant JMML. Oral Presentation, OHSU Research Week, May 2016.

Jenkins, Chelsea, Julia Maxson, Chris Eide, BH Chang, Jeffrey Tyner. PTPN11 mutations in JMML confer dasatinib sensitivity in a TNK2 dependent manner. Poster, OHSU Research Week, May 2014. Oral Presentation OHSU Research Week, May 2015.

ACADEMIC AND PROFESSIONAL HONORS

Awards:

Mentor Recognition, 2017 OHSU F.L.A.M.E. Awards
Best Student Oral Presentation Award, OHSU Research Week 2016
Best Poster, OHSU Research Week 2014
Phi Beta Kappa, University of Oregon 2007

Fellowships and Scholarships:

2016	OHSU Graduate Student Organization Travel Award
2015-2016	Friends of Doernbecher Grant Recipient
2015-2016	OCTRI OSLER TL1 Training Grant Recipient
2015-2014	Tartar Trust Fellowship Recipient
2014-15	Ruth L. Kirchstein T32 Training Grant Recipient, Program in Molecular and Cellular Biosciences
2013	OHSU Cancer Program Travel Award
2002-2006	Dan Konnie Memorial Scholarship
2002-2006	University of Oregon Presidential Scholarship

SKILLS:

Cloning, PCR, and mutagenesis. Tissue culture and cell line viral transduction. Western blot and CoIP protein analysis. Primary mouse bone marrow harvest, transduction, and transformation assay setup. Mouse xenograft and syngeneic transplant model design, maintenance, and analysis.

REFERENCES:

Jeffrey Tyner Ph.D.
Associate Professor of Medicine,
School of Medicine, OHSU
3181 SW Sam Jackson Park Road
Mail Code: L592
Portland, OR 97202
tynerj@ohsu.edu

Phone: 503-494-5599

Bill Chang M.D. Ph.D.
Associate Professor of Pediatrics,
Division of Hematology and Oncology
School of Medicine, OHSU
3181 SW Sam Jackson Park Road
Mail Code: L592
Portland, OR 97202
changb@ohsu.edu

Phone: 503-494-1543

Maureen Hoatlin Ph.D.
Associate Professor of Biochemistry & Molecular Biology
and Molecular & Medical Genetics,
School of Medicine, OHSU
3181 SW Sam Jackson Park Road
Mail Code: L224
Portland, OR 97202
hoatlinm@ohsu.edu

Abstract

The development of targeted therapeutics using small-molecule inhibitors was pioneered in hematologic malignancies and has revolutionized the treatment of subsets of cancers. Further experience with these inhibitors has led to the identification of select mutations that may respond to specific inhibitors. This dissertation presents data about one of these mutant proteins, PTPN11. PTPN11 is a tyrosine phosphatase implicated in the pathogenesis of JMML, AML, and other malignancies. Activating mutations of PTPN11 are known to increase proliferative signaling and cell survival, but the signaling upstream of PTPN11 is not well understood. It is important to understand this upstream signaling, because PPTN11 is an activator of multiple downstream proliferative pathways that may compensate in response to targeted inhibitors. There is an increasing body of literature that suggests a link between the multi-kinase inhibitor dasatinib and mutated PTPN11.

Our lab has developed *ex vivo* functional assays with small-molecule kinase inhibitors and RNAi targeting to screen primary patient samples for specific pathway dependence. Using these assays, we found that mononuclear white

blood cells from a patient with recurrent PTPN11-mutant JMML were sensitive to dasatinib. The sample also showed significantly reduced viability in the presence of siRNA targeting the TNK2 gene product. However, there was no known link between PTPN11 mutations and dasatinib sensitivity or between PTPN11 and the kinase TNK2.

This dissertation presents novel evidence that PTPN11 is activated by an upstream kinase, TNK2. PTPN11-mutant JMML and AML primary patient cells have displayed significant sensitivity to TNK2 inhibition by dasatinib. My research has revealed that PTPN11 and TNK2 interact directly, allowing for TNK2-dependent phosphorylation of PTPN11. There is a subsequent PTPN11-dependent dephosphorylation of TNK2, suggesting a tightly coupled regulatory signaling loop. Consequent to increased PTPN11 phosphorylation, co-expression of TNK2 and mutant PTPN11 synergistically increases MAP kinase proliferative signaling and mouse bone marrow colony formation. These increases can be significantly blocked with chemical inhibition of TNK2. Clinically, a patient with recurrent JMML who was treated with dasatinib had a therapeutic response. Collectively, these data indicate TNK2 as a promising target for PTPN11-mutant cancers.

Chapter 1 : Background

1-1: Introduction

Leukemia cells are liquid tumors that arise in the bone marrow, where normal hematopoiesis occurs[1]. Cell intrinsic factors like mutations in proteins that control cell proliferation or cell death can drive blood cells to proliferate uncontrollably, filling up the marrow and spilling out to the rest of the body; into other hematopoietic organs like the liver and spleen[2]. Infiltration of the marrow leads to both overcrowding and microenvironmental signaling to impair normal hematopoiesis. This results in cytopenias in neutrophils, erythrocytes and platelets leading to immune dysfunctions, anemia, and bleeding. Further, other organ infiltration can lead to pain and organ failure.

Conventional therapies using cytotoxic chemotherapy have shown great benefit in the treatment and cure of many hematologic malignancies [2, 3]. In

[1] Henry William Fuller was the first to publish a case report describing the diagnosis of leukemia in a live patient in 1846, though others before him had identified and named the disease from post-mortem specimens [1]

[2] Specifically, activating mutations in proto-oncogenes transform them into oncogenes, which drive tumorigenesis. A class of proteins known to negatively regulate cell proliferation and survival called tumor suppressors can acquire loss-of-function mutations, which lead to unregulated cell proliferation and mutagenesis.

the early 2000's targeted therapies revolutionized treatment with the use of the small-molecule inhibitor imatinib, proving the efficacy of targeting specific driver mutations [4]. While conventional and targeted therapies have some success (in some cases, complete success) in curing patients, more work needs to be done to identify treatment strategies for subsets of these patients.

My work has focused on leukemia driven by mutations in PTPN11 or tyrosine-protein phosphatase non-receptor type 11, (also known as Src homology 2 domain-containing phosphatase 2, or SHP2), a tyrosine phosphatase that normally has a positive effect on cellular proliferation. Somatic monoallelic activating mutations in this gene lead to aberrant proliferative signaling in hematopoietic stem cells, resulting in leukemia [5]. Although select mutations increase inherent PTPN11 activity, its activity can be further enhanced through phosphorylation of its C-terminal tyrosine residues [6]. This dissertation describes a kinase upstream of PTPN11, TNK2, which when targeted by an inhibitory drug, imparts increased susceptibility to killing in PTPN11-mutant leukemia cells. TNK2 increases PTPN11 phosphorylation—thereby activating it—and is part of a regulation loop whereby PTPN11 activity negatively regulates TNK2.

My research began by looking at a mutant-PTPN11 driven childhood leukemia, Juvenile Myelomonocytic Leukemia (JMML), and has expanded to

include samples from patients with Acute Myeloid Leukemia (AML). JMML, like many rare diseases, provides an important model for proof-of-principal research that might then be applied to broader populations of patients with more heterogeneous disease, like AML. Because other tumor types also harbor PTPN11 mutations, it is my hope that targeting of TNK2 can be effective for the treatment of a diverse population of patients. This introduction will describe the background and rationale for targeting TNK2 in PTPN11 mutant leukemias.

1-2: Cellular signaling is critical for normal hematopoietic cells and leukemia transformation

The study of cellular signaling has led to landmark developments in targeted therapies for leukemia. Cellular signaling pathways function to transduce extracellular signals (via a receptor like a receptor tyrosine kinase) through a diverse network of intracellular pathways. These signals can induce many effects, including cellular growth, proliferation, senescence, or death [7]. Cellular signaling is dependent on post-translational protein modifications, most commonly the addition or removal of a phosphate group from target proteins [8, 9].

Phosphate addition to a Serine, Threonine, or Tyrosine residue on a target protein is catalyzed by protein kinases, which transfer a phosphate from a high energy Adenosine Triphosphate (ATP) molecule. Phosphorylation is generally an activating event, although there are exceptions [8, 9]. Enzymes called phosphatases catalyze the hydrolysis reaction removing a phosphate, which is typically an inhibitory or inactivating event [10]. This creates a finely tunable system in which regulation can occur at many levels. For example, cells can regulate the amount or rate of phosphorylation or dephosphorylation independently, allowing them to integrate multiple input systems simultaneously.

These signaling pathways are essential for cellular homeostasis, and perturbations in rates of phosphorylation or dephosphorylation can cause dramatic effects. In cancer, mutation or dysregulation of an activating member of a proliferative signaling pathway (a proto-oncogene) can be a driving event in tumorigenesis. Alternately, an inactivating mutation or silencing of a regulatory member of a proliferative pathway (a tumor suppressor or positive regulator of apoptosis) can lead to tumorigenesis as well.

Defining the mechanisms of cellular signaling in cancer is essential for determining pathways that drive cellular proliferation and survival, or

pathways that prevent programmed cell death. Once we understand how these pathways work, we can understand their dysfunctional state in cancer and develop therapies to target them.

1-3: Tyrosine kinase inhibitors in treatment of hematologic malignancies

The advent of targeted therapies came with experiments to target HER-2 transformed cells with a monoclonal antibody [11] which was developed into the drug Herceptin for breast cancer[3]. This was a pioneering discovery, because it illustrated that tumor cells could be eliminated by therapies that specifically target the molecular drivers of cancer. Prior to this development, the only available tumor therapies were cytotoxic chemotherapies and radiation, which can cause debilitating side effects [3]. While Herceptin targets a receptor on the surface of breast cancer cells, the most successful targeted therapy to date is a tyrosine kinase inhibitor, imatinib mesylate.

[3] Herceptin, also known as Trastuzimab was developed jointly by UCLA and Genentech, and began testing in clinical trials in 1992 and was approved by the FDA in 1998 [12]

The drug imatinib mesylate (Gleevec) is an inhibitor of the Abelson kinase ABL1[4]. In Chronic myelogenous leukemia (CML), ABL1 is the C-terminal portion of the fusion oncoprotein breakpoint cluster region/Abelson (BCR-ABL), which is the result of a chromosomal translocation between chromosomes 9 and 22. BCR-ABL causes increased proliferative signaling through aberrant phosphorylation of downstream signaling pathways. Inhibition of ABL1 kinase activity by imatinib successfully treats CML, and patients are able to stay in remission with a daily dose of the drug with minimal side effects [4]. Imatinib works by binding to the ATP pocket of the ABL moiety of BCR-ABL, preventing its activity [13]. It has been shown to selectively bind the inactive conformation of ABL1 kinase [13]. Drug resistance does develop in a portion of these patients, most commonly due to a "Gatekeeper" mutation that changes a key threonine residue, T315, to an isoleucine, which eliminates an important hydrogen bonding site for imatinib [14]. Dasatinib, a second generation Src-family kinase inhibitor, has a 325-fold higher affinity for the ATP-binding pocket than imatinib and can bind the active form of the kinase, but is not effective against the gatekeeper mutation [14]. The newer drug ponatinib does have the ability to bind the

[4] Imatinib mesylate or Gleevec, also known by the drug molecule name sti-571 was developed by Novartis with Dr. Brian Druker. It entered clinical trials in 1998 and was approved by the FDA for use in 2001 [4]

gatekeeper mutant, though a number of patients develop alternate methods of resistance [14].

These drugs were developed in a rational way to target proteins responsible for oncogenic transformation. It is only through understanding of oncogenic transformation that we can continue to develop new specific inhibitors. These targeted inhibitors are particularly required to treat malignancies for which conventional therapy is not successful.

1-4: The Ras/MAPK pathway

Mitogen activated protein kinases (MAPK's) are essential for cell signal transduction from cell surface receptors to the cytoplasm to effect changes in cellular signaling and transcription. MAPK proteins are necessary for the regulation of cell cycle, differentiation, growth, senescence, and apoptosis. MAPK proteins are a family of Ser/Thr kinases that are activated by serial phosphorylation events [15]. There are many proteins in the MAPK superfamily, but it is the Ras/Raf/MEK/ERK axis which is thought to control expansion, survival and differentiation in hematopoietic progenitors [15].

The Ras/MAPK pathway is initiated by activation of a membrane-associated Ras protein. Ras proteins, encoded by the genes for H-Ras, N-Ras[5] and K-Ras are small guanosine-nucleotide bound GTPases that cycle between an inactive GDP-bound state and an active GTP-bound state [17] Activating mutations in K-Ras and N-Ras are the most common forms of Ras in hematopoietic malignancies, with H-Ras almost never appearing as an oncogenic driver [18].

Activation of Ras is catalyzed by a guanosine nucleotide exchange factor (son of sevenless 1, or SOS1), which increases the exchange rate of GDP for GTP, driving the concentration of active Ras-GTP up. Active Ras recruits Raf to the cell membrane, where Raf can be activated by phosphorylation by other tyrosine kinases[6]. [20].

Activated Raf phosphorylates and activates MEK (MAPKK), which then phosphorylates MAPK p44/42 (ERK 1/2, MAPK 1/3, or extracellular signal-regulated kinase), perhaps through the formation of a Raf/MEK/ERK complex [19]. MEK1/2 also promotes expression of the anti-apoptotic protein BCL-2 [21]. MAPK p44/42 activates a large number of downstream proteins,

[5] H-Ras and K-Ras are named after rat sarcoma viruses that spawned their discovery by Scolnick et al. in 1982 [16] N-Ras was subsequently discovered and named for it prevalence in neuroblastoma cells [17]

[6] Raf can be activated by by PAK and Src Family Kinases (SFKs) at this point [19].

including transcription factors and protein kinases that exert a proliferative, pro-differentiation, and anti-apoptotic effect[7][18].

Activating mutations in the Ras/MAPK pathway are present in about 30% of all cancers [23]. Mutations in Ras proteins are driving events in many solid malignancies, most notably pancreatic, colon, melanoma, and lung tumors [24]. Mutations in Raf proteins are well known in melanoma, with targeted therapies currently in use against Raf [25]. Inactivating mutations in negative regulators of Ras signaling can also lead to proliferative disorders, especially in the case of neurofibramotosis, driven by inactivating mutations in the GAP NF1 protein [26]. While targeted therapies exist against downstream members of the pathway, Ras itself is considered to be undruggable [26].

1-5: PTPN11 in the Ras/MAPK pathway

In normal cells, Ras/MAPK signaling is dependent on PTPN11. PTPN11 is a ubiquitously expressed protein tyrosine phosphatase[8]. It resides in the

[7] Targets regulated by MAPK p44/42 include: RSK, c-Myc, EIF4E, c-PLA2, C-Fos, MNK, ELK1, BRF, and UBF [22].
[8] PTPN11, a homolog of the Corkscrew protein in *Drosophila*, was first identified by Freeman et al. in 1992 [27]. It was later shown to link PDGFR signaling to Ras/MAPK activation by Bennett *et al.* in 1994 [28].

cytoplasm where it acts downstream of receptor tyrosine kinases like FLT3, FGFR, EGFR, PDGFRA and PDGFRB [28-31]. PTPN11 dephosphorylates targets in many signaling pathways including Ras/MAPK, PI3K/Akt, focal adhesion kinase (FAK), and JAK/Stat, as further described below. Unlike many other tyrosine phosphatases, PTPN11 promotes cellular proliferation [32].

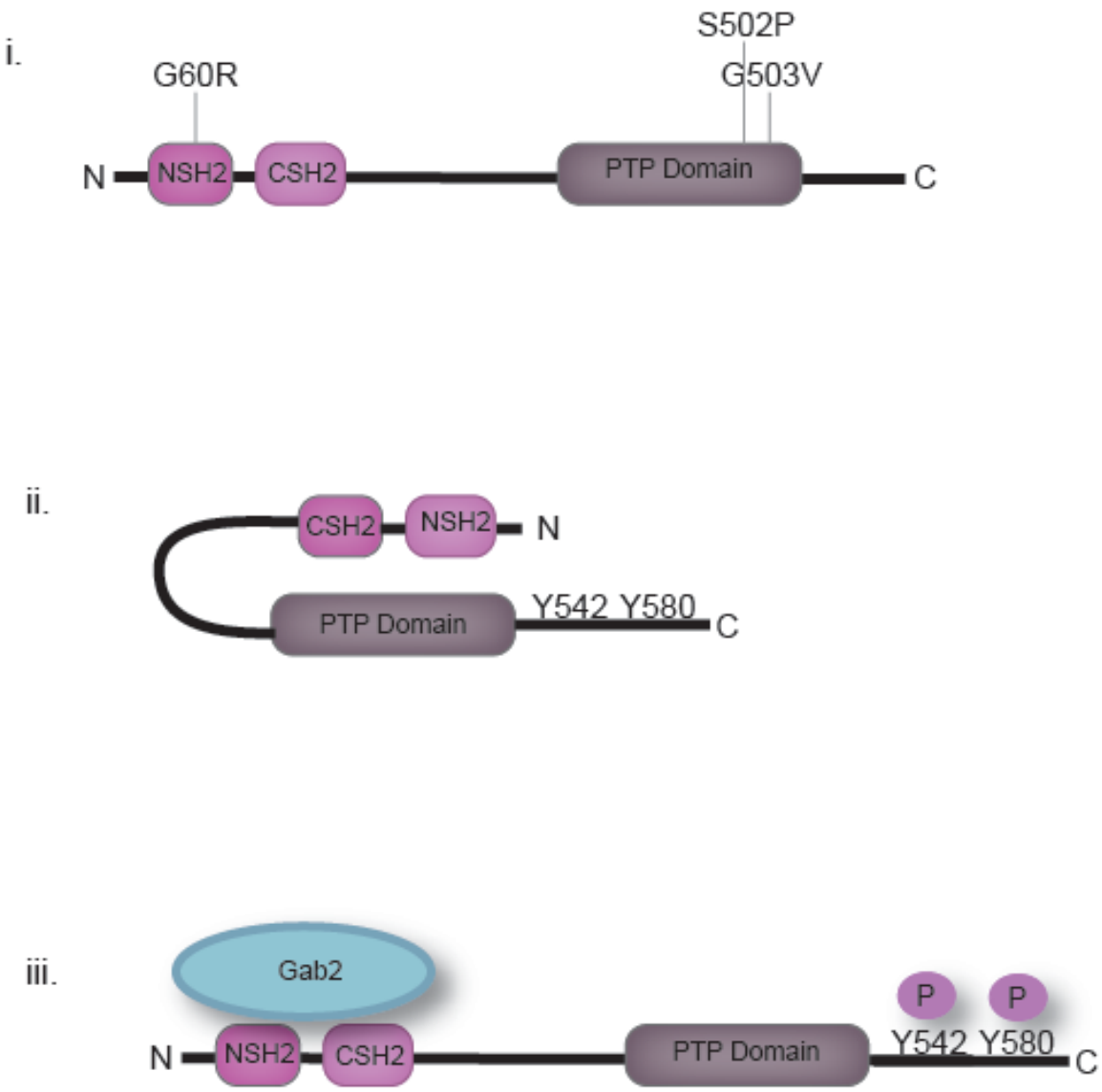

Figure 1-1: PTPN11 domains and mechanism of activation. Adapted from [6].

i. Activating mutations occur in SH2 and PTP domains. ii. PTPN11 is autoinhibited through association of SH2 and PTP domains. Activating mutations relieve this autoinhibtion. iii. Phosphorylation of C-terminal Tyrosine residues Y542 and Y580 help to relieve PTPN11's autoinhibited conformation. Binding of scaffold protein Gab2 to SH2 domains locks PTPN11 in the active position.

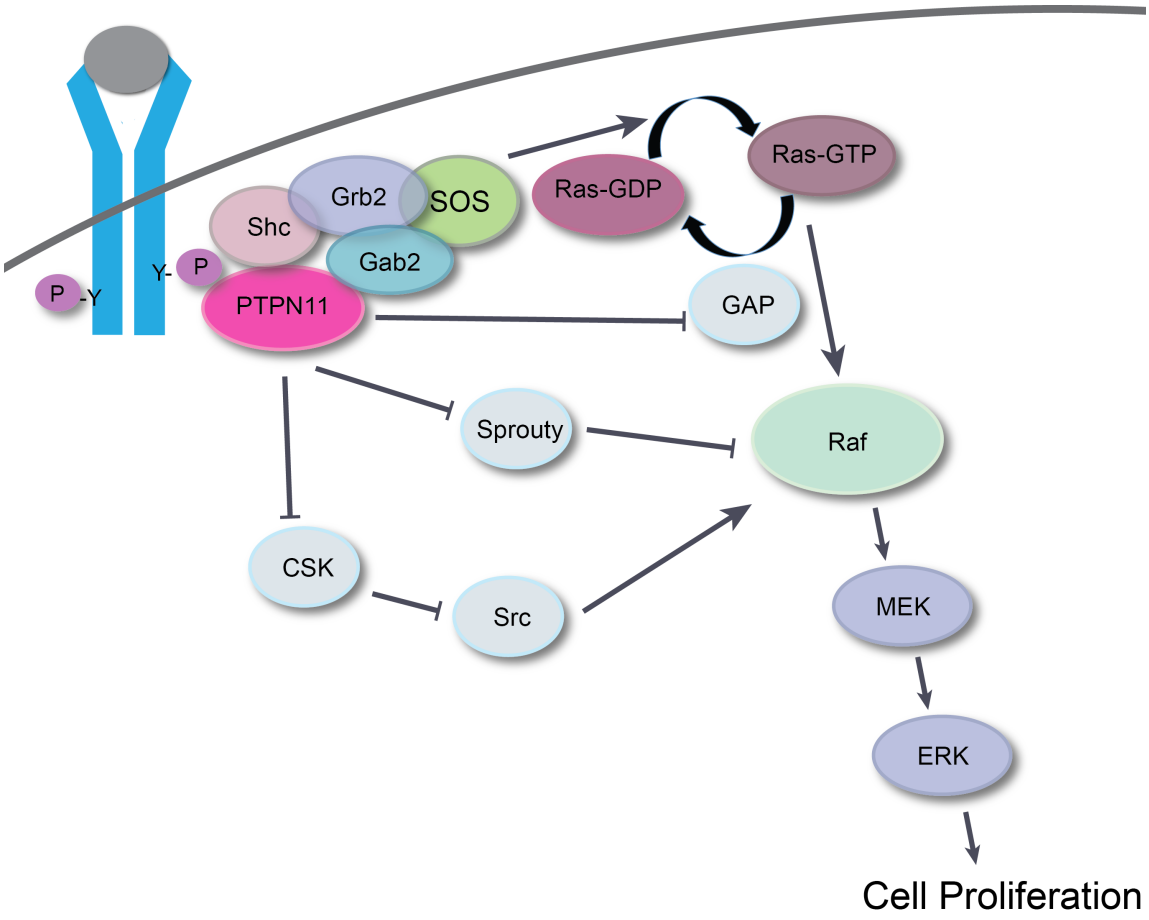

Figure 1-2: Detailed Shp2/Ras/MAPK signaling diagram. Adapted from [6].

PTPN11 removes phosphate residues from Ras-GAP, Sprouty, and CSK, which are all negative regulators of Ras signaling. PTPN11 also acts as a scaffold for proteins including SOS1, which directly activates Ras. Activated ERK (MAPK p44/42) acts as a proliferative transcription factor.

PTPN11 has three major functional domains: two N-terminal Src-homology 2 or SH2 domains that bind phosphorylated tyrosine residues on other proteins, and a central phosphatase domain (Fig1-1). PTPN11 also has a C-terminal tail with two tyrosyl phosphorylation sites and a proline-rich motif. PTPN11 is autoinhibited in its basal state, with the N-SH2 domain blocking the catalytic domain of the PTP domain, and is activated in part by phosphorylation of tyrosine residues Y542 and Y580 in its C-terminus [33]. There is some evidence that phosphorylation of the C-terminal tyrosine residues is co-regulated, with phosphorylation of Y580 depending on Y542 phosphorylation [6]. After phosphorylation of the C-terminal tyrosine residues, the N-SH2 domain of PTPN11 binds to phosphorylated tyrosyl residues of scaffold proteins such as Gab1 or Gab2 (Grb2-associated binding protein 1 or 2), relieving autoinhibition [33]. These scaffold proteins are activated by phosphorylation by adaptor molecules such as Grb2 (growth factor receptor-bound protein 2) or SHC (Src homology 2 domain-containing proteins), which directly bind phosphorylated tyrosines on the intracellular portion of receptor tyrosine kinases. Scaffold proteins associated with PTPN11 recruit and stimulate GNEF (guanosine nucleotide exchange factor) proteins such as SOS1 (son of sevenless 1) which facilitate the transformation of Ras into its GTP-bound active state [34].

Although the exact mechanism of action of PTPN11 in the Ras/MAPK pathway remains elusive, PTPN11 has been shown to contribute to cell signaling in several ways (Fig. 1-2). It has been established that PTPN11 inactivates Ras-GAP[9] and Sprouty, which are direct inhibitors of Ras signaling [10, 36]. PTPN11 also indirectly reduces phosphorylation of CSK (via Paxillin and PAG[10]), which usually adds an inhibitory phosphate to C-Src, an activator of the Ras/MAPK pathway [10, 37]. Recent research suggests that PTPN11 may also directly remove an inhibitory phosphate from a conserved tyrosine residue on Ras (Tyr 32), increasing its propensity to form Ras/Raf dimers [38].

PTPN11 has important roles in normal hematopoietic cellular signaling. Embryonic stem cells lacking PTPN11 are unable to contribute to hematopoiesis in chimeric mice, suggesting that PTPN11 is required for hematopoiesis [39]. Deletion of a floxed conditional PTPN11 allele in a hematopoietic stem cell transplant model in mice causes bone marrow aplasia, loss of hematopoietic stem cells and multi-lineage progenitors,

[9] Ras-GAP is prevented from translocation to the plasma membrane (where it is normally activated) through dephosphorylation of key residues on RTKs by PTPN11 [35].

[10] PAG is also known as: Phosphoprotein asscociated with glycosphingo-lipid-enriched membrane microdomains.

pancytopenia, and early lethality [40]. These data suggests a dependence on PTPN11 for hematopoietic stem cell pool maintenance in adults [40].

1-6: PTPN11 mutations evoke pathogenesis

Disease-associated mutations in PTPN11 perturb the equilibrium of its autoinhibition, resulting in a constitutively active protein [33]. Most of these mutations disrupt the interaction between the N-SH2 domain and the PTP catalytic domain [41].

Mutant PTPN11 has been identified as the most common driver of JMML, found in 35% of patients (Table 1-1) [42, 43]. Further, mutations in drivers of the MAPK pathway, namely *NF1*, *NRAS*, *KRAS*, *PTPN11* or *CBL* occur in 85% of patients, with poorer prognosis for patients as RAS pathway mutation number increases [43]. The most common PTPN11 mutation found in JMML, E76K, has been identified as having the highest phosphatase activity [5, 42].

Table 1-1: Frequency of JMML and Top 20 AML mutations. Adapted from [44, 45]

JMML Mutation	Frequency
PTPN11	35%
N-Ras/K-Ras	20%
NF1	15%
CBL	15%
Other	15%

AML Mutation	Frequency
FLT3	33.8%
NPM1	28.3%
DNMT3A	23.1%
N-Ras	16.2%
complex	10.5%
TET2	9.9%
minus7/7q	9.5%
plus8/8q	9.3%
IDH2	9.2%
RUNX1	8.8%
CEBPA	8.2%
PTPN11	7.7%
IDH1	6.8%
TP53	6.4%
SRSF2	5.8%
MLL	5.6%
inv(16)	5.3%
WT1	4.7%
K-Ras	4.0%

i. Normal Hematopoiesis

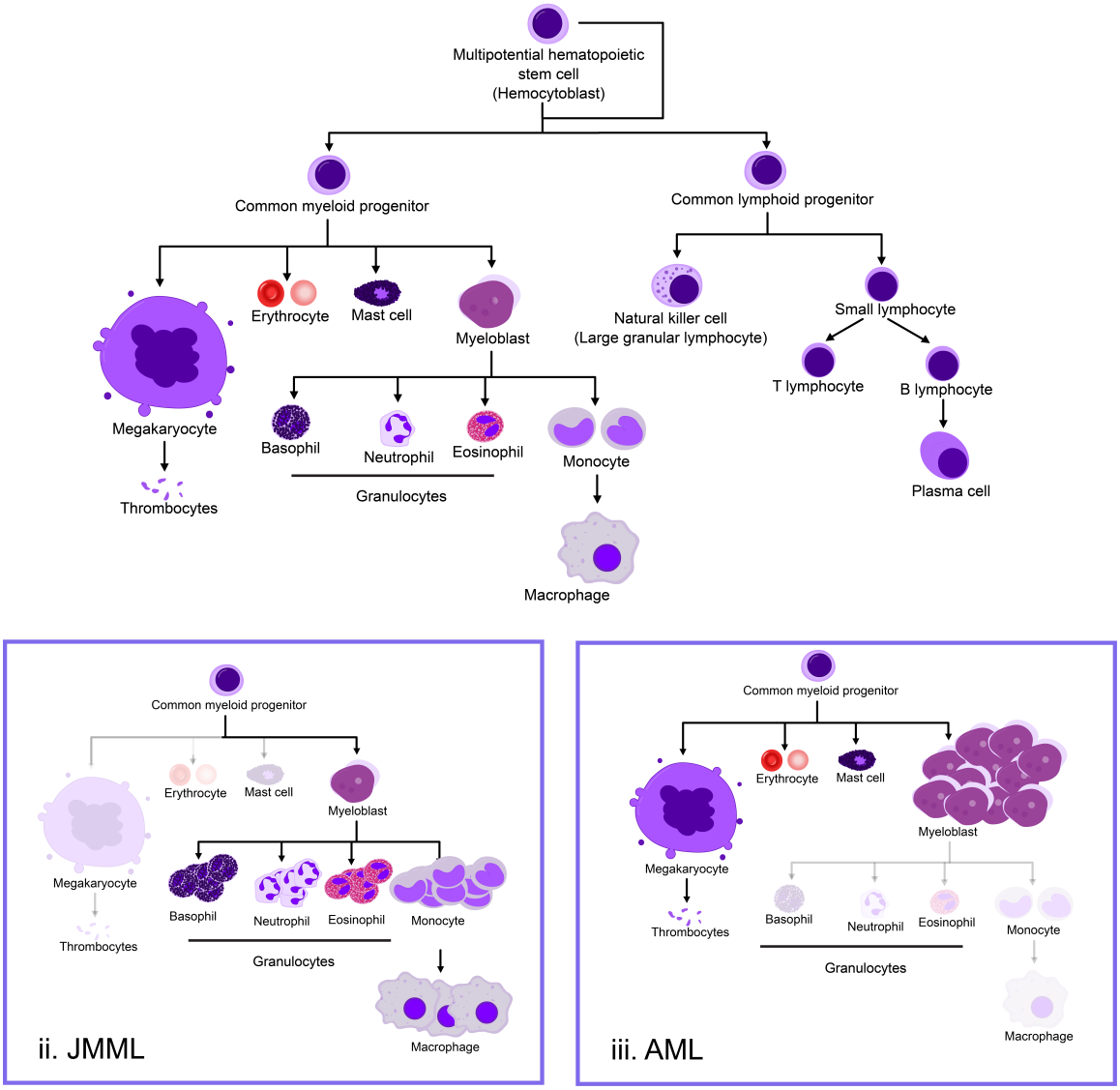

Figure 1-3: Normal hematopoiesis vs. JMML and AML adapted from [46].

i. Normal hematopoiesis. ii. JMML causes increases in monocyte and granulocytes, with concurrent anemia and thrombocytopenia. iii. AML cells proliferate at the immature blast phase preventing differentiation to monocytes or granulocytes.

JMML is a rare clonal myeloproliferative disorder characterized by overproduction of the myeloid lineage monocytes and granulocytes[11] (Fig. 1-3) without differentiation arrest with infiltration of the spleen, lung and intestines [48, 49]. Patients present at a median age of 2 years with fever, thrombocytopenia, failure to thrive, splenomegaly, and hepatomegaly [49-51]. JMML has poor response to chemotherapy, and the only current curative treatment for JMML is allogeneic hematopoietic stem cell transplant, which fails in 50% of patients by 5 years [52].

Gain-of-function, germline PTPN11 mutations, often slightly different than those that cause JMML, occur in 50% of cases with Noonan Syndrome (NS) which imparts a susceptibility to JMML [33]. In addition to increased leukemic potential, patients with NS also present with short stature, skeletal abnormalities, learning disabilities and cardiac defects [53]. Germline mutations in PTPN11 are also present in a related LEOPARD syndrome[12]. Many, but not all of the same codons affected in JMML are affected in NS, but the codon substitutions are generally different [42]. These different codon

[11] In normal myeloid hematopoiesis, common myeloid progenitor cells give rise to megakaryocytes, erythrocytes, mast cells, and myeloblasts (Fig 1-3). Myeloblasts give rise to granulocytes (basophils, neutrophils, and eosinophils), and monocytes. Monocytes can give rise to macrophages [47].

[12] LEOPARD Syndrome patients present with: Lentigenes, electrocardiograph conduction defects, ocular hypotelorism, pulmonary stenosis, abnormalities of genitals, retarded growth, and deafness.

substitutions impart a "weaker" mutational phenotype that may explain why many infants with NS have transient myeloproliferative disorders that resolve with time. Interestingly, mutant-PTPN11 driven NS is more likely to be familial than NS caused by other mutations in the Ras/MAPK pathway [53].

Similar mutations in PTPN11 are also present in ~5-10% of cases with AML, and have been associated with B-cell acute lymphoblastic leukemia, breast and lung tumors (Table 1-1) [42, 43, 45, 54-57]. AML differs from JMML in its heterogeneity of driver mutations. AML can be driven by aberrant signaling through multiple proliferative pathways (notably including Ras/MAPK), and, partially due to later onset of disease, patients are more likely to have multiple genetic lesions.[13]

Clinically, AML patients present with increased myeloblast (or blast) count with concurrent cytopenias in the granulocyte and monocyte compartments (Fig 1-3). Current standard-of-care treatment for AML includes an initial intensive remission induction phase (often just called induction) where

[13] A "two-hit" requirement theory has been proposed, whereby AML occurs as a result of two genetic aberrations: one to increase proliferative advantage, and one to arrest differentiation or prevent apoptosis [58]. These are termed "Class I and Class II" mutations, with PTPN11 and other Ras pathway mutations falling into the proliferative Class I subgroup.

patients are typically given a combination of the chemotherapeutic drugs cytarabine and daunorubicin[14]. Following induction, patients undergo a consolidation phase of treatment where they may receive additional high dose cytarabine treatment or allogeneic stem cell transplant with the goal of completely eliminating the disease. PTPN11 mutations in AML or JMML are not an indicator of prognosis, but some differential effects are seen depending on the patient's co-occurring mutations [45, 61].

1-7: TNK2 in cellular signaling

TNK2 (Tyrosine Kinase Nonreceptor 2), also known as ACK1 (Activated CDC42 Kinase 1) is a cytoplasmic kinase that can interact with activated receptor tyrosine kinases (RTKs) including EGFR, HER2, and MERTK, suggesting that TNK2 can act as a major integrator of cellular signaling[15] [63, 64]. TNK2 belongs to a family of kinases including the closely related TNK1[16] [65]. While TNK2 is ubiquitously expressed, TNK1 is only expressed in hematopoietic cells of the umbilicus [66]. TNK2 was originally identified based on its interaction with the cell migration regulator CDC42, whereby

[14] Cytarabine and daunorubicin both interrupt DNA replication: Cytarabine acts as a cytosine analog, and daunorubicin acts as a DNA intercalator. This is thought to be especially toxic in replicating cells [59, 60].
[15] TNK2 was identified as an inhibitor of CDC42 GTPase activity in 1993 [62].
[16] ACK family members include TNK2/ACK1, ACK2, DACK, TNK1, ARK-1, DPR2, and Kos1.

TNK2 and CDC42 work together to regulate cellular attachment and migration [62, 67].

It has been suggested that TNK2's multiple domains may be the source of its ability to function in different cellular compartments and with a variety of targets [68]. Among the functional domains of TNK2 are a sterile alpha motif (SAM) domain, a tyrosine kinase domain, a Src Homology domain 3 (SH3), a CDC42/RAC-interactive (CRIB) domain, a putative EGFR-Binding (EBD) domain (known as the Mig6-homology region or MHR), and a ubiquitin-association domain (Fig. 1-4) [69]. Phosphorylation of a key tyrosine residue (Tyr 284) of the activation loop of the kinase domain of TNK2 is activating, and *in vitro* studies suggest that this can be mediated by SRC kinase (FIG. 1-4) [70]. TNK2 activation occurs when activated RTKs interact with the MHR domain, which is thought to abrogate an autoinhibited conformation of the MHR with the TNK2 kinase domain [71]. Recent work also suggests that an additional (or alternate) step in TNK2 activation involves symmetric dimerization (via the SAM motif) leading to transphosphorylation [65]. Multiple modes of activation may allow TNK2 to switch between them in different cellular contexts [68].

Figure 1-4: TNK2 Domains. Adapted from [68].

SAM: Sterile Alpha Motif, Kinase Domain, SH3: Src homology 3, C: CRIB domain, CL: Clathrin binding domain, P: PPXY motif or WW domain-interacting region. MHR: Mig6 homology region or EGFR binding domain, UBA: Ubiquitin binding domain.

In addition to interacting with CDC42, activated TNK2 has been shown to activate pro-tumorigenic and pro-survival pathways in the cell. TNK2 activates Akt through phosphorylation of a novel tyrosine residue, downregulates the tumor-suppressor WWOX in hepatocellular carcinoma, and promotes androgen-independent prostate cancer growth through phosphorylation of the androgen receptor (Fig. 1-5) [72, 73]. Interestingly, the specificity and kinetics of TNK2 activation are cell-type dependent, making TNK2 function very dynamic [68].

TNK2 downregulation is moderated by polyubiquitylation and degradation in a context-dependent manner. Two types of ubiquitin E3 ligases have been implicated in this process: Nedd4-2 and the SIAH proteins SIAH1 and SIAH2 [74, 75]. Nedd4-2 regulation is coupled with EGFR activation in a signaling-dependent degradation mechanism. TNK2 associates with EGFR and clathrin in vesicles, where it has been shown to be associated with Nedd4-2 [75]. SIAH ubiquitin ligase enzymes have been shown to bind to TNK2 at the UBA domain in a ligand-independent mechanism [74]. SIAH protein levels are negatively regulated in the presence of TNK2 [74]. Additional regulatory mechanisms have likely not been discovered, especially given the cell-context specific activity of TNK2 [68].

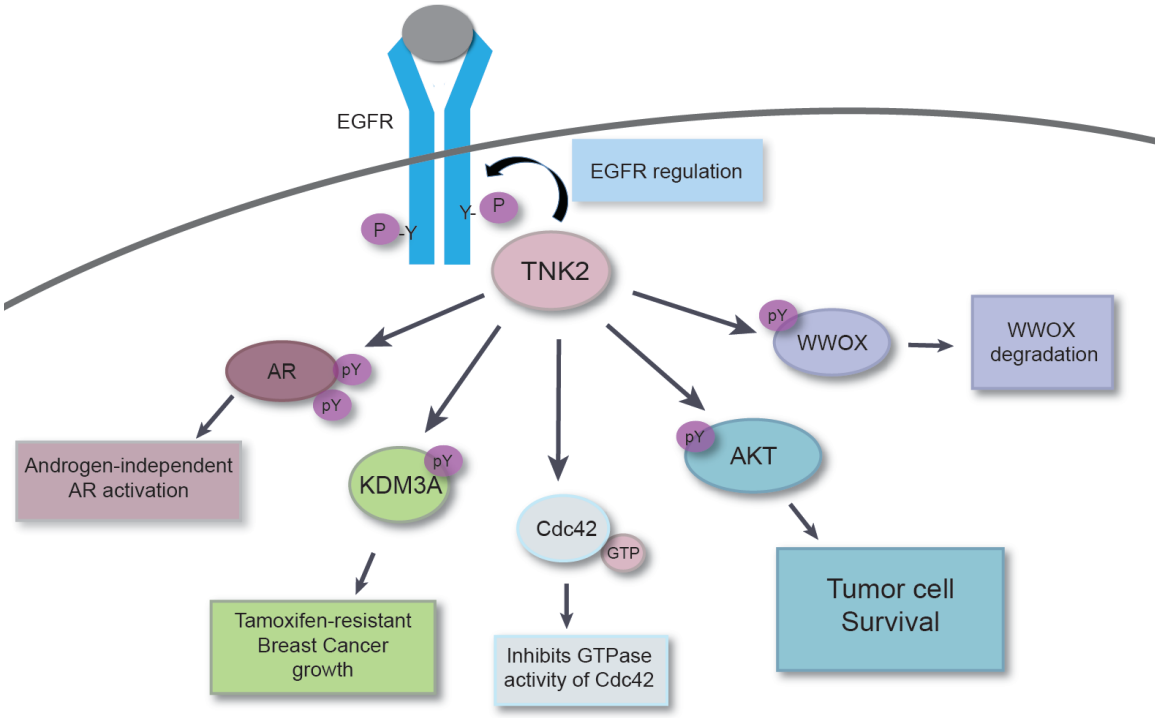

Figure 1-5: TNK2 positively regulates many proliferative pathways.

Clockwise: TNK2 is activated by phosphorylation downstream of RTKs including EGFR. TNK2 has a regulatory function on EGFR levels once activated. TNK2 phosphorylates WWOX at Tyr287, leading to its polyubiquitylation and degradation in hepatocellular carcinoma. TNK2 phosphorylates AKT at a novel residue Tyr176, leading to PI3K-independent activation and tumor cell survival. TNK2 inhibits the GTPase activity of Cdc42, which has positive effects on cell survival and migration. TNK2 phosphorylates KDM3A at Tyr 1114, leading to tamoxifen-resistant cell growth. TNK2 phosphorylates two residues on the Androgen Receptor, Tyr267 and Tyr363, leading to testosterone independent AR activation. Adapted from [68].

1-8: TNK2 pathogenesis

TNK2 is overexpressed in many solid tumors [68]. Select reports have identified point mutations [65, 76], gene amplifications [77], or ligand-dependent[17][73, 78] signaling roles for TNK2 in solid tumors of the prostate [73, 79-81], breast [82], gastrointestinal tract [83], kidney [76], pancreas [84], or lung [77, 78]. We and others have recently characterized the importance of TNK2 signaling in certain hematologic malignancies and solid tumors by regulating signaling downstream of pathways including EGFR [85], SRC [70], and CSF3R [86]. Additionally, overexpression of TNK2 has been associated with tumor aggressiveness and poor patient outcome in breast cancer [87]. The role of TNK2 in PTPN11-mutant tumors was uncharacterized prior to data presented in this dissertation.

1-9: Evidence for a link between PTPN11 and TNK2

Recent research has suggested a link between mutations in PTPN11 and sensitivity to the multi-kinase inhibitor dasatinib. Dasatinib was designed to have a strong affinity to ABL kinase, but it targets many other kinases, including TNK2 [88].

[17] TNK2 has been shown to be activated downstream of the ligands EGF, Gas6, Heregulin, Insulin growth factor, and insulin [68].

Research in a mouse model of PTPN11-mutant lung cancer suggests that dasatinib may inhibit proteins upstream of PTPN11 [54]. Induced PTPN11 E76K expression in mouse lung cells resulted in adenoma and adenocarcinoma in a transgenic mouse model [54]. Mutant PTPN11 induced phosphorylation of its scaffold protein Gab1 in these tumors. Work in cell lines expressing mutant PTPN11 showed that dasatinib treatment reduced the interaction of PTPN11 with Gab1 by co-immunoprecipitation and reduced the subsequent phosphorylation of Gab1. This work suggests that dasatinib can suppress the observed effects of activated PTPN11.

Pretreating MCF-10a human epithelial cells with dasatinib was shown to reduce phosphorylation of PTPN11 and Gab1 after EGFR stimulation, suggesting a dependence on dasatinib targets for PTPN11 activation downstream of EGFR [89]. Dasatinib was also shown to abrogate GM-CSF hypersensitivity and RAS signaling in primary JMML cells from a single PTPN11-mutant patient, which may be mediated through inhibition of SRC family kinases[90].

Most recently, work in a mouse model of NS by Yi et al. demonstrates the efficacy of low-dose dasatinib in selectively improving cardiac dysfunction, but does not identify mechanisms of action for dasatinib[89]. Researchers determined that Protein Zero-related (PZR), a protein that binds the SH2

domains of the open conformation of PTPN11 and is hyperphosphorylated in the presence of mutant PTPN11, has reduced phosphorylation with low dose dasatinib treatment. PZR is highly expressed in heart tissues, and abrogation of its hyperphosphorylation seems to account for the improvement in cardiac dysfunction.

While this body of evidence suggests a link between treatment with dasatinib and reduction of mutant PTPN11-dependent signaling, the mechanisms linking PTPN11 to dasatinib have not yet been identified. This dissertation addresses those mechanistic questions, and describes experiments performed to support my central hypothesis: TNK2 is necessary for PTPN11-mutant leukemia survival.

1-10: Synthetic lethality in cancer

Synthetic lethality is a genetic concept developed by yeast geneticists in the early 20th century [91] that has been co-opted by cancer researchers in more recent years [92]. Two genes are considered synthetic lethal if perturbation in both genes is lethal to cells or an organism. Iglehart et al. define synthetic lethality in the case of cancer therapeutics as two

genes, of which one can be targeted for mutation or inhibition, and the second is only mutated in tumor cells [92].

The advantage of a synthetic lethal approach in cancer therapy is that treatments become targeted to tumor cells bearing a mutation, and not the surrounding cells that do not. A synthetic lethality window can be determined by comparing viability curves of cells harboring a pathogenic mutation and wild-type cells [93]. The "window" is the range of concentrations of drug that kills mutant cells but does not affect normal cells. For the purposes of this dissertation, TNK2 has a synthetic lethal relationship to mutant-PTPN11, with TNK2 inhibition being lethal only in the context of leukemia cells harboring activating PTPN11 mutations.

1-11: Summary

PTPN11 is a ubiquitous tyrosine phosphatase that drives signaling through the Ras/Raf/MEK/ERK signaling axis. Over-activation of this pathway by mutant PTPN11 has been implicated in a number of hematologic malignancies, especially JMML and AML. Current literature suggests a link between mutant PTPN11 and dasatinib sensitivity, but the molecular mechanisms underlying this sensitivity have not been described. The central

hypothesis of my work has been that TNK2 is necessary for PTPN11-mutant leukemia survival. This dissertation identifies the kinase TNK2 as a key activator of mutant PTPN11 and describes the mechanism by which cells with mutant PTPN11 are sensitive to dasatinib. Additionally, this work describes a closely coupled regulatory feedback loop from PTPN11 to TNK2, and posits that patients with PTPN11-mutant leukemias may benefit from dasatinib treatment.

Chapter 2 : Results

2-1: A primary specimen from a patient with PTPN11-mutant JMML demonstrates dasatinib sensitivity and TNK2-dependence

2-1.1: A primary JMML specimen with PTPN11 G60R demonstrates TNK2-dependence.

In order to identify functional targets in a primary patient sample, peripheral mononuclear white blood cells from a patient with recurrent JMML carrying a PTPN11 G60R (g180c transversion) mutation (Fig. 2-1) were assayed against *ex vivo* panels of small-molecule kinase inhibitors or siRNAs [94, 95]. The sample showed significantly reduced viability in the presence of siRNA targeting TNK2, suggesting that these JMML cells exhibited dependence on TNK2 for cell survival (Fig. 2-2 and Table 2-1).

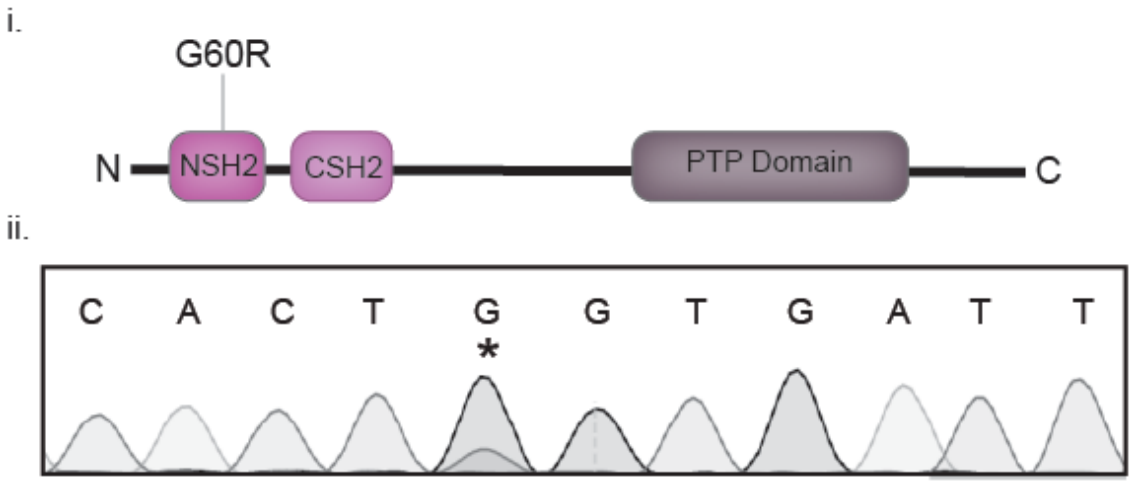

Figure 2-1*:* PTPN11 mutation in a JMML sample.

The PTPN11 mutation G60R (i) was first identified in a patient with recurrent JMML by whole exome sequencing, and confirmed by Sanger sequencing (ii).

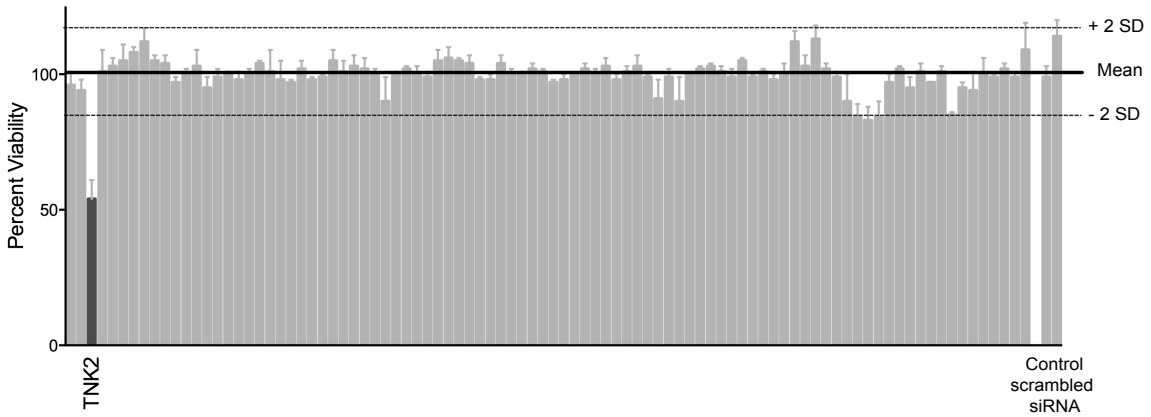

Figure 2-2: Patient sample screening identifies TNK2 as a functional target.

Peripheral blood mononuclear cells from this patient were incubated with an siRNA library. Each bar represents cell viability after silencing of an individual kinase. Values represent percent mean viability ± SEM (n = 3).

Table 2-1: JMML patient siRNA panel data

siRNA	Cell	Std Error
ABL1	96	5
ABL2	94	4
TNK2	54	7
ALK	101	8
AXL	103	3
BLK	105	6
BMX	108	2
BTK	112	5
TP53RK	105	2
CSF1R	104	3
CSK	97	2
DDR1	100	2
DDR2	103	6
STYK1	95	4
EGFR	99	3
EPHA1	100	1
EPHA2	98	3
EPHA3	100	2
EPHA4	104	1
EPHA7	101	8
EPHA8	98	7
EPHB1	97	1
EPHB2	102	3
EPHB3	98	1
EPHB4	99	1
EPHB6	105	4
ERBB2	101	4
ERBB3	103	4
ERBB4	102	4
FER	100	2
FES	90	9
FGFR1	100	1
FGFR2	102	1
FGFR3	100	3
FGFR4	99	2
FGR	105	4
FLT1	106	4
FLT3	105	1
FLT4	104	3
FRK	98	1
FYN	98	2
HCK	104	3
IGF1R	100	2
INSR	100	1
ITK	102	2
JAK1	101	1
JAK2	97	1
JAK3	98	2
KDR	100	0
LMTK2	102	2
KIT	100	2

siRNA	Cell	Std Error
LCK	103	3
LTK	98	2
LYN	101	2
MATK	103	4
MERTK	99	1
MET	91	7
MST1R	99	3
MUSK	90	9
NTRK1	100	1
NTRK2	102	1
NTRK3	103	1
PDGFRA	101	2
PDGFRB	99	3
PTK2	105	1
PTK2B	99	1
PTK6	101	1
PTK7	98	2
PTK9	100	4
PTK9L	112	4
RET	103	4
ROR1	113	5
ROR2	102	2
ROS1	99	2
RYK	90	10
SRC	84	5
SYK	83	5
TEC	84	6
TEK	97	3
TIE	102	1
TNK1	95	4
TXK	101	3
TYK2	97	0
TYRO3	101	2
YES1	85	1
ZAP70	95	2
N-RAS	94	7
K-RAS	100	6
EPHA5	99	1
EPHA6	102	2
SRMS	99	2
AATK	109	10
Control 1	99	4
Control 2	114	6

2-1.2: A primary JMML specimen with a PTPN11 G60R mutation demonstrates dasatinib sensitivity.

Treatment of this patient's cells with a panel of small-molecule inhibitors revealed hypersensitivity to the multi-target kinase inhibitor, dasatinib, with an IC_{50} of 36 nM (Table 2-2 and 2-5). The median IC_{50} for dasatinib from a diverse cohort of 151 primary leukemia patient specimens was 401 nM. This patient's mononuclear cells were, therefore, 10-fold more sensitive to dasatinib than the average leukemia sample from this previously published patient cohort [96] (Fig. 2-3). Because TNK2 is a reported target of dasatinib [88], this raised the possibility that leukemic cells with PTPN11 mutations might be sensitive to drugs that target TNK2, such as dasatinib.

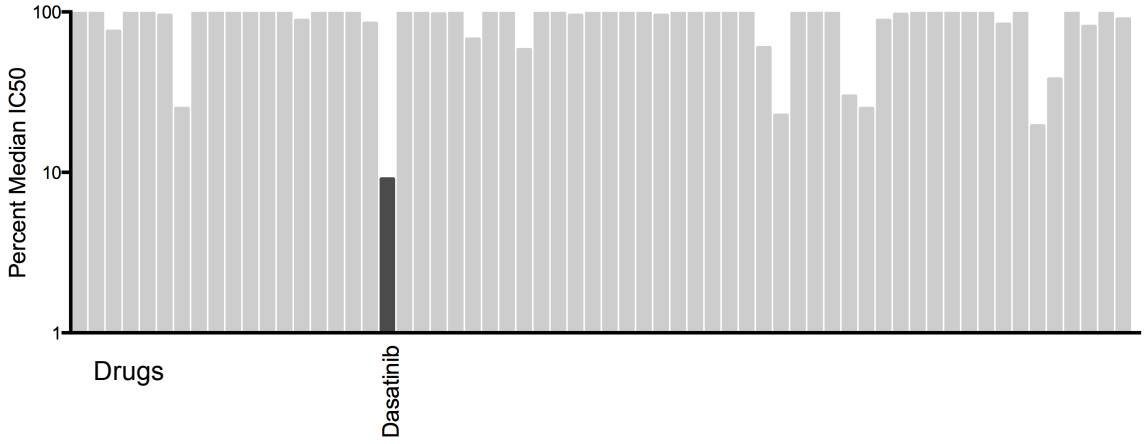

Figure 2-3: Patient sample screening identifies TNK2 as a functional target.

Peripheral blood mononuclear cells from the same JMML patient were incubated with graded concentrations of 66 different small-molecule kinase inhibitors for 3 days. Cell viability was determined and the IC_{50} for each drug was calculated with respect to cells incubated in the absence of drug. These IC_{50} values were compared to the median IC_{50} for each drug across 151 patient samples. Each bar represents the percent of median IC_{50} for an individual kinase inhibitor. (n=3).

Table 2-2: JMML patient inhibitor panel data

Drug	Percent Median IC50
ABT-869	169.15
AG490	100.00
AKT IV	75.81
AKT X	153.67
AMG-706	100.00
AMPK	95.25
AP24534	25.04
AST-487	158.82
AZD-1152	100.00
BIRB-796	100.00
BMS-387032	5259.19
CAL101	100.00
CHIR-258	142.29
CHIR-265	88.62
CI-1033	138.21
CP-690550	100.00
CYC-202	100.00
CYT387	84.90
Dasatinib	9.08
EGFR	100.00
EKB-569	122.11
Erlotinib	97.04
Flavopiridol	109.77
Gefitinib	67.75
Gš6976	100.00
GW-2580	100.00
GW-786034	58.26
H-89	100.00
Imatinib	100.00
JAK3	95.12
JNJ-7706621	149.45
JNK II	267.03
KN92	100.00
KN93	100.00
Lapatinib	95.20
LY-333531	210.30
LY294002	110.21
MEK1/2	100.00
MLN-518	100.00
MLN-8054	100.00
NF-kB	59.85

Drug	Percent Median IC50
Nilotinib	22.70
p38	100.00
PD153035	100.00
PD98059	100.00
PI-103	29.87
PKC-412	25.00
PP2	88.46
PTK787	96.53
SB-202190	100.00
SB-203580	100.00
SB-431542	100.00
Sorafenib	99.12
SRC	100.00
Staurosporine	83.64
STO609	100.00
SU-14813	19.50
Sunitinib	38.21
SYK	100.00
VX-680	81.26
VX-745	100.00
ZD-6474	90.25

2-1.3: PTPN11 G60R mutant increases Ras/MAPK signaling.

The most common PTPN11 mutation in JMML, E76K, has been identified as having the highest phosphatase activity of any activated PTPN11 mutant [5, 42]. Next we examined the capacity of the PTPN11 G60R mutation to activate the MEK/ERK pathway. We performed heterologous studies using transfected human expression constructs containing wild-type PTPN11, PTPN11 G60R or PTPN11 E76K into human endothelial kidney 293T17 cells, a highly transfectable derivative of the human embryonic kidney (HEK293) cell line. Immunoblots of 293T17 cells expressing either PTPN11 G60R or E76K showed significantly increased levels of p44/42 MAPK phosphorylation (ERK1/2, MAPK 1/3) compared with cells expressing wild-type PTPN11 (Fig. 2-4).

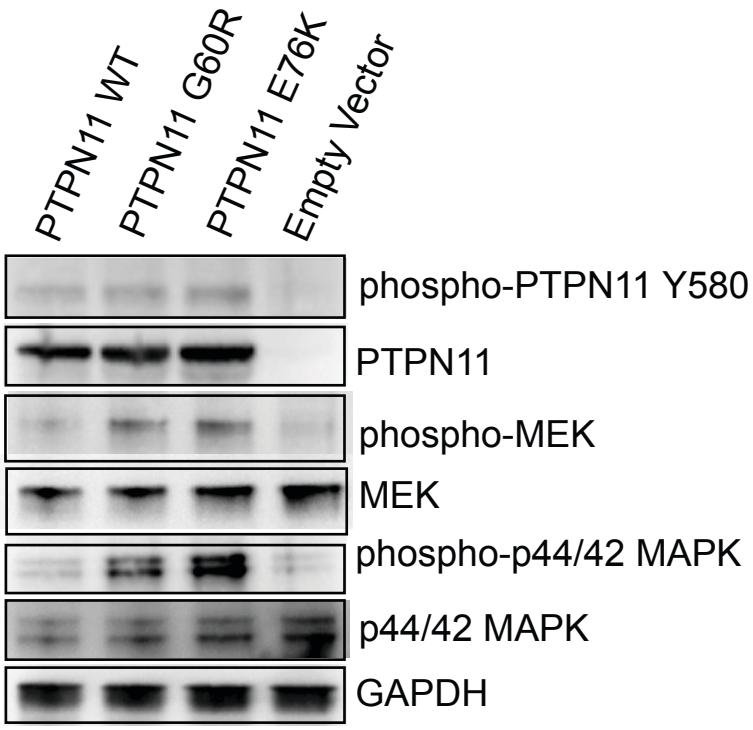

Figure 2-4: PTPN11 G60R increases signaling through Ras/MAPK in 293T17 cell lysates.

293T17 cells were transiently transfected with expression constructs containing PTPN11, PTPN11 G60R, PTPN11 E76K, or empty vector, and lysates were subjected to immunoblot. Representative blot of 3 biological replicates.

2-1.4: PTPN11 G60R increases GM-CSF sensitivity in bone marrow colony formation assay.

To test granulocyte macrophage colony-stimulating factor (GM-CSF) hypersensitivity – a hallmark of PTPN11 mutations and JMML [97], mouse bone marrow cells were transduced with constructs expressing PTPN11 mutations or wild-type. Consistently, both PTPN11 E76K and G60R showed GM-CSF hypersensitivity in mouse bone marrow methylcellulose colony formation assays (Fig. 2-5, $p<0.05$). Since the PTPN11 G60R and E76K mutations appeared to have the same gain-of-function phenotype, and because the PTPN11 E76K mutation is the most commonly occurring PTPN11 variant seen in JMML, we conducted further experiments for this study primarily using the PTPN11 E76K mutant.

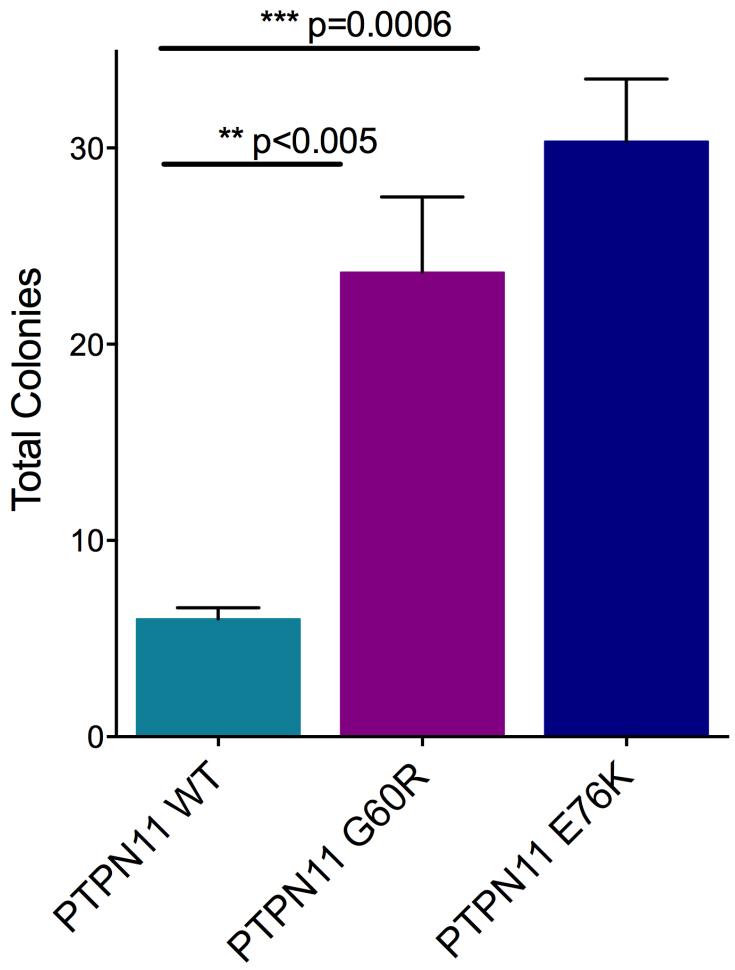

Figure 2-5: PTPN11 G60R increases GM-CSF sensitivity in mouse bone marrow colony formation assay.

Mouse bone marrow cells were transduced to express PTPN11, PTPN11 G60R, or PTPN11 E76K and plated in a methylcellulose GM-CSF sensitivity colony formation assay. Colonies were counted at 14 days [GM-CSF]=0.05nM. (n=3). **p<0.005 ***p=0.0006 by one-way ANOVA. Error bars represent SEM.

2-2: TNK2 enhances signaling of mutant PTPN11 through RAS/MAPK

2-2.1: 293T17 lysates expressing mutant PTPN11 and TNK2 reveal novel signaling events.

In order to examine the potential impact of TNK2 on signaling of PTPN11 mutants, 293T17 cells were co-transfected with constructs expressing mutant or wild-type PTPN11 with or without TNK2 co-expression. Signaling activity was then assessed by immunoblot (Fig. 2-6). Co-expression of PTPN11 E76K and TNK2 resulted in significantly increased levels of phosphorylated p44/42 MAPK ($p=0.0005$) when compared to cells expressing PTPN11 E76K or TNK2 alone (Fig. 2-7). We also observed that co-expression of TNK2 with PTPN11 results in elevated phosphorylation of PTPN11 at residues Y542 and Y580 ($p=0.0005$) (Fig. 2-6,7). Interestingly, phosphorylation of TNK2 at its primary activating tyrosine residue, Y284, was reduced when co-expressed with PTPN11, and this reduction of TNK2 phosphorylation was especially pronounced with mutant PTPN11 compared with wild-type (Fig. 2-6,7). The Y284 residue of TNK2 has been shown to be important for TNK2 activation, with SRC kinase implicated as a possible kinase upstream of TNK2 that phosphorylates this site[68]. This decrease in phospho-TNK2 is also observed, though not at statistically significant levels, when wild-type PTPN11 is co-transfected with TNK2 (Fig. 2-7).

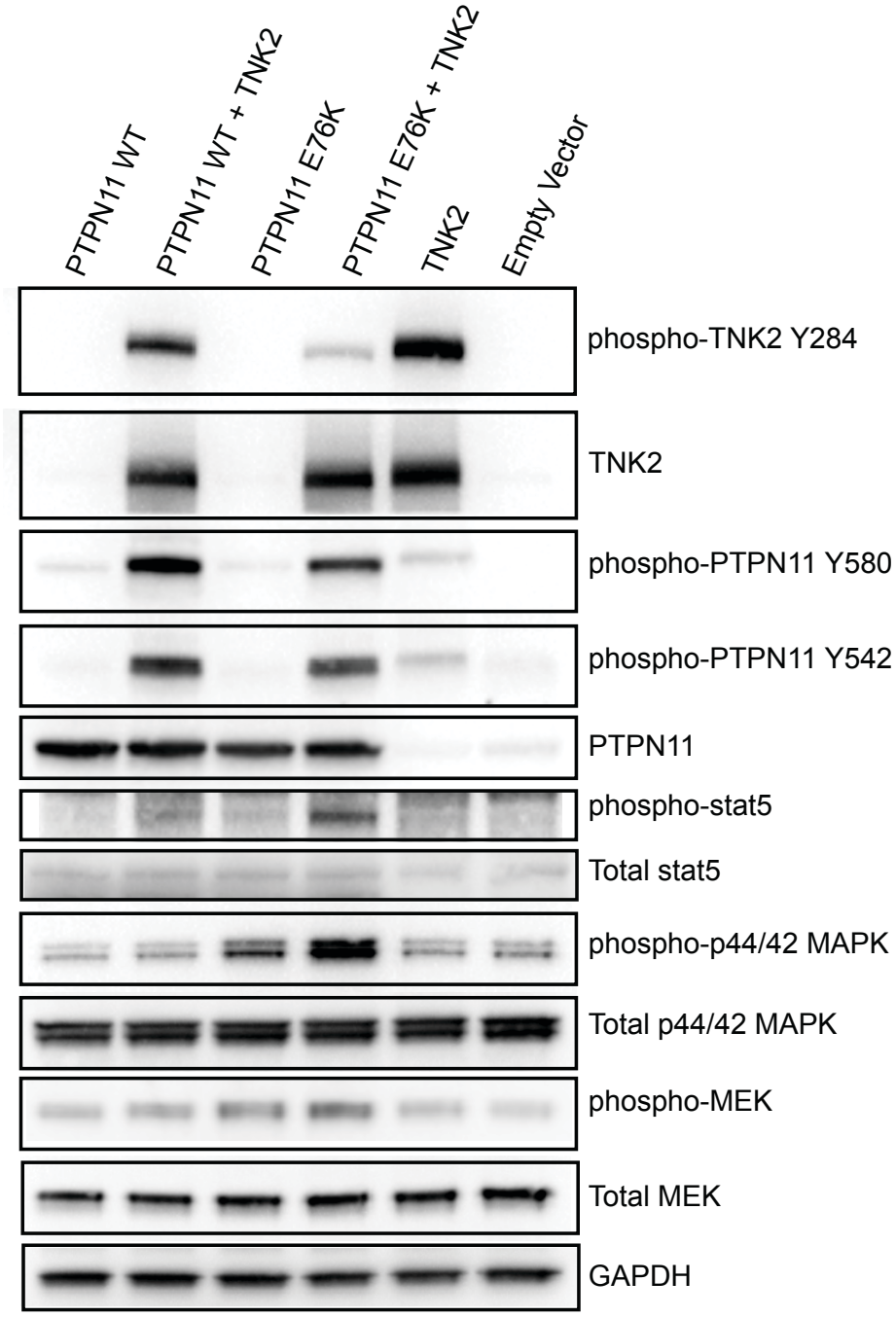

Figure 2-6: 293T17 cell lysates expressing mutant PTPN11 and TNK2 reveal novel signaling events.

293T17 cells were co-transfected with overexpression constructs containing PTPN11, PTPN11 E76K, TNK2, or empty vector controls. Lysates were collected at 48 hours and subjected to immunoblot. Representative blot of 4 biological replicates.

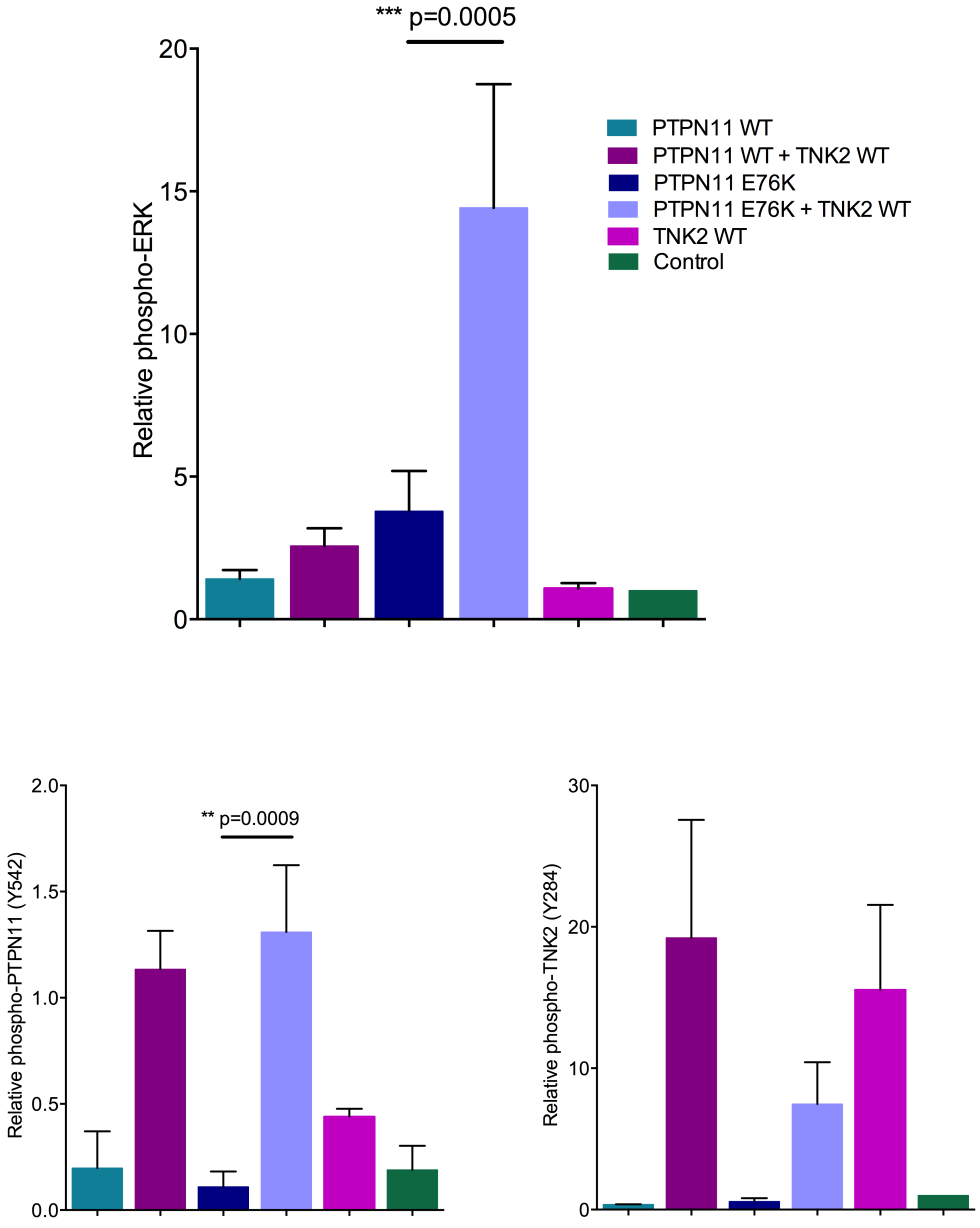

Figure 2-7: Quantification of Western blots represented in Fig 2-6.

Relative phospho-p44/42 MAPK (phospho-ERK1/2), relative phospho-TNK2 (Y284), and relative phospho-PTPN11 values were calculated with GAPDH as a loading control. (n=4). *** p=0.0005, ** p=0.0009 by one-way ANOVA. Error bars represent SEM.

2-2.2: Increase in PTPN11 activity is TNK2 kinase dependent.

Since TNK2 is dephosphorylated while enhancing activation of p44/42 MAPK downstream of mutant PTPN11, we next wanted to test the impact of mutations that activate or de-activate the TNK2 kinase domain. We generated a mutation at the TNK2 "gatekeeper" residue, TNK2 T205I, which has increased kinase activity compared with WT TNK2 and has been shown previously to block sensitivity to kinase inhibitors, as described with gatekeeper mutants of other tyrosine kinases, such as BCR-ABL [98, 99]. We also generated a kinase inactive version of TNK2 with a mutation at the critical tyrosine residue in the kinase domain, Y284F. We observed that the enhancement of p44/42 MAPK phosphorylation by TNK2 and mutant PTPN11 co-expression was further enhanced with co-expression of the activated TNK2 T205I with mutant PTPN11. This was abrogated by co-expression of mutant PTPN11 with the kinase inactive TNK2 Y284F (Fig. 2-8) These data suggest that kinase activity of TNK2 is required to enhance mutant PTPN11 signaling.

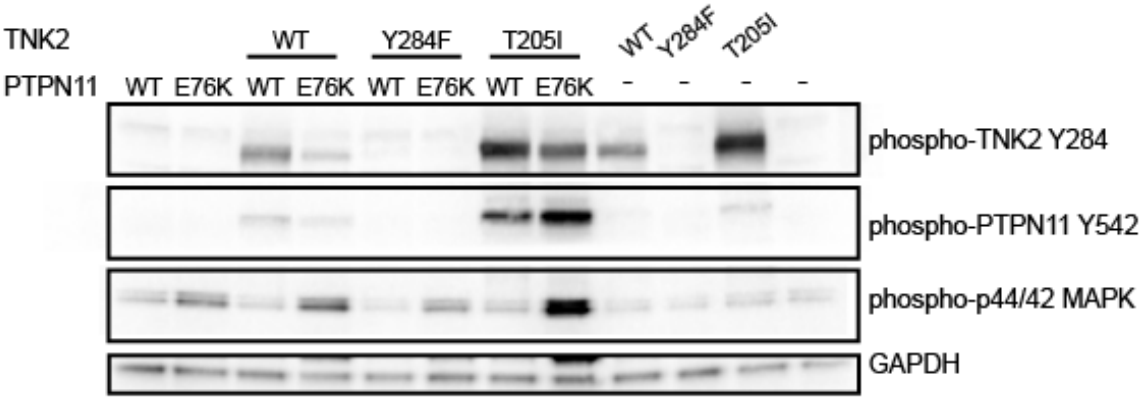

Figure 2-8: Increase in PTPN11 activity is TNK2 kinase dependent.

293T17 cells were co-transfected with overexpression constructs containing PTPN11, PTPN11 E76K, TNK2, TNK2 Y284F, TNK2 T205I, or empty vector controls. Lysates were collected 48 hours post-transfection and subjected to immunoblot. Representative blot of 2 biological replicates.

2-2.3: TNK2 kinase activity is dependent of phosphorylation.

To test that reduced TNK2 phosphorylation correlated with reduced TNK2 kinase activity, an in vitro kinase assay was performed on lysates from 293T17 cells transfected to express wild-type or mutant forms of TNK2 (Fig. 2-9). TNK2 mutant expression constructs were generated with mutations at the reported phosphorylated Tyrosine residues Y284, Y518, and Y859. In addition to these mutants we also examined the kinase activity of the two activating TNK2 mutants D163E and T2015I. To increase specificity of the assay, TNK2 was immunoprecipitated prior to assessing the kinase activity. As expected, mutation of TNK2 to reduce tyrosine phosphorylation reduced its kinase activity with respect to wild-type TNK2, suggesting that its dephosphorylation results in lower TNK2 activity in this context.

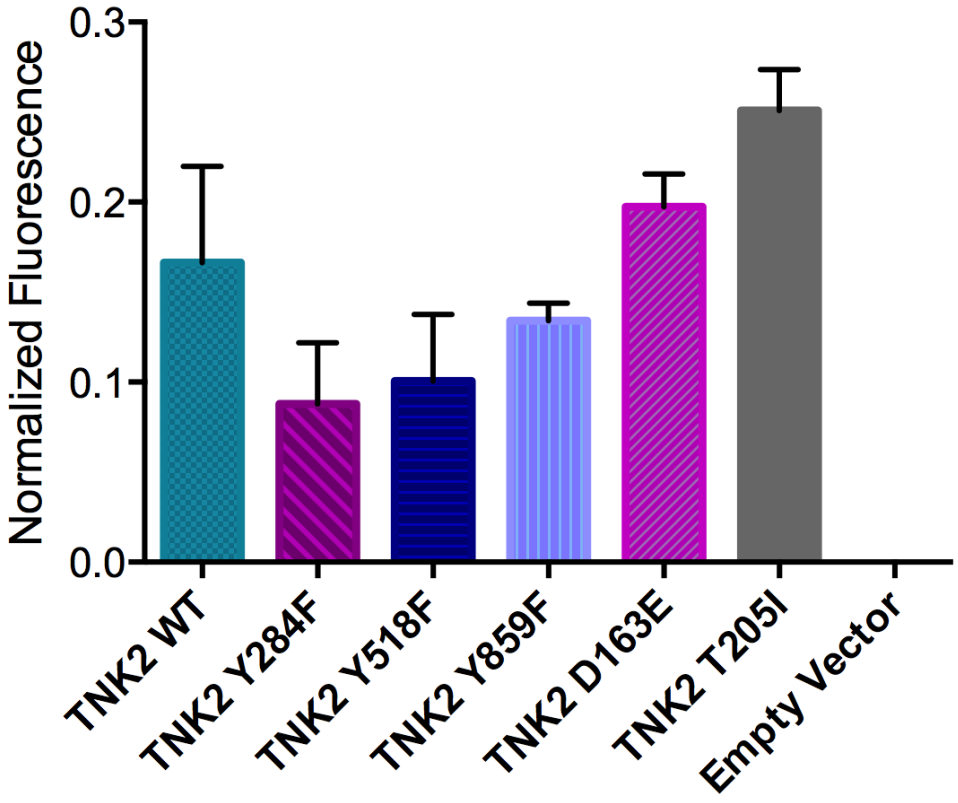

Figure 2-9: TNK2 kinase activity is dependent on phosphorylation.

293T17 cells were co-transfected with constructs containing TNK2, TNK2 Y284F, TNK2 Y518F, TNK2 Y859F, TNK2 D163E, TNK2 T205I, or empty vector controls. Lysates were collected 48 hours post-transfection and subjected to *in vitro* kinase assay. Values normalized to empty vector control.

2-2.4:Additional PTPN11 activating mutants follow observed signaling patterns.

To test whether the observed effect was not specific to JMML-related mutations in PTPN11, several other mutant PTPN11 expression constructs were generated. These mutants derive from AML (N58K, G503V), CML (G503V) or kidney cancer cell lines (SN12C). These mutant constructs were co-expressed in 293T17 cells with TNK2, and immunoblots were performed (Fig. 2-10). The observed effect of synergy with TNK2 with regard to the increase of Ras/MAPK signaling and reduction of phospho-TNK2 was recapitulated with these constructs, and seems to be a global characteristic of activated PTPN11.

i.

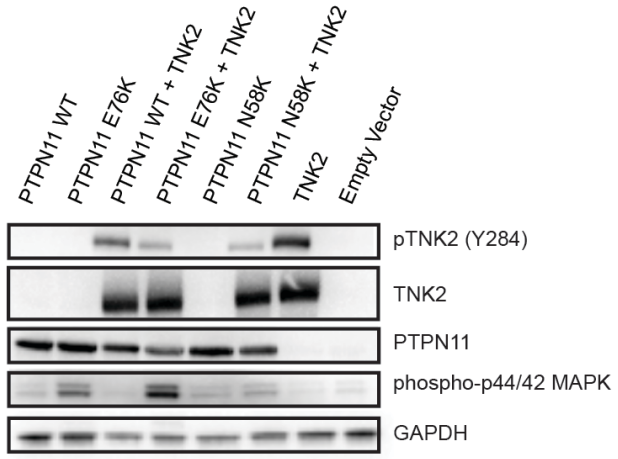
PTPN11 WT
PTPN11 E76K
PTPN11 WT + TNK2
PTPN11 E76K + TNK2
PTPN11 N58K
PTPN11 N58K + TNK2
TNK2
Empty Vector
pTNK2 (Y284)
TNK2
PTPN11
phospho-p44/42 MAPK
GAPDH

ii.

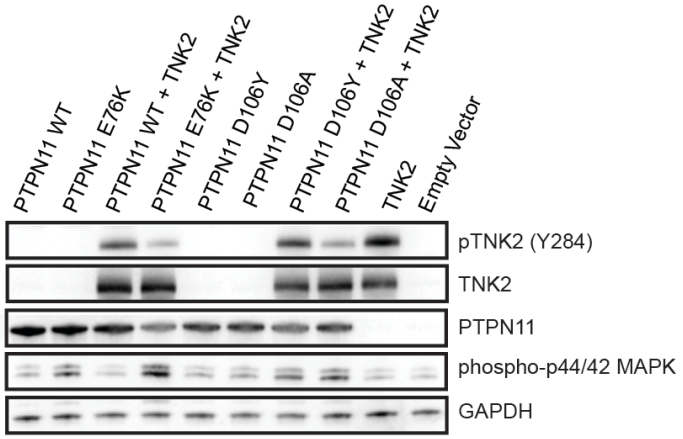
PTPN11 WT
PTPN11 E76K
PTPN11 WT + TNK2
PTPN11 E76K + TNK2
PTPN11 D106Y
PTPN11 D106A
PTPN11 D106Y + TNK2
PTPN11 D106A + TNK2
TNK2
Empty Vector
pTNK2 (Y284)
TNK2
PTPN11
phospho-p44/42 MAPK
GAPDH

iii.

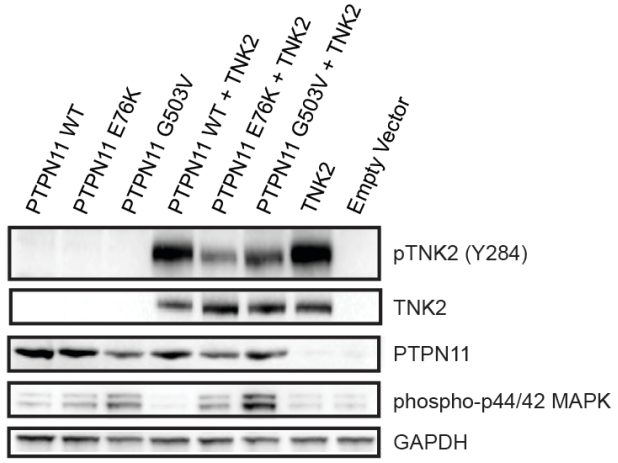
PTPN11 WT
PTPN11 E76K
PTPN11 G503V
PTPN11 WT + TNK2
PTPN11 E76K + TNK2
PTPN11 G503V + TNK2
TNK2
Empty Vector
pTNK2 (Y284)
TNK2
PTPN11
phospho-p44/42 MAPK
GAPDH

Figure 2-10: Additional PTPN11 activating mutants follow observed signaling patterns.

i. 293T17 cells were transiently co-transfected with expression constructs containing PTPN11, PTPN11 E76K, PTPN11 N58K, TNK2, or empty vector controls. Lysates were subjected to immunoblot. Representative blot from 2 biological replicates. ii. 293T17 cells were transiently co-transfected with expression constructs containing PTPN11, PTPN11 E76K, PTPN11 D106Y, PTPN11 D106A, TNK2, or empty vector controls. Lysates were subjected to immunoblot. Representative blot from 2 biological replicates. iii. 293T17 cells were transiently co-transfected with expression constructs containing PTPN11, PTPN11 E76K, PTPN11 G503V, TNK2, or empty vector controls. Lysates were subjected to immunoblot. Representative blot from 3 biological replicates.

2-2.5: PTPN11 and TNK2 co-immunoprecipitate.

Collectively, the enhanced signaling observed with TNK2/PTPN11 co-expression as well as the reciprocal increase in PTPN11 phosphorylation and decrease in TNK2 phosphorylation suggested that PTPN11 and TNK2 might be directly interacting with PTPN11 as a target of TNK2 kinase activity. To test this hypothesis, we performed a co-immunoprecipitation experiment using FLAG-tagged PTPN11 constructs. 293T17 cells were co-transfected with TNK2 and PTPN11 WT FLAG or PTPN11 G60R FLAG constructs and lysates were harvested then subjected to immunoprecipitation and immunoblot (Fig. 2-11). We were able to detect robust co-immunoprecipitation of PTPN11 and TNK2, suggesting these proteins do interact. In addition to detection of interaction between our FLAG-tagged constructs and TNK2, TNK2 immunoprecipitation in cells transfected with TNK2 and empty vector control resulted in co-immunoprecipitation of endogenous phosphorylated PTPN11, supporting immunoblot data showing phosphorylation of endogenous levels of PTPN11 in cells overexpressing TNK2 (Fig. 2-6).

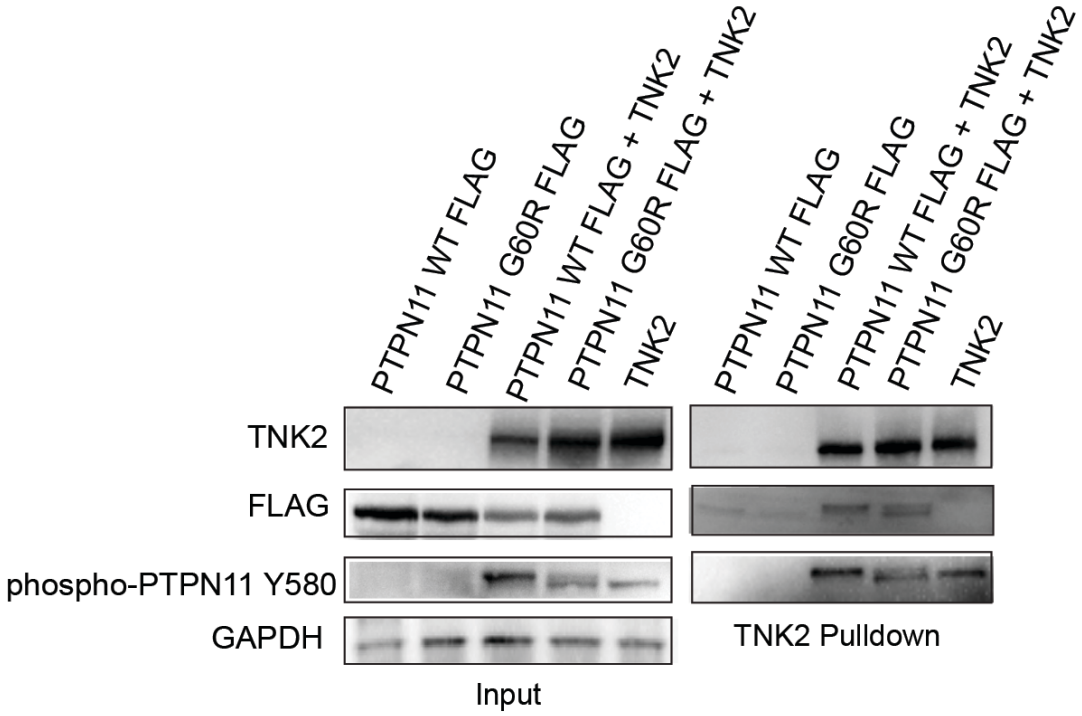

Figure 2-11: PTPN11 and TNK2 co-immunoprecipitate.

293T17 cells were co-transfected with overexpression constructs containing PTPN11 WT FLAG or PTPN11 G60R FLAG constructs, TNK2, or empty vector controls. Lysates were collected at 48 hours and subjected to TNK2 immunoprecipitation, followed by Western blot.

2-2.6: PTPN11 activation is dependent on C-terminal tyrosine residues.

In order to determine whether phosphorylation of C-terminal PTPN11 residues is necessary for activated mutant-PTPN11 activation in the presence of TNK2, PTPN11 mutant expression constructs were generated and 293T17 cells were transiently transfected to express mutant PTPN11, TNK2, or empty vector control (Fig. 2-12). We again observed a significant increase in phospho-p44/42 MAPK with the co-expression of PTPN11 E76K and TNK2 (Fig. 12-12,13). Mutation of either Y542 or Y580 reduced phospho-p44/42 MAPK. However, mutation of PTPN11 at both Y542 and Y580 resulted in similar levels of phospho-p44/42 MAPK (Fig. 2-13). Interestingly, PTPN11 with the activating E76K mutant, which is thought to allow PTPN11 to constitutively adopt the open active conformation, requires phosphorylation of Y542 and Y580 for full activation (Fig. 2-13). These data suggest that phosphorylation of the C-terminal residues of PTPN11, seen here to increase significantly in the presence of TNK2, is imperative for full PTPN11 activity.

In agreement with the observation that activated mutant PTPN11 E76K greatly reduces phospho-TNK2 levels (Fig. 2-7) TNK2 dephosphorylation from these experiments coordinates with PTPN11 activity (Fig. 2-14). Reduced PTPN11 activity correlates with higher levels of TNK2 phosphorylation, suggesting that this event is PTPN11-dependent.

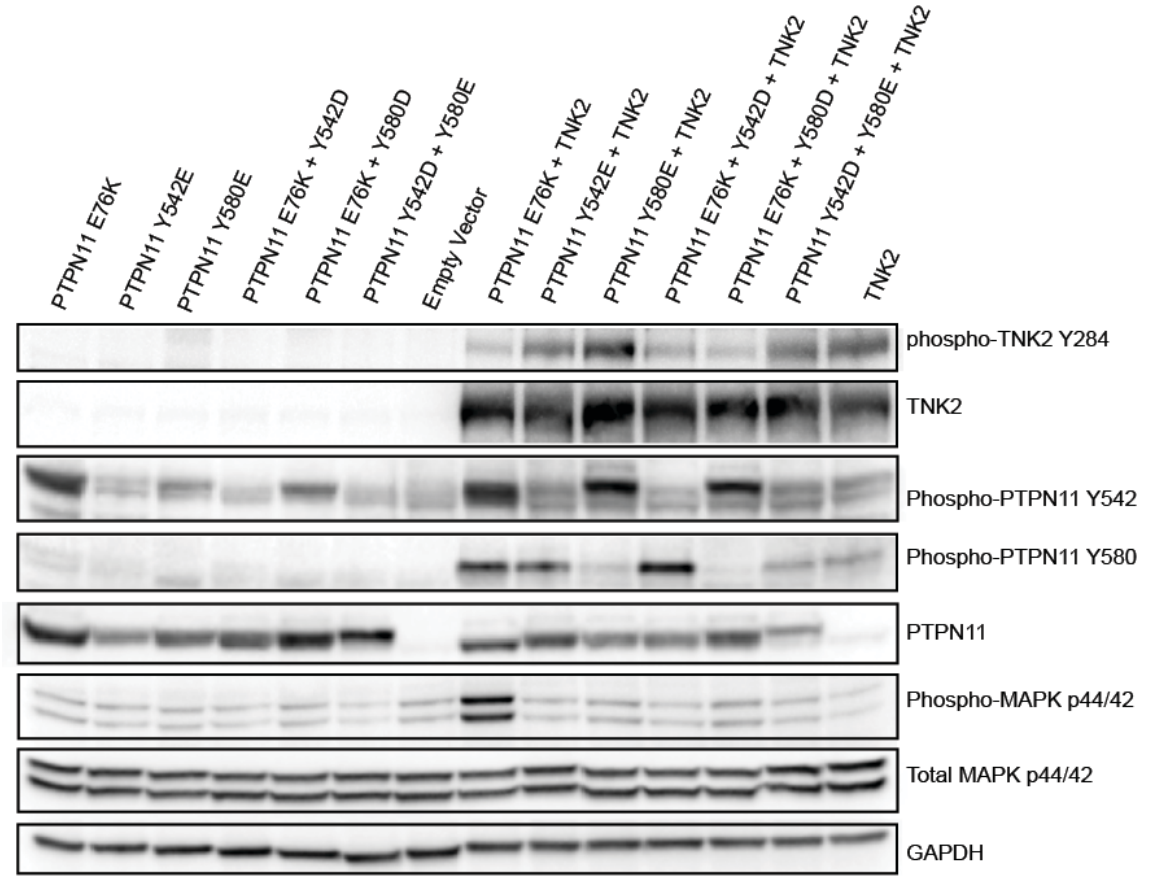

Figure 2-12: PTPN11 activation is dependent on phosphorylation of C-terminal Tyrosine residues by TNK2:

293T17 cells were co-transfected with expression constructs containing PTPN11, mutant PTPN11, TNK2, or empty vector controls. Lysates were collected 48 hours post-transfection and subjected to immunoblot. Representative blot. (n=3.)

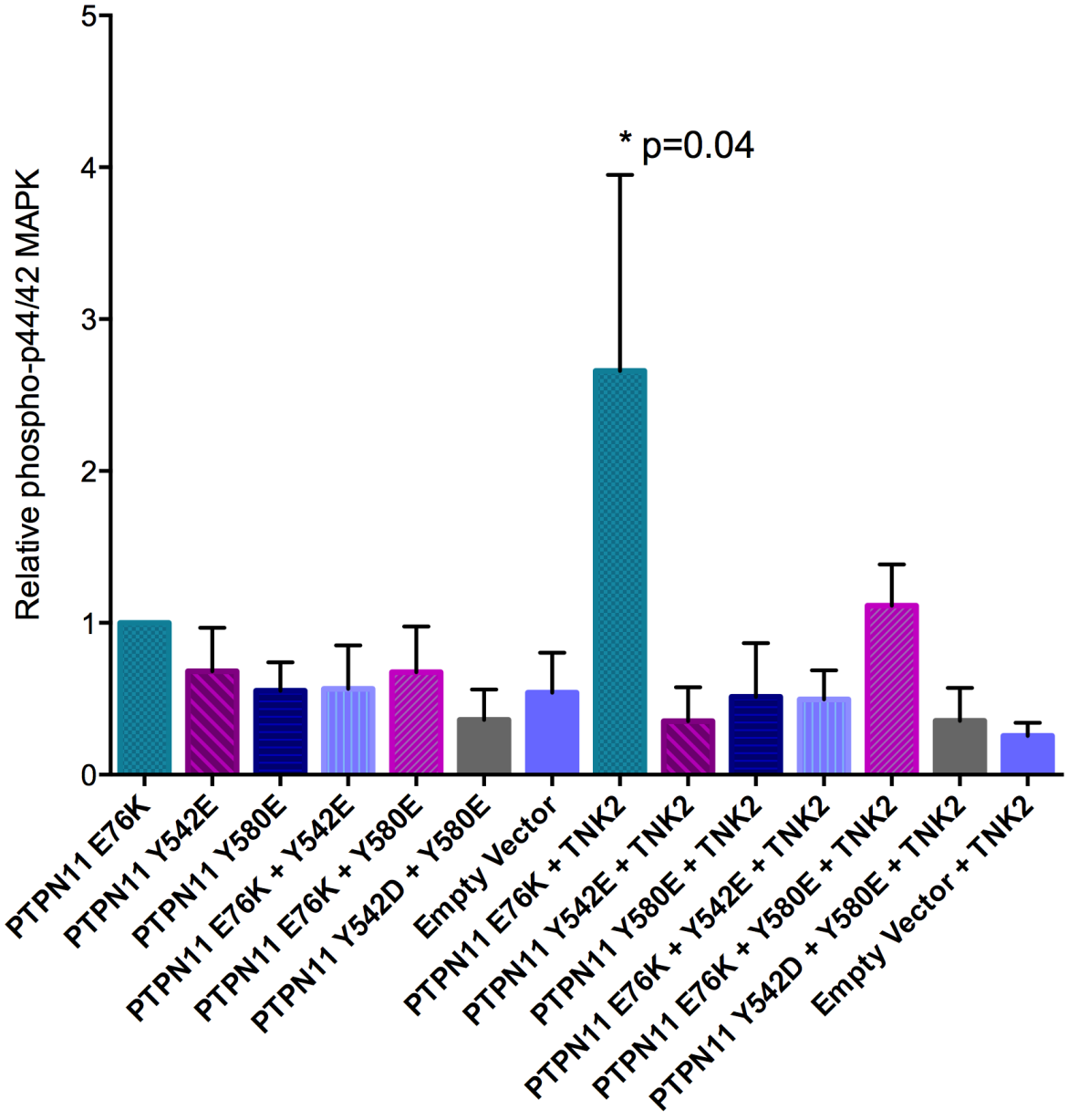

Figure 2-13: Synergy between TNK2 and mutant PTPN11 to increase phosphorylation of p44/42 MAPK is dependent on PTPN11 C-terminal tyrosine phosphorylation.

Quantification of Fig. 2-12. (n=3). Error bars represent SEM.

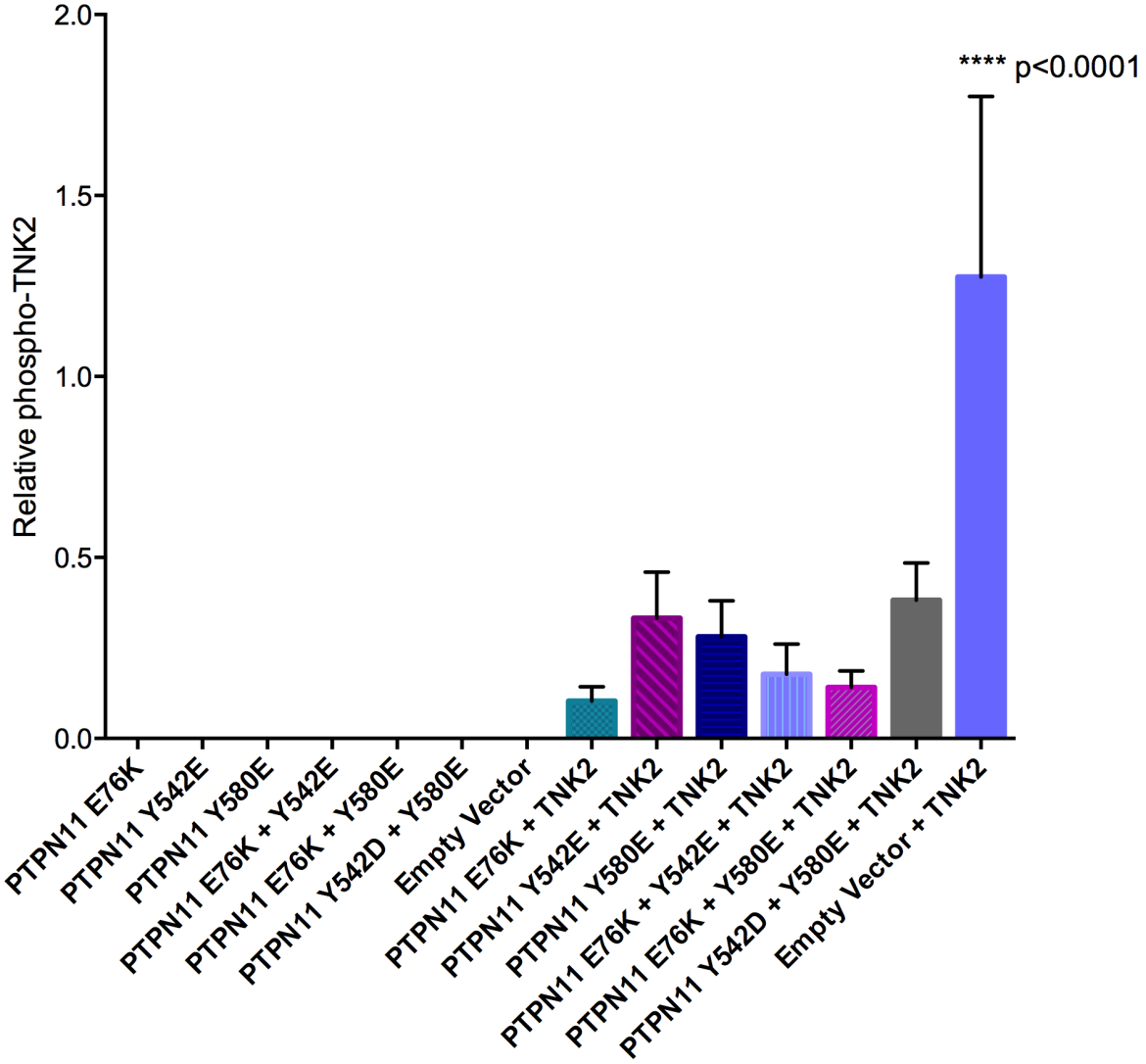

Figure 2-14: TNK2 dephosphorylation is dependent on PTPN11 activity.

Quantification of Fig. 2-12. (n=3). Error bars represent SEM.

2-3: Inhibition of TNK2 reduces signaling through PTPN11/RAS/MAPK

2-3.1: TNK2 inhibition reduces signaling through Ras/MAPK.

Since our data suggested that TNK2 positively regulates PTPN11 signaling, we next sought to determine the impact of TNK2 inhibition on mutant PTPN11 signaling. To test this, we co-expressed mutant or wild-type PTPN11 with wild-type or gatekeeper-mutant TNK2 T205I. The gatekeeper mutant is resistant to dasatinib as well as the TNK2-selective inhibitor, AIM-100 [98, 100]. 293T17 cells expressing these constructs were treated with either dasatinib or AIM-100 for 2 hours and signaling pathway activity was assessed by immunoblot (Fig. 2-15). Inhibition of TNK2 by either dasatinib or AIM-100 resulted in significantly reduced phospho-p44/42 MAPK levels ($p<0.0001$ for dasatinib $p<0.0001$ for AIM-100) in cells co-expressing mutant PTPN11 and TNK2 wild-type (Fig. 2-15,16.). In contrast, cells co-transfected with PTPN11 E76K constructs and the inhibitor-resistant gatekeeper TNK2 T205I mutant showed no significant reduction in MAPK signaling (Fig. 2-16). In addition, phospho-Y542 PTPN11 and phospho-Y580 PTPN11 were both reduced in the presence of TNK2 inhibition (Fig 2-17), though only when expressing wild-type TNK2. Phosphorylated PTPN11 levels were unaffected

by inhibitors in the context of the drug-resistant, gatekeeper TNK2 mutant. Taken together, these data suggest that TNK2 is an upstream activator of PTPN11, and that targeting of TNK2 abrogates PTPN11 signaling, impacting on PTPN11 capacity to activate the downstream MAPK pathway.

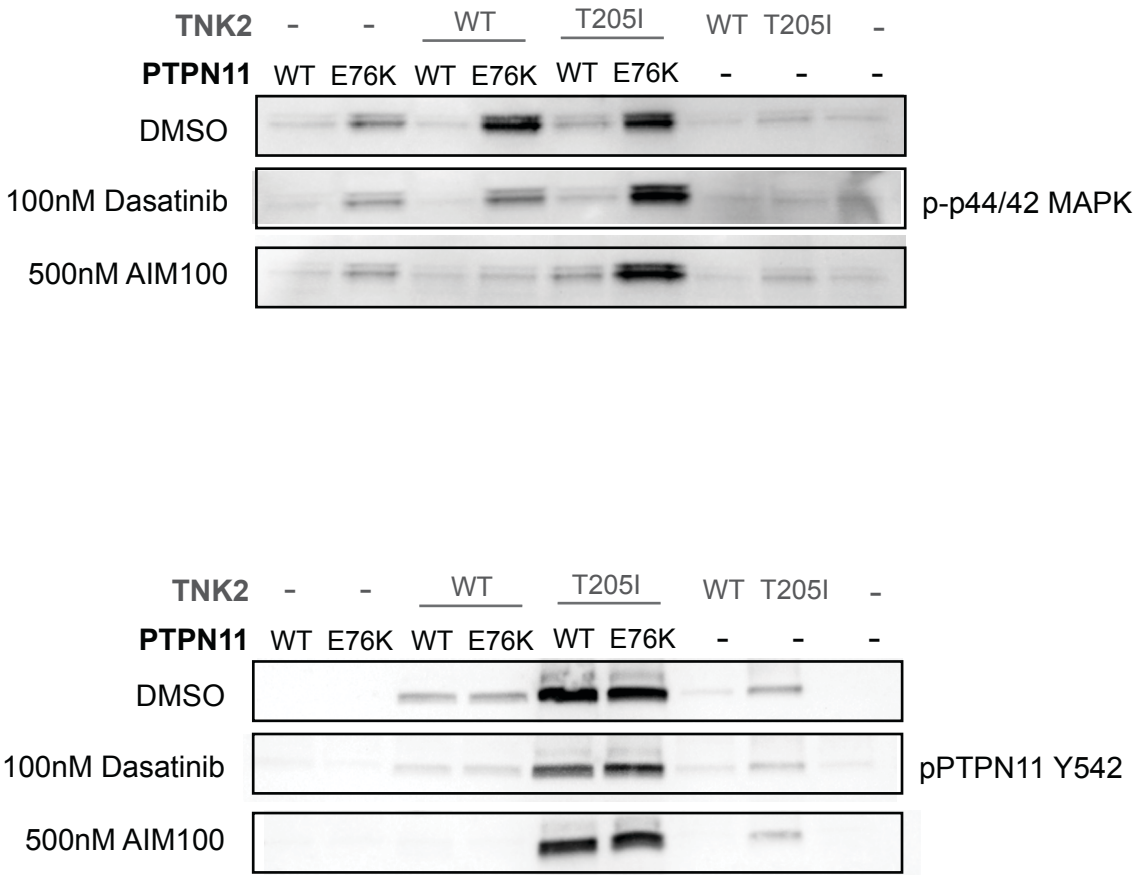

Figure 2-15: TNK2 inhibition reduces signaling through Ras/MAPK in 293T17 lysates.

Phospho-p44/42 MAPK (phospho-ERK ½) in 293T17 cells treated with TNK2 inhibitors. HEK293 T17 cells were co-transfected with overexpression constructs containing PTPN11, PTPN11 E76K, TNK2, TNK2 T205I, or empty vector controls. Cells were treated with Dasatinib (100nM), AIM100 (500nM) or 0.05% DMSO vehicle control for two hours at 48 hours post-transfection. Lysates were subjected to immunoblot. Representative blot of 4 biological replicates.

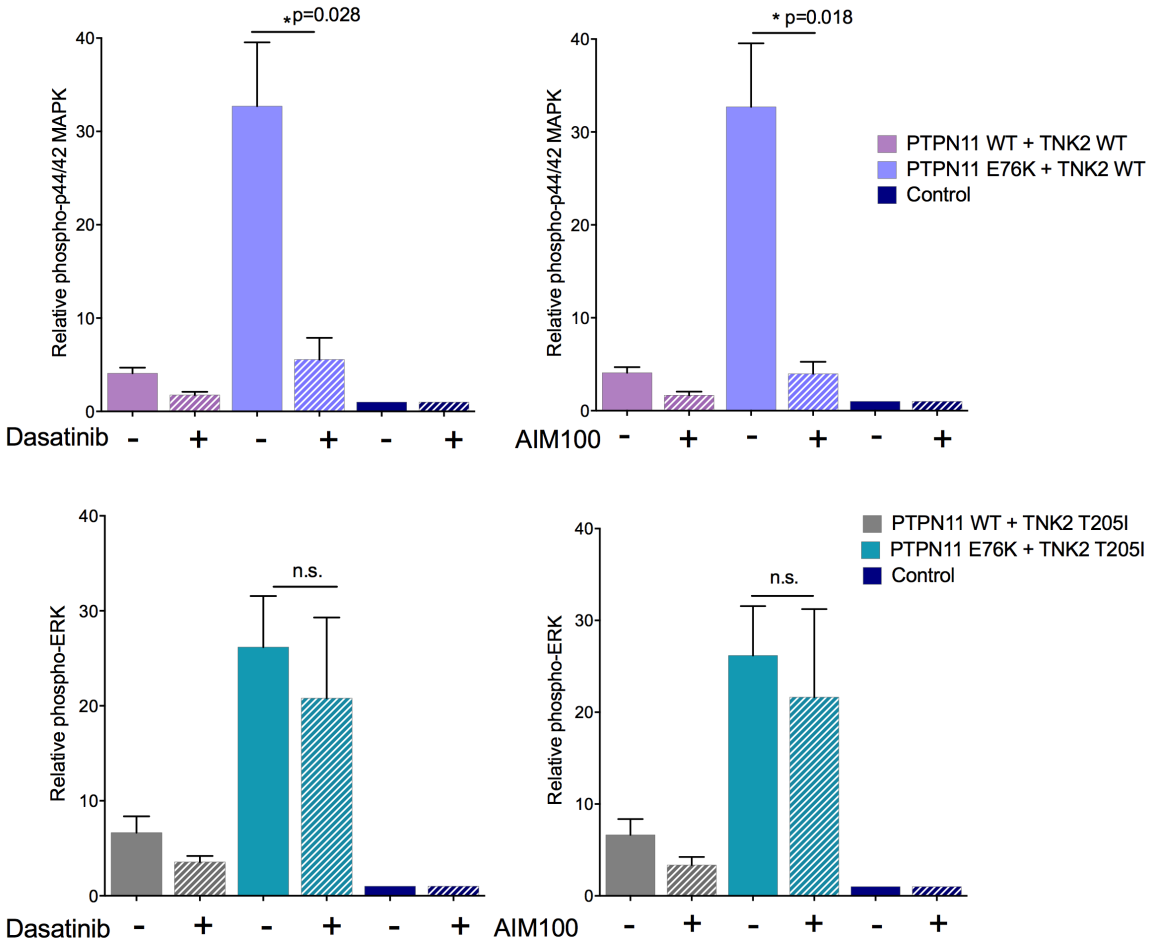

Figure 2-16: Quantification of Western blots represented in Fig 2-15.

Relative phospho-MAPK p44/42 (phospho-MAPK ½), values were calculated with GAPDH as a loading control. (n=4). P-values calculated by one-way ANOVA. Error bars represent SEM.

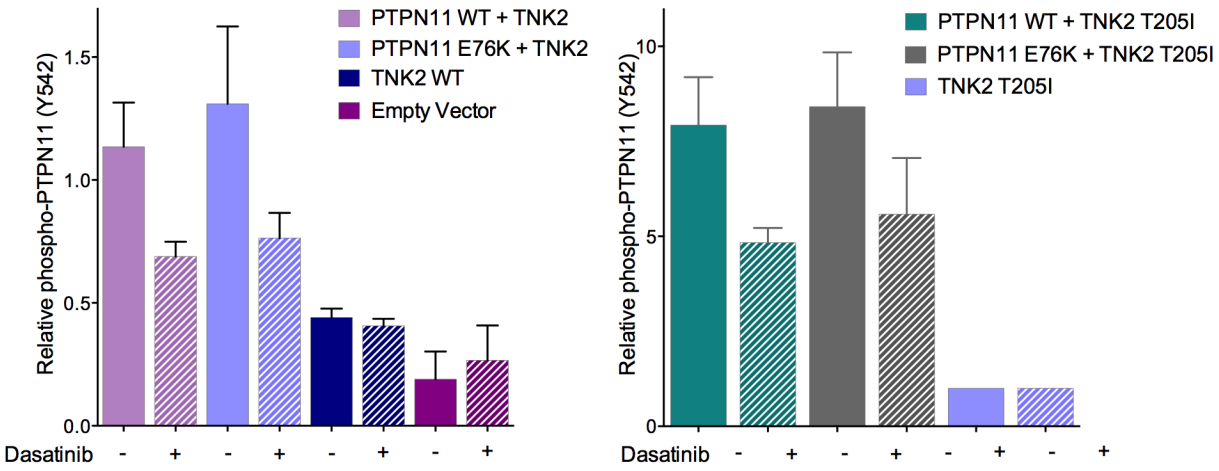

Figure 2-17: Quantification of Western blots represented in Fig. 2-15.

Relative phospho-PTPN11 (Y542) values were calculated with GAPDH as a loading control. (n=4). Error bars represent SEM.

2-3.2: TNK2 dephosphorylation is dependent on PTPN11 activity.

Since small-molecule TNK2 inhibitors appeared to block the TNK2-mediated phosphorylation of PTPN11, we next determined whether inhibition of PTPN11 could block the reciprocal dephosphorylation of TNK2. To test this, we used a newly developed allosteric inhibitor of PTPN11, SHP099 [101, 102] (Fig. 2-18,19,20). Inhibition of PTPN11 with SHP099 in cells transfected with PTPN11 and TNK2 overexpression constructs resulted in decreased phosphorylation of p44/42 MAPK at concentrations similar to those published [102], suggesting that the increase in MAPK signaling induced by the addition of TNK2 is dependent on PTPN11. Inhibition of PTPN11 also resulted in increased phosphorylation of TNK2 in a dose-dependent manner, consistent with our hypothesis that PTPN11 activity is responsible for the reduction in TNK2 phosphorylation. Interestingly, levels of phospho-PTPN11 increased concomitantly with the increases in phospho-TNK2, consistent with the model that activated TNK2 phosphorylates PTPN11[18]. Collectively, these data support a feedback mechanism in which TNK2 phosphorylates and activates PTPN11 and is, in turn, deactivated through a PTPN11-dependent dephosphorylation event.

[18] This compound was not effective in the presence of activated PTPN11 (Fig. 2-19).

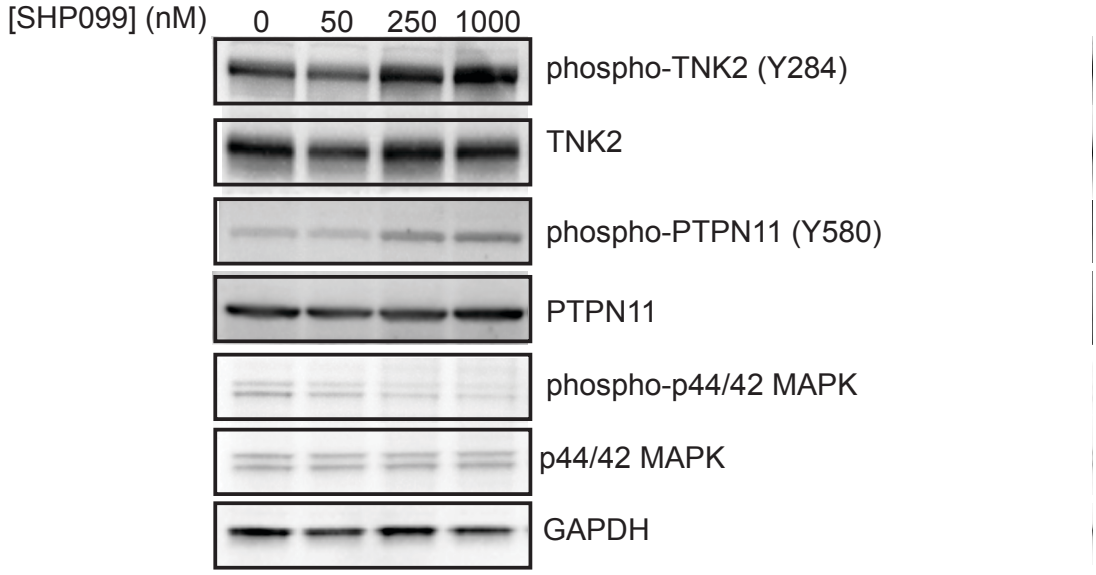

Figure 2-18: Inhibition of PTPN11 in cells co-transfected with PTPN11 WT and TNK2 vectors.

Cells were treated with SHP099 or vehicle control in increasing doses for two hours at 48 hours post-transfection. Lysates were subjected to Western blot. Representative blot of 5 biological replicates.

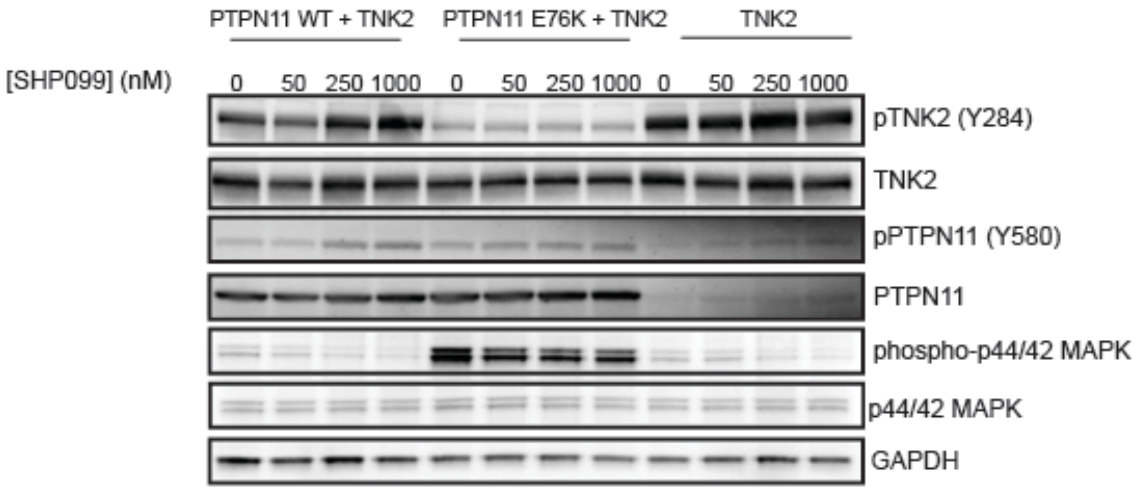

Figure 2-19: Inhibition of PTPN11 in cells co-transfected with PTPN11 WT and TNK2, PTPN11 E76K and TNK2, or TNK2 and empty vector control.

Cells were treated with SHP099 or vehicle control in increasing doses for two hours at 48 hours post-transfection. Lysates were subjected to Western blot. Representative blot of 5 biological replicates.

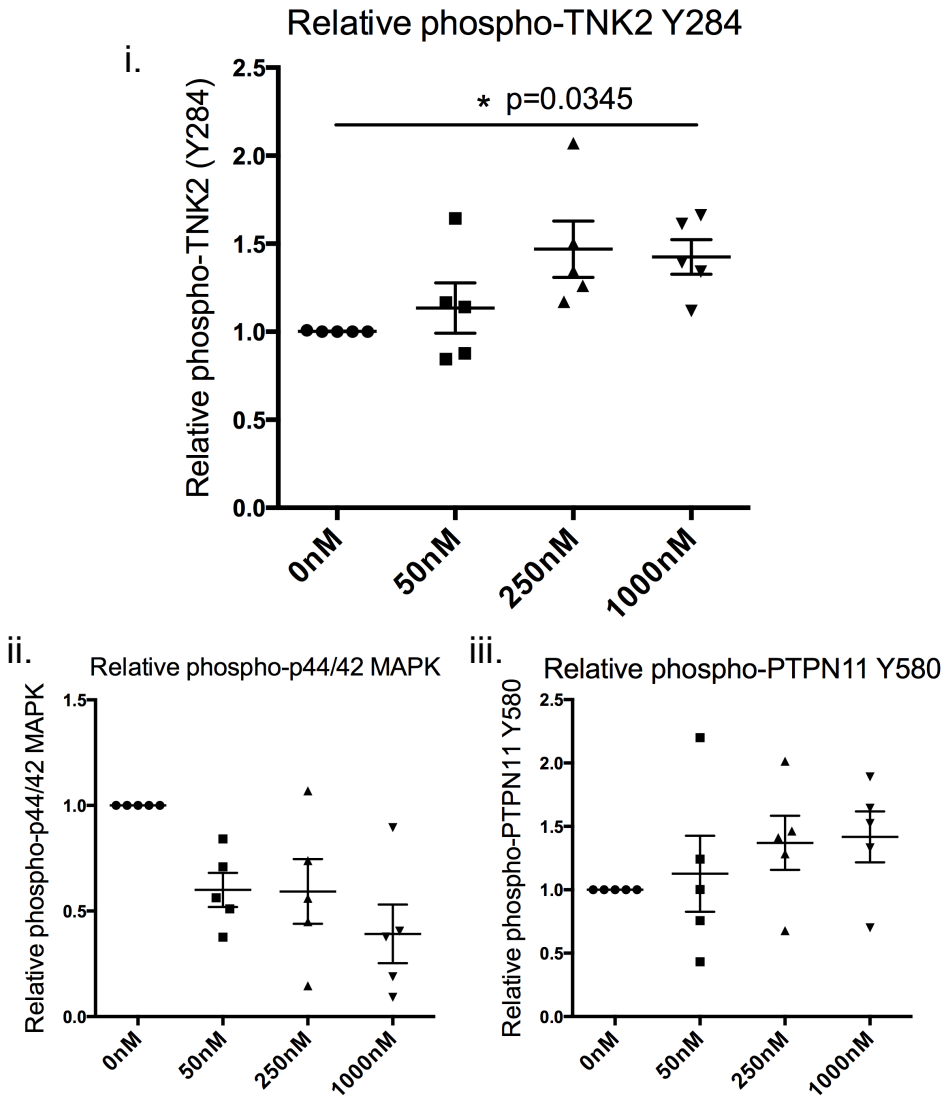

Figure 2-20: PTPN11 inhibition by SHP099 increases phospho-Y284 TNK2 and phospho-Y580 PTPN11.

i. Relative phospho-TNK2 Y284 in 293T17 lysates. 293T17 cells were co-transfected with overexpression constructs containing PTPN11 and TNK2. Cells were treated with 0.05% DMSO vehicle control or increasing concentrations of SHP099 for two hours at 48 hours post-transfection. Lysates were subjected to immunoblot. n=5. ii. Relative phospho-PTPN11 Y580 in 293T17 lysates. iii. Relative phospho-p44/42 MAPK in 293T17 lysates.

2-4: TNK2 is a functional target for PTPN11-mediated transformation

2-4.1: Mutant PTPN11 and TNK2 significantly increase GM-CSF sensitivity in mouse bone marrow colony formation assay and are sensitive to dasatinib treatment.

Increased hypersensitivity of cells to the cytokine GM-CSF in colony formation assays is a hallmark of JMML pathogenesis [32, 97]. Having established that TNK2 co-expression can enhance the signaling activity of mutant PTPN11, we next wanted to determine whether TNK2 can also enhance transformation potential of mutant PTPN11 in a functional assay and whether targeting of TNK2 can mitigate PTPN11-mediated colony formation. Accordingly, unselected mouse bone marrow cells were transduced with mutant-PTPN11 with or without TNK2 co-expression. We observed significantly increased colony formation when mutant PTPN11 and TNK2 were co-expressed compared to mutant-PTPN11 alone, TNK2 alone, or wild-type PTPN11 co-expressed with TNK2 ($p<0.0001$) (Fig. 2-21,22). To test whether PTPN11-mediated colony formation can be successfully targeted with TNK2 inhibitors, we performed mouse bone marrow colony assays expressing two different PTPN11 mutant constructs (E76K and G60R) with endogenous levels of TNK2 and treated cells with graded concentrations of dasatinib. Dasatinib reduced colony formation in a dose-dependent fashion

(Fig. 2-23). We also examined colony reduction by dasatinib and AIM-100 in bone marrow cells co-transduced with PTPN11 E76K and TNK2, and we observed reduced colony formation in the presence of both TNK2 inhibitors, suggesting a reliance on TNK2 for PTPN11 transformation potential (Fig. 2-24). Lack of synergy with the treatment of both drugs suggests that dasatinib and AIM-100 target proteins in the same pathway.

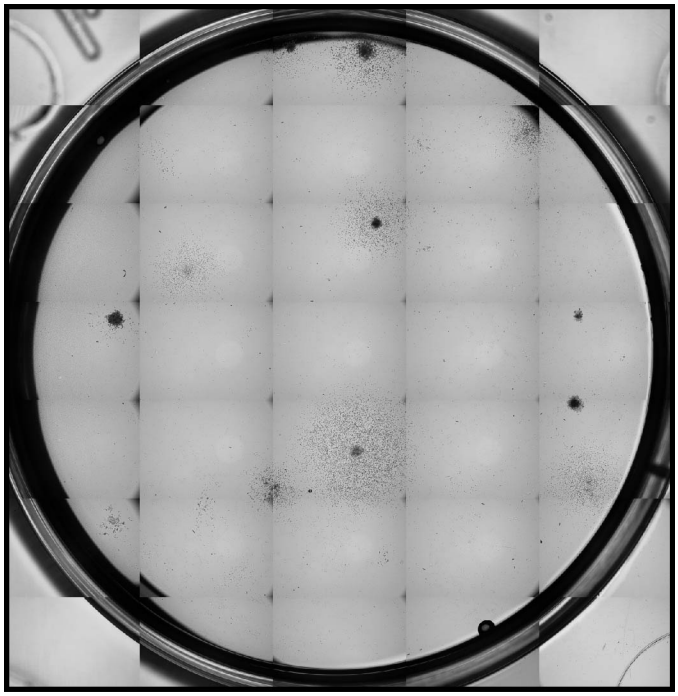

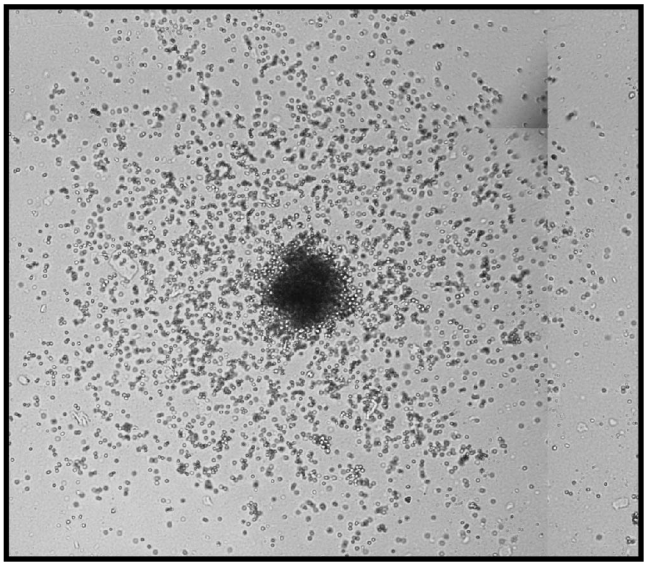

Figure 2-21: Representative colonies from bone marrow colony formation assay. Colonies are GM-CFU, indicating response to GM-CSF.

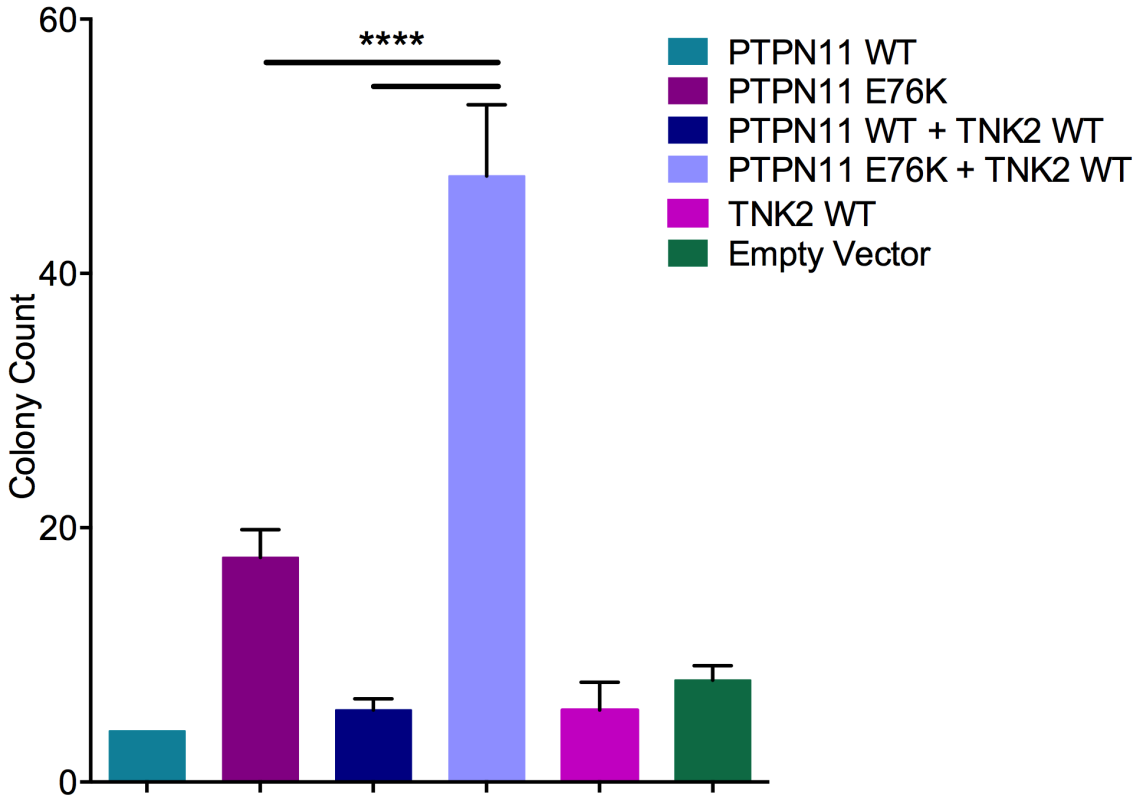

Figure 2-22: Mutant PTPN11 and TNK2 significantly increase GM-CSF sensitivity in mouse bone marrow colony formation assay.

Total colony formation in mouse bone marrow colony formation assay. Mouse bone marrow cells were co-transduced to overexpress PTPN11, PTPN11 E76K, TNK2 or empty vector controls. Cells were selected for GFP+ and puromycin resistance and plated in a methylcellulose GM-CSF sensitivity colony formation assay. Colonies were counted at 14 days [GM-CSF]=0.05nM. (n=3). **** p<0.0001 by one-way ANOVA. Error bars represent SEM.

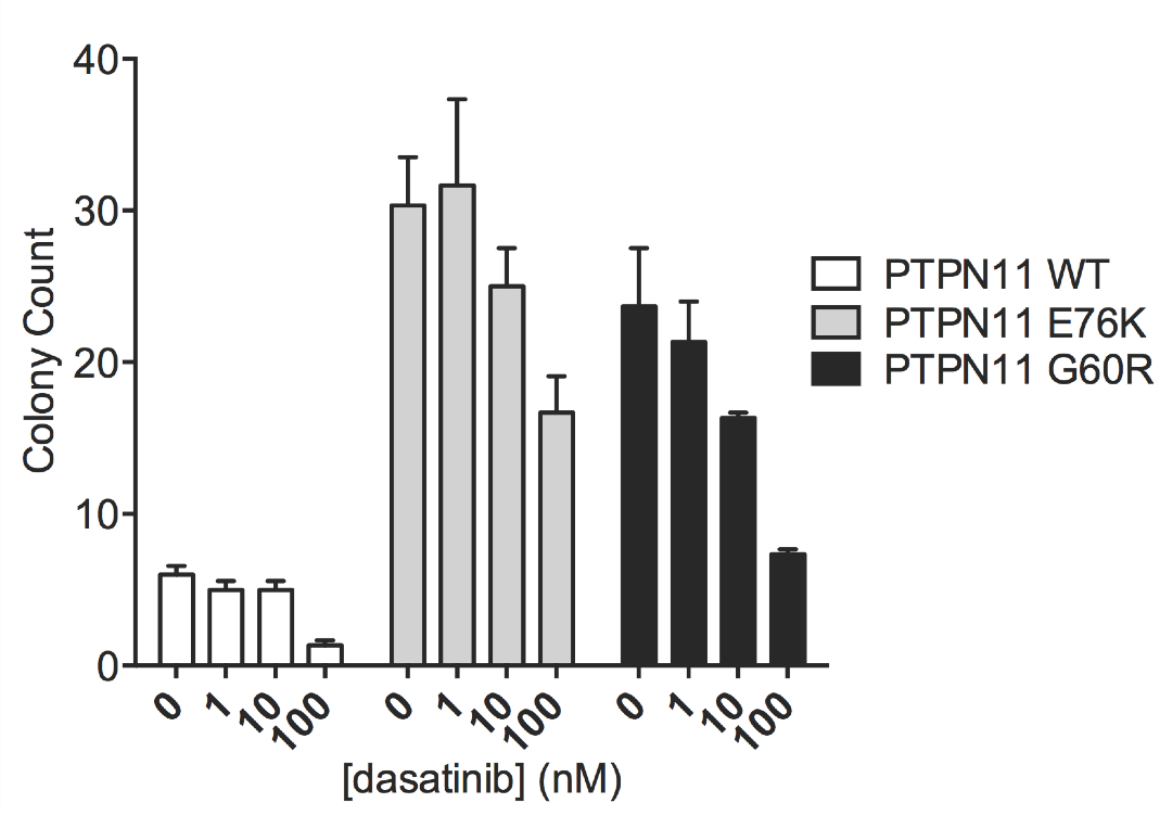

Figure 2-23: Mouse bone marrow cells expressing mutant PTPN11 are sensitive to dasatinib treatment.

Total colony formation in mouse bone marrow colony formation assay in cells transduced with PTPN11, PTPN11 E76K or PTPN11 G60R. Cells were sorted for GFP+. Cells were plated with increasing concentrations of dasatinib. Error bars represent SEM. (n=3).

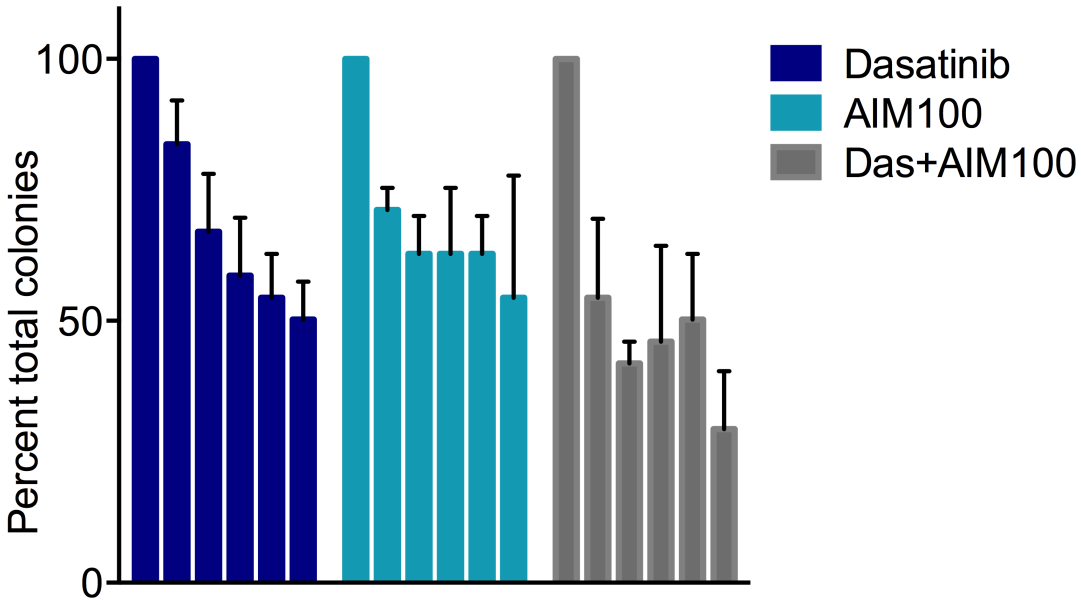

Figure 2-24: Mouse bone marrow cells expressing mutant PTPN11 and TNK2 are sensitive to TNK2 inhibition.

Percent of untreated colony formation for mouse bone marrow cells co-transduced with PTPN11 E76K and TNK2 and treated with dasatinib (0, 10, 50, 100, 500, or 1000nM), AIM100 (0, 10, 50, 100, 500, or 1000nM), or dasatinib (100nM) and AIM100 (0, 10, 50, 100, 500, or 1000nM). Cells were selected for GFP+ and puromycin resistance. (n=6). Error bars represent SEM.

2-4.2: Targeted inhibition of parallel signaling pathways to Ras/MAPK in mouse bone marrow colony formation assays.

To determine the effect of other known pharmacological inhibitors of proliferative signaling pathways in cells transduced with mutant PTPN11 and TNK2, additional mouse bone marrow colony formation assays were conducted (Fig. 2-25). Cells were plated in methylcellulose in the presence of AIM-100, vemurafenib (a Raf inhibitor), dasatinib, SCH77298 (a p44/42 MAPK/ERK inhibitor), selumetinib (a MEK inhibitor), GS1101 (a PI3K inhibitor) and ruxolitinib (a JAK/Stat inhibitor). Only ruxolitinib, a potent inhibitor of the GM-CSF signaling upstream of PTPN11 prevented colony growth more than dasatinib. This suggested to us that the effect we observe is upstream of PTPN11.

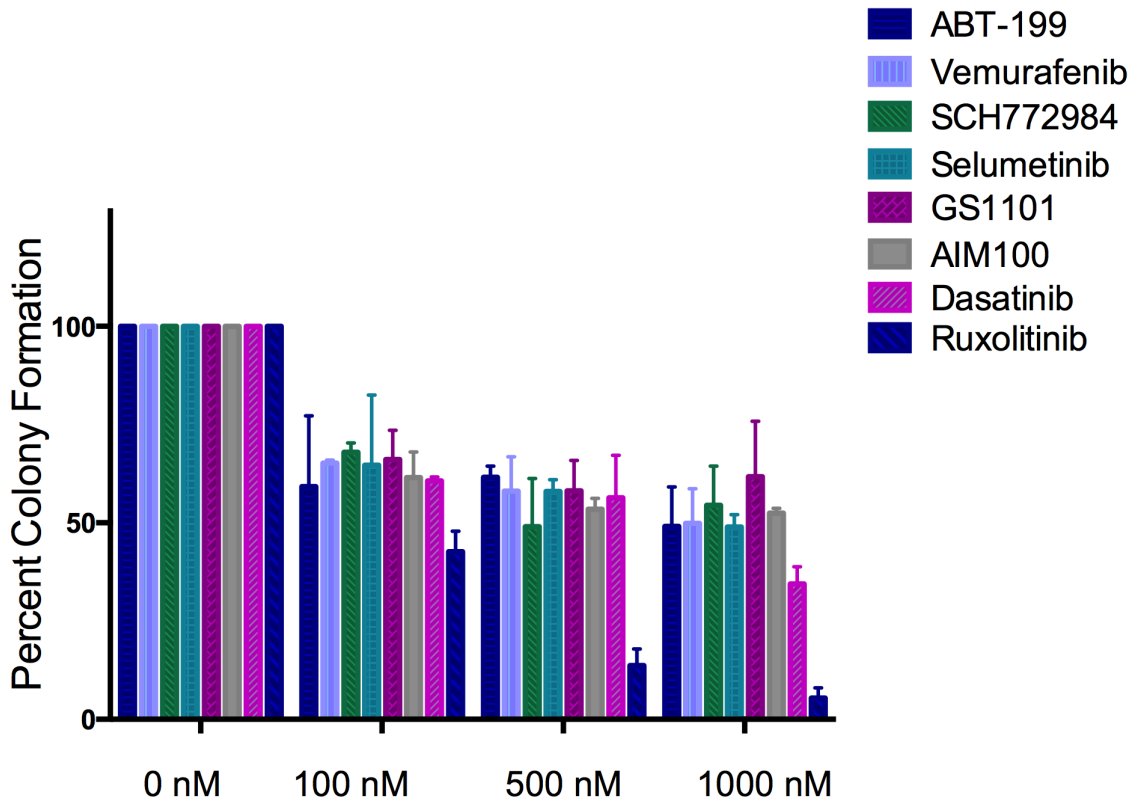

Figure 2-25: Targeted inhibition of alternate signaling pathways to Ras/MAPK in mouse bone marrow colony formation assays.

Percent of untreated colony formation for mouse bone marrow cells co-transduced with PTPN11 E76K and TNK2 and treated with AIM100, vemirafinib, dasatinib, SCH772984, selumetinib, GS1 101, or ruxolitinib (0,10, 50, 100, 500, or 1000 nM). Cells were selected for GFP+ and puromycin resistance. (n=3). Error bars represent SEM.

2-5: PTPN11 mutations confer dasatinib sensitivity in acute myeloid leukemia

2-5.1: AML patient samples harboring PTPN11 mutations display significant sensitivity to dasatinib in an *in vitro* assay.

Because a significant percentage of AML cases also harbor gain-of-function mutations in PTPN11, we examined dasatinib sensitivity profiles in primary AML patient samples that have mutant or wild-type PTPN11. 128 samples from patients diagnosed with AML were assessed for *ex vivo* dasatinib sensitivity and IC_{50} values were calculated, representing drug sensitivity. A comparison of the average IC_{50} value for samples with PTPN11 mutations versus samples with wild-type PTPN11 reveals that the PTPN11-mutant samples are significantly more sensitive to dasatinib than the wild-type samples ($p=0.018$)(Fig. 2-26). To ensure that this relationship is specific to activation of PTPN11, we also assessed the dasatinib sensitivity profiles of KRAS and NRAS-mutant relative to wild-type samples in this same cohort. There was no difference in average dasatinib sensitivity of NRAS mutant versus NRAS wild-type specimens, suggesting dasatinib sensitivity is TNK2-dependent in PTPN11 mutant samples, and does not occur with mutations that occur further downstream in the RAS/MAPK pathway. None of these samples had activating mutations in targets of dasatinb, and none were

positive for BCR-ABL (Table 2-3). To further investigate whether other targets of dasatinib might be responsible for this observed sensitivity, we analyzed RNAseq expression data from a cohort of 356 primary AML patient samples, 10 of which contained PTPN11 mutations (Table 2-4, Fig. 2-32). PTPN11 mutant samples showed no significant increase in mRNA transcripts for any of the 35 top DNA target proteins when compared to PTPN11 WT samples. While mRNA levels are not a strict indicator of protein activity, the lack of mutation or overexpression of other dasatinib targets in these samples supports TNK2 as the key target in these patient samples.

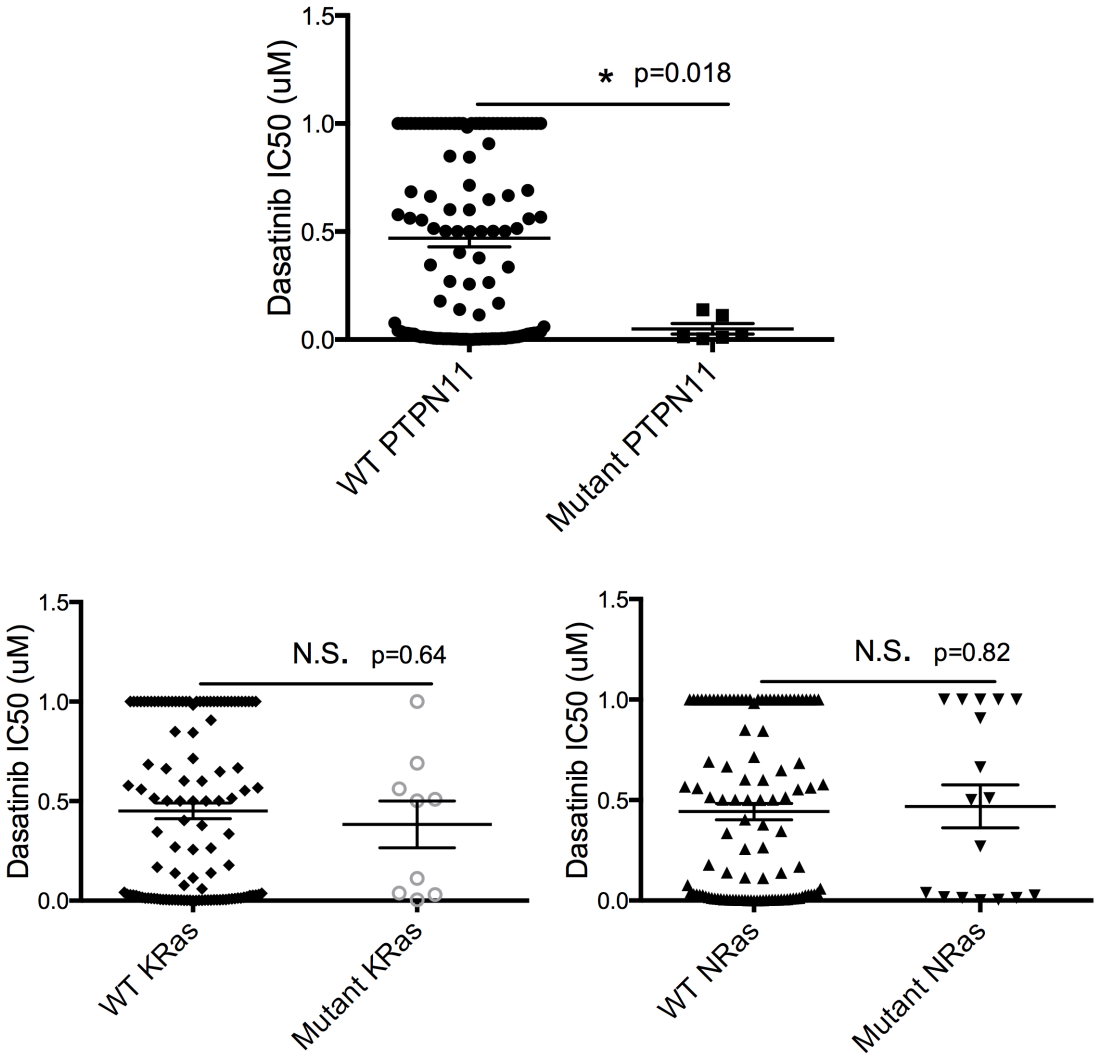

Figure 2-26: AML patient samples harboring PTPN11 mutations display significant sensitivity to dasatinib in an *in vitro* assay.

Mean dasatinib IC_{50} of AML patients by PTPN11, NRAS or KRAS mutation status. If no IC_{50} reached, IC_{50}=1uM. n=128. p-values determined by two-tailed student's t-test.

2-5.2: Signaling effects and dasatinib sensitivity of PTPN11 S502P mimic those seen with other PTPN11 activating mutations.

We identified one AML-specific PTPN11 mutation (S502P) in multiple dasatinib-sensitive patient samples and confirmed its presence by Sanger sequencing (Fig. 2-29). To investigate the transformation potential of this variant, PTPN11 S502P was introduced into 293T17 cells or mouse bone marrow (Fig. 2-27,30). Cell lysates from 293T17 cells expressing PTPN11 S502P showed significant increases in MAPK signaling as well as a reduction of phospho-TNK2 compared with wild-type. Additionally, MAPK signaling was reduced after dasatinib exposure (Fig. 2-28). In mouse bone marrow colony formation assays, we observed that the PTPN11 S502P mutation confers GM-CSF hypersensitivity. This increase in colony formation is reduced in the presence of dasatinib. Collectively, these data suggest that the S502P variant of PTPN11 is phenotypically similar to the variants seen in JMML, consistent with the data from primary samples harboring the S502P mutation.

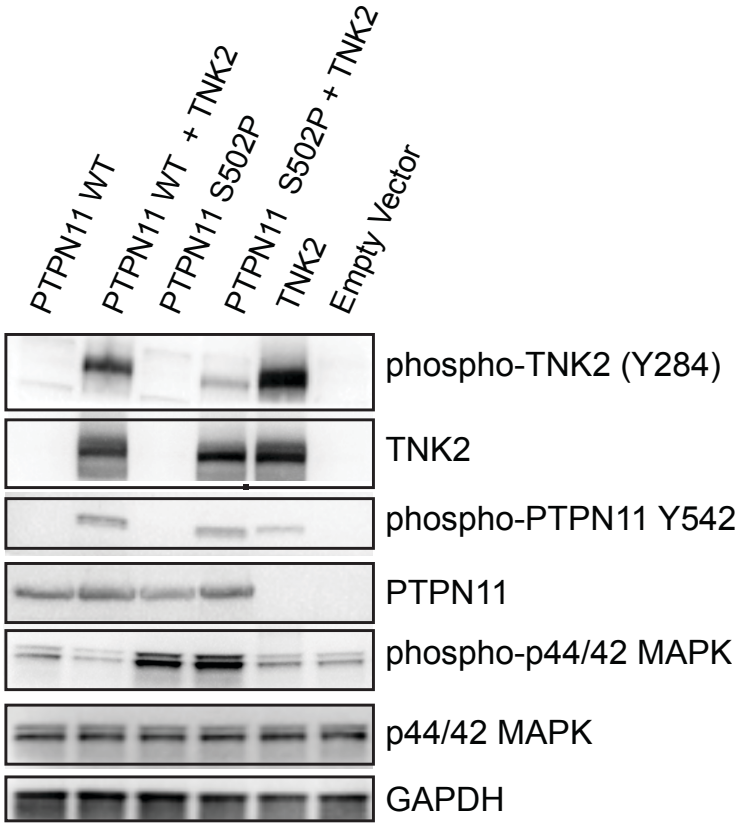

Figure 2-27: Signaling effects of PTPN11 S502P mimic those seen with other PTPN11 activating mutations.

293T17 cells were transiently co-transfected with expression constructs containing PTPN11, PTPN11 S502P, TNK2, or empty vector controls. Lysates were subjected to immunoblot. Representative blot from 5 biological replicates.

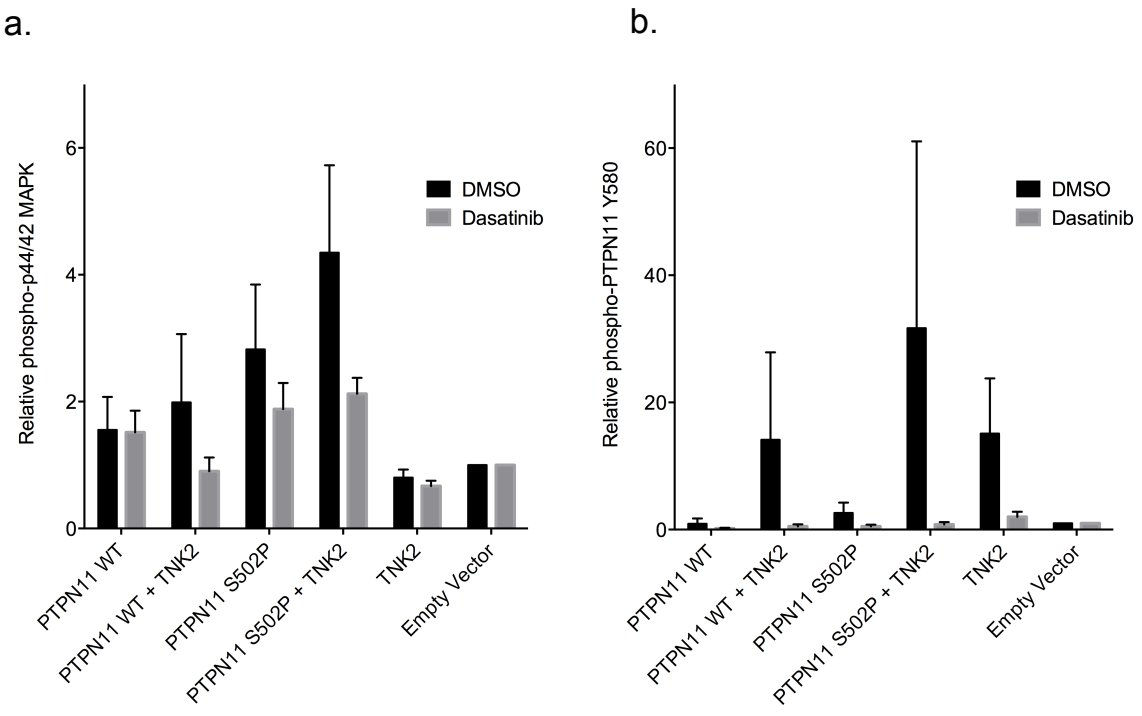

Figure 2-28: PTPN11 mutation from AML patient confers dasatinib sensitivity.

a) Relative phospho-p44/42 MAPK quantification. 293T17 cells were co-transfected with overexpression constructs containing PTPN11, PTPN11 S502P, TNK2, or empty vector controls. Cells were treated with 0.05% DMSO vehicle control or Dasatinib (100nM) for two hours at 48 hours post-transfection. Lysates were subjected to immunoblot. (n=5).

b) Relative phospho-PTPN11 Y580 in 293T17 lysates. (n=5).

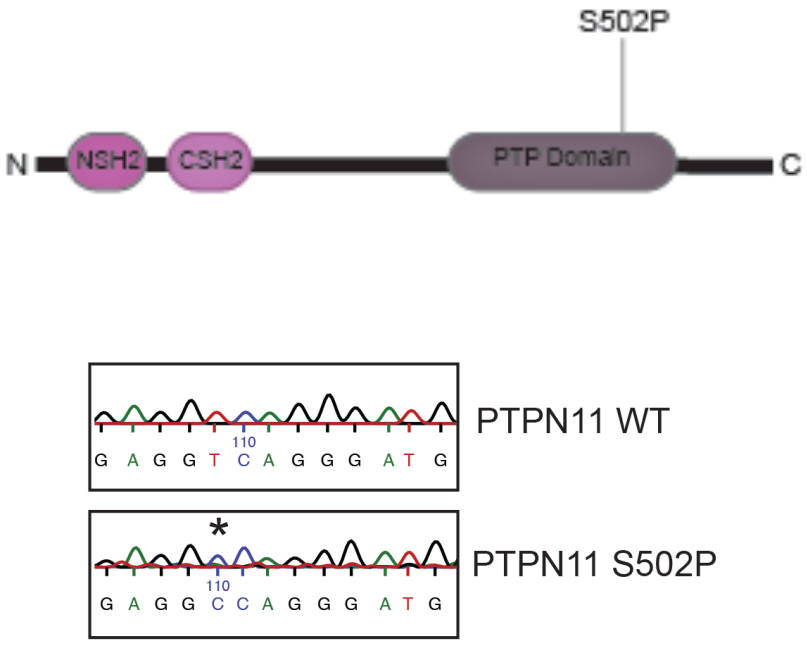

Figure 2-29: Sanger sequencing of AML patient sample PTPN11 S502P mutation.

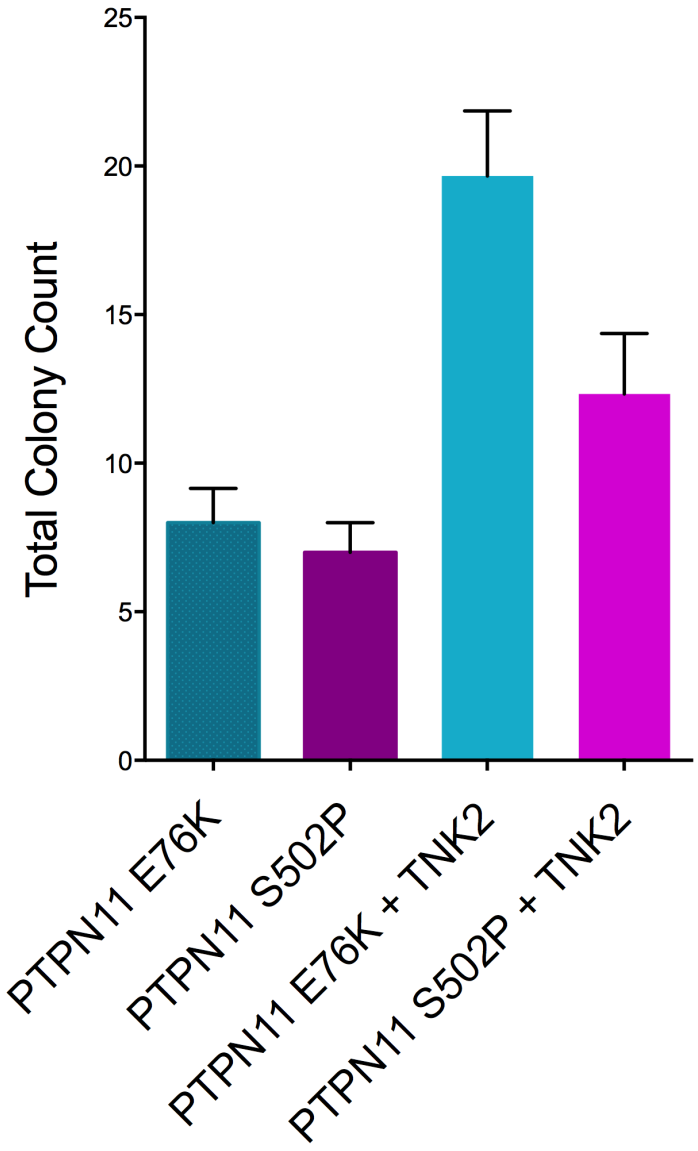

Figure 2-30: PTPN11 S502P increases GM-CSF sensitivity in mouse bone marrow colony formation assay.

Total colony formation in mouse bone marrow colony formation assay. Mouse bone marrow cells were co-transduced to express PTPN11, PTPN11 E76K, PTPN11 S502P, TNK2 or empty vector controls, and plated in a methylcellulose GM-CSF sensitivity colony formation assay. Colonies were counted at 14 days [GM-CSF]=0.05nM. (n=3). Error bars represent SEM.

2-6: Clinical Validation

The leukemia sample used for initial siRNA and drug sensitivity studies (shown in Figures 2-2 and 2-3) was obtained from a 6 year old Caucasian male with JMML with mutant PTNPN11 diagnosed at age 5 who had failed to respond to two matched sibling donor bone marrow transplants using myeloablative conditioning. Since his leukemia cells were sensitive to TNK2 silencing and dasatinib *in vitro* (Fig. 2-2), the family elected to initiate dasatinib therapy at 60mg/m^2/day as an alternative to palliative care under an investigational drug exemption. The patient had a rapid decrease in WBC counts to within normal range (Fig 2-31). One month after starting dasatinib the patient presented with fevers and leukocytosis and was therefore started on mercaptopurine, a chemotherapeutic agent. A repeat marrow at the time showed no overt evidence of disease, but a blood culture at that time grew *Klebsiella bacteria*. After identification of the bacteria and marrow results, mercaptopurine was discontinued. Once treatment for bacteremia was initiated, this patient had a slow resolution of his leukocytosis and his thrombocytopenia improved after mercaptopurine was discontinued. He achieved a sustained hematologic remission in response to dasatinib therapy and was then eligible to receive a third allogeneic stem cell transplant using an unrelated cord blood donor, which afforded an additional year of life. He

eventually died from relapsed disease at age of 7 years. This case study, along with the *ex vivo* data from PTPN11-mutant AML patients provided the rationale for further investigations into the efficacy of dasatinib or other TNK2 inhibitors in PTPN11-mutant leukemias.

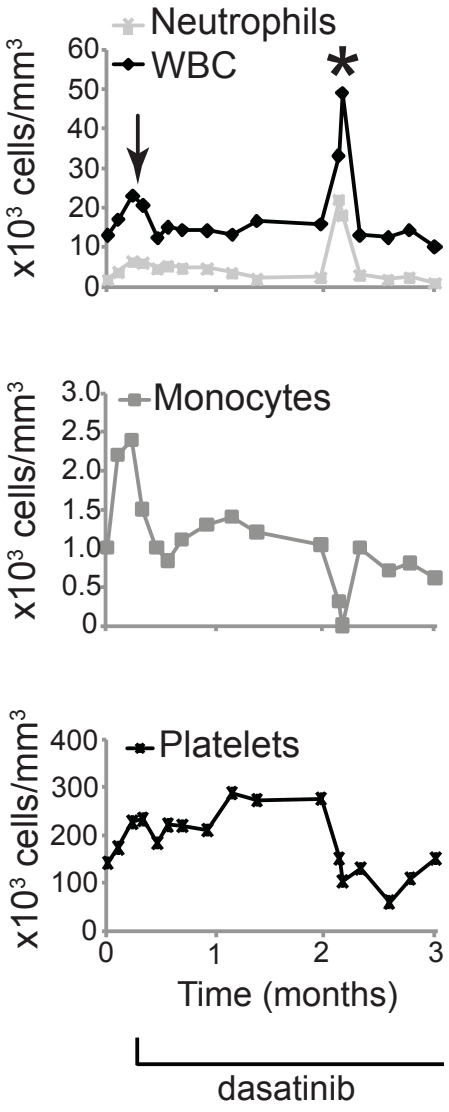

Figure 2-31: Peripheral blood counts for JMML patient at the time of recurrence after second bone marrow transplant.

Dasatinib therapy is shown over a three-month period. The patient was diagnosed with Klebsiella bacteremia (denoted by *), which resolved with antibiotic therapy.

2-7 Supplementary Figures

Table 2-3: Mutations identified in PTPN11-mutant patient samples from figure 2-26.

Sample ID	Mutated Gene	Type	Mutation
1078	DNMT3A	misssense	R882H
1078	NPM1	frameshift	L287LCX
1078	PTPN11	misssense	F285S
1104	ASXL1	frameshift	A619X
1104	FLT3	misssense	D835H
1104	PTPN11	misssense	D61H
1104	TET2	misssense	F1300L
1286	PTPN11	misssense	E76V
1315	ETV6	misssense	L398Q
1315	KRAS	misssense	Q61P
1315	PTPN11	misssense	G503V
1315	U2AF1	misssense	S34F
1438	BCOR	frameshift	S841X
1438	PTPN11	misssense	D61Y
1438	WT1	frameshift	R370X
1532	DNMT3A	misssense	R882C
1532	NPM1	frameshift	L287LCX
1532	PTPN11	misssense	E76Q
1988	KRAS	misssense	G13D
1988	NPM1	frameshift	L287LCX
1988	NRAS	misssense	G13D
1988	PTPN11	misssense	T73I
2295	FLT3	misssense	D835E
2295	IKZF1	misssense	H474Q
2295	PTPN11	misssense	A72V

Table 2-4: Kd values of top dasatinib targets

Adapted from HMS LINCS Project Dasatinib KINOMEscan - Dataset (ID:20196)

https://lincs.hms.harvard.edu/db/datasets/20196/smallmolecules?sort=facility_salt

ABL1(M351T)-phosphorylated	0.02
ABL1(F317L)-nonphosphorylated	0.03
ABL1(H396P)-nonphosphorylated	0.03
ABL1-nonphosphorylated	0.03
ABL1(F317I)-phosphorylated	0.04
ABL1(Q252H)-nonphosphorylated	0.04
EPHB6	0.04
ABL1(E255K)-phosphorylated	0.05
ABL1(H396P)-phosphorylated	0.05
ABL1-phosphorylated	0.05
ABL1(Q252H)-phosphorylated	0.06
ABL1(Y253F)-phosphorylated	0.06
EPHA3	0.09
ABL1(F317I)-nonphosphorylated	0.1
ABL2	0.17
LCK	0.2
BLK	0.21
SRC	0.21
EPHA5	0.24
EPHA8	0.24
YES	0.3
FRK	0.31
EPHB4	0.34
HCK	0.35
EPHB2	0.39
EPHB1	0.45
PGFRA	0.47
FGR	0.5
KIT(L576P)	0.57
LYN	0.57
CSF1R	0.58
PGFRB	0.63
KIT(A829P)	0.66
KIT(V559D)	0.68
DDR1	0.69
FYN	0.79
KIT	0.81
EPHA2	0.85
CSK	1
EPHA4	1.2
BMX	1.4
BTK	1.4
KIT(D816H)	1.6
TXK	2.1
GAK	2.6
KIT(D816V)	2.6
KIT(V559D,V654A)	2.7
DDR2	3.2
MP2K5	3.3
SIK1	3.9
EPHA1	4.1
TNK2	5.6

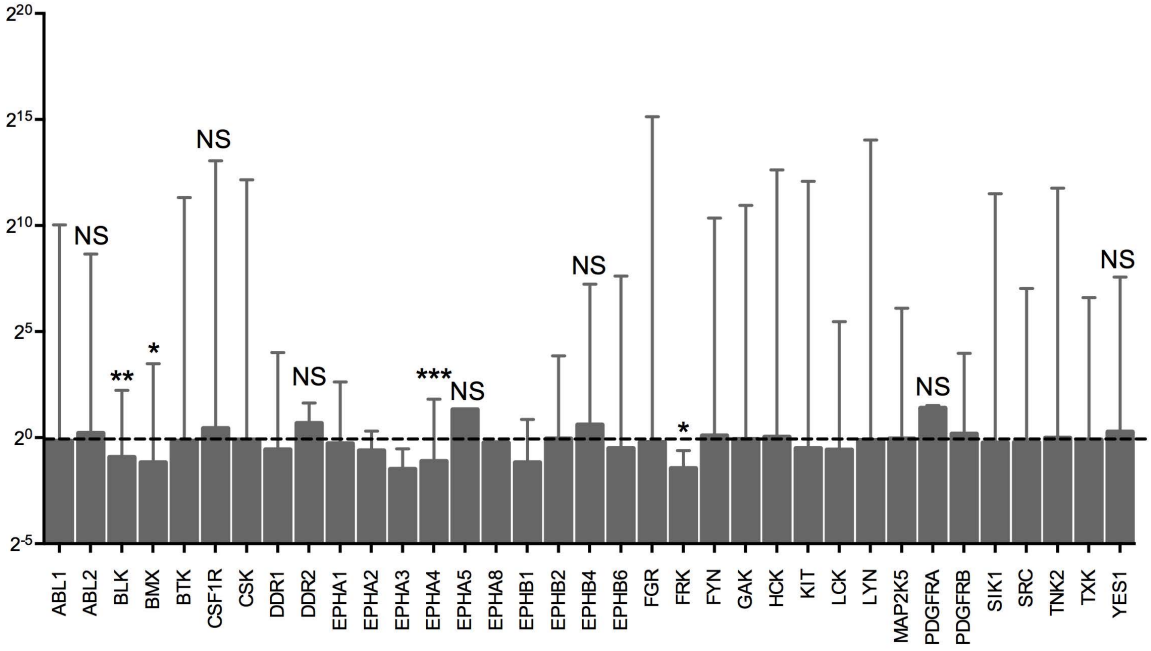

Figure 2-32: Relative mRNA expression of dasatinib targets in AML patient samples from figure 2-26.

n=356. Values represent mean of the RNA counts per million for PTPN11 mutant samples (n=10)/mean of the RNA counts per million for PTPN11 WT samples (n=346). Error bars represent SEM of the quotient. Student's two-tailed T-test with Welch's correction was used to calculate p-values for each gene's difference of means.

Table 2-5: Targets of inhibitors from Table 2-2.

Inhibitor	Other name	Target	Pathway
ABT-869	Linifanib	VEGFR/PDGFR/KDR/CSF1R/Flt-1/3	Tyrosine Kinase
AG490	tryphostin	JAK2	JAK/STAT
AKT IV		AKT	PI3K/Akt/mTOR
AKT X		AKT	PI3K/Akt/mTOR
AMG-706	Motesanib Diphosphate	VEGFR1,2,3/PDGFR/cKIT/RET	Tyrosine Kinase
AMPK		AMPK/KDR/VEGFR2/ALK2/BMPR1	Tyrosine Kinase
AP24534	Ponatinib	BCR/ABL T315I /FLT3/RET/KIT/FGFR/PDGFR/SRC	Tyrosine Kinase
AST-487		RET kinase	Tyrosine Kinase
AZD-1152	Barasertib	Aurora B	JAK/STAT
BIRB-796	Doramapimod	p38a MAPK	MAPK
BMS-387032	SNS-032	CDK2	Cell cycle
CAL-101/GS-1101	Idelalisib	PI3K	PI3K/Akt/mTOR
CHIR-258	Dovitinib	FLT3/c-KIT/FGFR1/FGFR3/VEGFR1,2,3,/PDGFR/CSF1R	Tyrosine Kinase
CHIR-265		B-RAF/VEGFR	Tyrosine Kinase
CI-1033	Canertinib	EGFR/ERB2	Tyrosine Kinase
CP-690550	Tofacitinib	JAK	JAK/STAT
CYC-202	Seliciclib/Roscovitine	cdc2/cdk2,5/cyclin	Cell cycle
Cytopia	Cyt387	JAK1/JAK2	JAK/STAT
Dasatinib	Sprycel	BCR/ABL, SRC, c-Kit	Tyrosine Kinase
EKB-569	Pelitinib	ERB1,2,4	Tyrosine Kinase
Erlotinib	Tarceva	EGFR/JAK2V617F	Tyrosine Kinase
Flavopiridol	Alvocidib	cdk1,2,4,6	Cell cycle
Gefitinib	Iressa	EGFR	Tyrosine Kinase
Go6976		PKC	Tyrosine Kinase
GW-2580		CSFiR	Tyrosine Kinase
GW-786034	Pazopanib	VEGFR	Tyrosine Kinase
H-89		PKA	Tyrosine Kinase
Imatinib	Gleevec	BCR/ABL, KIT	Tyrosine Kinase
JAK3		JAK3	JAK/STAT
JNJ-7706621		CDK1,2/cyclin, AuroraA and B	Epigenetic modifier
JNK II		c-JUN	Tyrosine Kinase
KN92		CAMKII	Calmodulin-dependent kinase
KN93		CAMKII	Calmodulin-dependent kinase
Lapatinib	Tykerb	ERB2/EGFR	Tyrosine Kinase
LY-333531	Ruboxistaurin	PKCB	Tyrosine Kinase
LY294002		PI3K	PI3K/Akt/mTOR
MEK1/2		MEK1/2	MAPK
MLN-518	Tandutinib	FLT3, PDGFRB, KIT	Tyrosine Kinase
MLN-8054		Aurora A	Epigenetic modifier
NF-kB Activ Inhib	QNZ, EVP 4593	NF-kB	Apoptosis
Nilotinib	tasigna	BCR-ABL/KIT/LCK/EPHA/DDR	Tyrosine Kinase
p38		p38	MAPK
PD153035		EGFR	Tyrosine Kinase
PD98059		MEK1/2	MAPK
PI-103		P13K	PI3K/Akt/mTOR
PKC-412	Midostaurin	PKC/Syk/Akt/PKA/c-Kit/…	Tyrosine Kinase
PP2		Src family, LCK, FYN, HCK	Angiogenesis
PTK-787	Vatalanib	VEGFR, KIT, PDGFR	Tyrosine Kinase
SB-202190		MAPK	MAPK
SB-203580		MAPK	MAPK
SB-431542		ALK5	TGFb-SMAD
Sorafenib	Nexavar	VEGFR2, PDGFR, RAF1, B-RAF	Tyrosine Kinase
SRC		Src	MAPK
Staurosporine	AM-2282	PKC, wide range of targets	Tyrosine Kinase
STO609		CAMKK	Calmodulin-dependent kinase
Sunitinib Malate	Sutent, SU11248	PDGFR, VEGFR2, KIT, RET, CSF1R, FLT3	Tyrosine Kinase
SYK		SYK kinase	Tyrosine Kinase
VX-680	Tozasertib	pan-Aurora	Epigenetic modifier
VX-745		p38a MAPK	MAPK
XAV-939		TNKS1, 2 (wnt b-catenin pathway)	Wnt pathway
XL-880	Foretinib	MET, VEGFR2,KDR	Tyrosine Kinase
XL184	Cabozantinib	MET and VEGFR2	Tyrosine Kinase
ZD-6474	Vandetanib, Caprelsa	VEGFR2, EGFR, RET	Tyrosine Kinase

Chapter 3 : Materials and Methods

3-1: Patient Samples

All clinical specimens were collected with informed consent on a protocol approved by the Oregon Health & Science University Institutional Review Board.

3-2: siRNA and kinase inhibitor assays

The siRNA and small-molecule inhibitor screening of patient samples was conducted as previously described [96, 103]: Blood or bone marrow from patients was separated on a Ficoll gradient and mononuclear cells were treated with ammonium-chloride-potassium (ACK) lysis buffer. Cells were cultured in R10 [RPMI-1640 medium supplemented with 10% FBS (Atlanta Biologicals), L-glutamine, penicillin/streptomycin (Invitrogen), and fungizone (Invitrogen)] supplemented with 10^{-4}M 2-mercaptoethanol (Sigma).

Kinase inhibitors were stored at 10 to 100 mmol/L in dimethyl sulfoxide (DMSO; stock concentration was 1,000 times the final concentration of the highest tested dose). For creation of replicate plates of the library, each drug

concentration was diluted to twice the final concentration and 50 µL were plated into 96-well plates using a Hydra 96-channel automated pipettor (Matrix Technologies). Plates were sealed with adhesive lids (Bio-Rad; microplate seal B), wrapped in aluminum foil, and stored at −20°C until use. Upon receipt of a patient sample, plates were thawed at 37°C, 5% CO_2 for 1 hour and centrifuged at 800 × *g* before removal of adhesive lids. Subsequently, patient samples were suspended into culture media at a concentration of 1,000,000 cells per mL, such that addition of 50 µL to each well would deliver 50,000 cells to that well (this also dilutes the drugs to their final, desired concentration). Cells were incubated for 3 days at 37°C, 5% CO_2 and subjected to a CellTiter 96 AQueous one solution cell proliferation assay (MTS) (Promega). Each plate contained 7 wells without any drug. The average absorbance value of these 7 wells was used for data normalization and the kill curve of each drug gradient was assessed relative to this average no-drug point.

Patient blood or bone marrow was prepared as above and 2.25 x 10^7 cells were resuspended in 4.2 mL of siPORT buffer (Ambion). Cells were aliquoted at 42 uL per well onto a 96-well electroporator (Ambion), and 2 uL of siRNA at 20 uM was added to each well [tyrosine kinase library (Dharmacon) with single and pooled nonspecific siRNA, as well as siRNA against EPHA5,

EPHA6, SRC-related kinase lacking C-terminal regulatory tyrosine and N-terminal myristylation (SRMS), apoptosisassociated tyrosine kinase (AATK), LMTK3, N-RAS, K-RAS (all from Dharmacon) added separately]. Cells were electroporated at 1110 V (equivalent of 150 V per well), 200 us, 2 pulses, and 50,000 cells per well were replated into triplicate plates containing 100 uL per well of culture media. For determination of cell viability, cells were subjected to the CellTiter 96 AQueous one solution cell proliferation assay (MTS) (Promega). All values were normalized to the median plate value.

3-3: Sequencing of Patient Samples

Peripheral blood and bone marrow samples from patients with JMML or AML were processed by Ficoll gradient centrifugation followed by red blood cell lysis. Cell pellets for subsequent genomic analysis were snap frozen in liquid nitrogen. DNA was extracted using Qiagen DNeasy kits performed according to manufacturer protocols. For exome sequencing, we used Illumina Nextera capture probes and protocol with libraries run on a HiSeq 2500 using paired end 100 cycle protocols. Initial data processing and alignments were performed using our in-house workflows that we describe here briefly. For each flowcell and each sample, the FASTQ files were aggregated into single files for read 1 and 2. BWA MEM version 0.7.10-

r789[104] was used to align the read pairs for each sample-lane FASTQ file. As part of this process, the flowcell and lane information was kept as part of the read group of the resulting SAM file. The Genome Analysis Toolkit (v3.3) and the bundled Picard (v1.120.1579) were used[105] for alignment post-processing. The files contained within the Broad Institute's bundle 2.8 were used including their version of the build 37 human genome. The following steps were performed per sample-lane SAM file: (1) Sorting and conversion to BAM via SortSam; (2) MarkDuplicates was run, marking both lane level standard and optical duplicates; (3) Read realignment around indels from the reads–RealignerTargetCreator/IndelRealigner; (4) Base Quality Score Recalibration. The resulting BAM files were then aggregated by sample and an additional round of MarkDuplicates was carried out at the sample level. For genotyping, each AML sample BAM was realigned at the sample level and then genotyped for single nucleotide variations using Mutect v1.1.7[106] and Varscan2 v2.4.1[107]. Additionally, indels were produced using Varscan2. Each VCF file was annotated using the Variant Effect Predictor v83 against GRCh37[108]. The resulting VCF files were filtered to include only those annotated to a gene and converted to MAF format using the vcf2maf v1.6.6 tool[109] and converted to MAF format. Data was flltered to include patient samples for which dasatnib IC50 and PTPN11 mutation

status was known. The full results of this exome sequencing cohort are being prepared in a separate manuscript.

For RNA-Seq, libraries were constructed using the SureSelect stranded RNA-seq protocol (Agilent) on the Bravo robot (Agilent). Briefly, poly(A)+ RNA is chemically fragmented. Double stranded cDNAs are synthesized using random hexamer priming with 3' ends of the cDNA adenylated then indexed adaptors ligated. Library amplification is performed using three-primer PCR using a uracil DNA glycosylase addition for strandedness. Libraries are validated with the Bioanalyzer (Agilent) and combined to run 4 samples per lane, with a targeted yield of 200 million clusters. Combined libraries are denatured, clustered with the cBot (Illumina), and sequenced on the HiSeq 2500 using a 100 cycle paired end protocol. For each sample, FASTQ files are aggregated into single files for read 1 and 2. Alignment is performed using Subjunc aligner(1.4.6)[110]. SAM files obtained from Subjunc are used as inputs into featureCounts(1.4.6)[111] and reads summarization are performed.

3-4: Plasmid construction

TNK2 transcript variant 1 in pDONR was purchased from Genecopoeia (GC-Y4392). Gene mutations were made using the QuikChange II XL site-directed mutagenesis Kit (Agilent Technologies) and primers designed using Agilent Technologies primer design tool (http://www.genomics.agilent.com/primerDesignProgram.jsp) (Table 3-1, 3-2).

Table 3-1: PTPN11 mutagenesis primers

Primer Name	Primer Sequence
PTPN11 N58K F	5'-acccacatcaagattcagaagactggtgattactatgac-3'
PTPN11 N58K R	5'-gtcatagtaatcaccagtcttctgaatcttgatgtgggt-3'
PTPN11 G60R F	5'-cacatcaagattcagaacactcgtgattactatgacctgtatg-3'
PTPN11 G60R R	5'-catacaggtcatagtaatcacgagtgttctgaatcttgatgtg-3'
PTPN11 E76K F	5'-gagaaatttgccactttggctaagttggtccagtattac-3'
PTPN11 E76K R	5'-gtaatactggaccaacttagccaaagtggcaaatttctc-3'
PTPN11 D106Y F	5'-atcctctgaactgtgcatatcctacctctgaaagg-3'
PTPN11 D106Y R	5'-cctttcagaggtaggatatgcacagttcagaggat-3'
PTPN11 G503V F	5'-cctttcagaggtaggatatgcacagttcagaggat-3'
PTPN11 G503V R	5'-tctgtctggaccatcactgacctctgagacc-3'
PTPN11 Y542D F	5'-agcagaaaagcaagaggaaagggcacgaagagacaaatattaagtattctc-3'
PTPN11 Y542D R	5'-gagaatacttaatatttgtctcttcgtgccctttcctcttgcttttctgct-3'
PTPN11 Y542E F	5'-aagcaagaggaaagggcacgaagatacaaatattaagtattctcta-3'
PTPN11 Y542E R	5'-tagagaatacttaatatttgtatcttcgtgccctttcctcttgctt-3'
PTPN11 Y580D F	5'-gaagacagtgctagagtcgaggaaaacgtgggcctgatg-3'
PTPN11 Y580D R	5'-catcaggcccacgttttcctcgactctagcactgtcttc-3'
PTPN11 Y580E F	5'-aagacagtgctagagtcgatgaaaacgtgggcctg-3'
PTPN11 Y580E R	5'-caggcccacgttttcatcgactctagcactgtctt-3'

Table 3-2: TNK2 mutagenesis primers

Primer Name	Primer Sequence
TNK2 T205I F	5'-ccgcccatgaagatggtgatagagctggca-3'
TNK2 T205I R	5'-tgccagctctatcaccatcttcatgggcgg-3'
TNK2 D163E	5'-gcctgaagcccgaggtcctgagccagc-3'
TNK2 D163E	5'-gctggctcaggacctcgggcttcaggc-3'
TNK2 Y284F F	5'-ctacctcagaatgacgaccatttcgtcatgcagga-3'
TNK2 Y284F R	5'-tcctgcatgacgaaatggtcgtcattctgaggtag-3'
TNK2 Y518F F	5'-ggaggggtgaaaaaaccaacctttgaccctgtgag-3'
TNK2 Y518F R	5'-ctcacagggtcaaaggttggtttttcacccctcc-3'
TNK2 Y859F F	5'-cagcagcacccacttttacttgctgcccg-3'
TNK2 Y859F R	5'-cgggcagcaagtaaaagtgggtgctgctg-3'

Wild-type and mutated TNK2 were transferred into a Gateway-converted version of pMXs-IRES-Puro (Cell Biolabs, Inc.), pcDNA™3.2® (Invitrogen), or MSCV-IRES-GFP using a Gateway LR Clonase kit (Invitrogen). Plasmid sequencing was confirmed via Sanger Sequencing (Eurofins).

PTPN11 transcript variant 1 in pDONR was purchased from Genecopoeia (A0360). Gene mutations were made using the QuikChange II XL site-directed mutagenesis Kit (Agilent Technologies) and primers designed using Agilent Technologies primer design tool. Wild-type and mutated PTPN11 were transferred into a Gateway-converted version of p3X-CMV-FLAG14, MSCV-IRES-GFP, or pcDNA™3.2® (Invitrogen), or using a Gateway LR Clonase kit (Invitrogen). Plasmid sequencing was confirmed via Sanger Sequencing (Eurofins).

3-5: Cell culture, transfection, and retroviral production

The human embryonic kidney 293T17 cell line (ATCC) was grown in DMEM (Invitrogen) medium with 10% FBS (Atlanta Biologicals), L-glutamine, penicillin/streptomycin (Invitrogen) and amphotericin B (Hyclone). Murine retrovirus was created by cotransfecting TNK2 or PTPN11 plasmids and the EcoPac plasmid (provided by Dr. Richard Van Etten, U.C. Irvine) into 293T17 using FuGENE 6 (ProMega). Supernatants were harvested 72 hours later.

3-6: Inhibitor assays

293T17 cells were transfected or co-transfected using FuGENE 6 (promega) and cultured for 48 hours. Inhibitors: dasatinib (SellekChem), AIM-100 (CalBiochem; [84]), SHP099 (DC Chemicals), were diluted in DMEM to attain a final concentration in a 6-well plate at 1/2000 dilution. After the treatment period, media was aspirated, and lysates were collected as for immunoblot assays. Lysates were subjected to immunoblot.

3-7: Colony formation assays

Bone marrow was harvested from Balb/C (6-9 weeks old) mice by flushing the femur and tibia with medium. Cells were cultured at 5×10^5 per mL with viral supernatant, polybrene (American Bioanalyticals) and HEPES (4-(2-hydroxyethyl)-1-piperazineethanesulfonic acid) buffer by centrifugation at 2500rpm at 30C for 90 min, then placed back at 37°°C. After 24 hours, the medium was replaced with fresh retroviral "cocktail" and cells were centrifuged as above, then placed back at 37 °C for additional 24 hours. Next, cells were analyzed for GFP expression by FACS.

GFP^+ cells were then sorted and plated in triplicate L into M3234 methylcellulose (StemCell Technologies) supplemented with 50 ng/mL mSCF,

10 ng/mL mIL-3, and mIL-6 (Peprotech). Cells were enumerated at day 14 using the STEMVision colony counter (STEMCELL Technologies) with blinded manual counting to ensure accuracy. Mouse work was done in accordance with OHSU IACUC protocol IS00002358.

3-8: Co-Immunoprecipitation assays

Proteins were immunoprecipitated from cell lysates by incubation with rabbit anti-ACK1 09-142 (Millipore) or anti-IgG isotype control overnight at 4 °C on a rotator. Lysates were then incubated with protein G agarose beads (Millipore) for 1 hour at 4 °C on a rotator. FLAG-tagged proteins were incubated with antiFLAG M2 affinity gel (Sigma-Aldrich) overnight at 4 °C on a rotator. Beads or affinity gel were washed 3 times using cell lysis buffer (Cell Signaling Technologies) with added complete mini protease inhibitor tablets (Roche), phenylmethylsulfonyl fluoride, and Phosphatase Inhibitor Cocktail 2 (Sigma Aldrich). Proteins were disassociated from beads using SDS loading buffer for 5 min at room temperature and then subjected to immunoblotting analysis.

3-9: Immunoblotting

Transfected 293T17 lysates were spun at 8,000rpm for 10 minutes at 4°C to pellet cell debris, mixed 2:1 with 3X GS sample buffer (75mmol/L Tris (pH 6.8), 3% sodium dodecyl sulfate, 15% glycerol, 8% b-mercaptoethanol, and 0.1% bromophenol blue) and heated at 95°C for 5 minutes. Lysates were run on criterion 4% to 15% Tris-HCL gradient gels (BioRad), transferred to polyvinylidene difluoride membrane, and blocked for 30 minutes in TBS-T (Tris-buffered saline with Tween20) with 5% BSA. Blots were probed overnight at 4°C with the following antibodies: rabbit anti-ACK1 A-11 (Santa Cruz), rabbit anti-SHP2 (CST 3572), rabbit anti-phospho-ACK1 (Millipore), rabbit anti-p44/42 MAPK (Erk 1/2) (CST 9102) rabbit phospho-p44/42 MAPK (Erk1/2) (Thr202/Tyr204) (CST 9101), mouse anti-GAPDH 6C5 (Ambion, AM4300), rabbit anti-MEK 1/2 (CST 9122), rabbit anti-phospho-MEK Ser217/221 (CST 9121), rabbit anti-phospho-STAT5 (Y694) (CST 9351), mouse anti-STAT5 (BD 610192). Primary antibody was followed by anti-rabbit or anti-mouse IgG HRP conjugated secondary antibodies. Blots were developed using Clarity chemiluminescent substrate (BioRad) and imaged using a BioRad ChemiDoc MP imaging system.

Quantification of relative protein values was calculated as follows: Total and phospho-protein levels were analyzed using BioRad ImageLab software. Each of these values was normalized to GAPDH protein levels for each membrane to control for loading effects. We then normalized each normalized phospho-protein value to the normalized total protein value to get a relative phospho-protein value.

3-10: In vitro TNK2 kinase assay

293T17 cells were transfected with overexpression vectors for TNK2, TNK2 mutant, or empty vector control, lysates were collected using assay-specific lysis buffer at 48 hours. TNK2 was immunoprecipitated using rabbit anti-ACK1 A-11 (Santa Cruz). The *in vitro* kinase activity of TNK2 mutants was measured using a non-radioactive isotope solid-phase enzyme-linked immunosorbent assay using the Universal Tyrosine Kinase Assay kit (Takara, clontech) according to the manufacturer's suggested protocol.

3-11: Statistical analysis

Mean values ± SEM are shown unless otherwise stated. One-way ANOVA or two-tailed student's T-test were used for comparisons. Welch's T-test was used in cases where population variances were not equal as described in each figure legend. Statistical analysis was conducted using GraphPad Prism Version 6.0. Sample sizes are consistent with those reported in similar studies and provide sufficient power to detect changes with the appropriate statistical analysis.

Chapter 4 : Summary and Discussion

4-1: Summary

Aberrant cell signaling events can lead to uncontrolled cell proliferation and survival, leading to malignancy. In some types of leukemia, a mutated, constitutively active tyrosine phosphatase, PTPN11, increases cell signaling through the Ras/MAPK proliferative pathway. Our lab identified a PTPN11-mutant leukemia patient whose cells were sensitive to siRNA-mediated knockdown of the kinase TNK2 and to the tyrosine kinase inhibitor dasatinib. Additionally, AML patient samples with PTPN11 mutations were significantly more sensitive to dasatinib than those with wild-type PTPN11 as determined by our functional assays. This difference was not observed in samples with mutant versus wild-type K-Ras or mutant versus wild-type N-Ras.

These studies are the first to identify TNK2 as the target of dasatinib in PTPN11-mutant leukemias. Current literature suggests a link between mutant PTPN11 and dasatinib sensitivity, but the molecular mechanisms underlying this sensitivity have not been described. The central hypothesis of

my work has been that TNK2 is necessary for PTPN11-mutant leukemia survival.

This dissertation describes a novel interaction between PTPN11 and TNK2. My research identified that TNK2 and PTPN11 interact with one another, with a TNK2-dependent activation of PTPN11. TNK2's activating effect synergizes with activating PTPN11 mutations, significantly increasing Ras/MAPK signaling and transformation potential as measured by mouse bone marrow colony formation assays. Both of these effects are nullified in the presence of dasatinib or the TNK2-specific inhibitor AIM-100.

Interestingly, TNK2 phosphorylation is reduced in a PTPN11-dependent manner, suggesting a negative feedback mechanism between PTPN11 and TNK2. These data has led us to develop a model to explain the interaction between PTPN11 and TNK2 (Fig. 4-1). This novel interaction between PTPN11 and TNK2 could explain the sensitivity of PTPN11-mutant patient samples to dasatinib, and could lead to promising new therapies for patients with PTPN11-dependent leukemias.

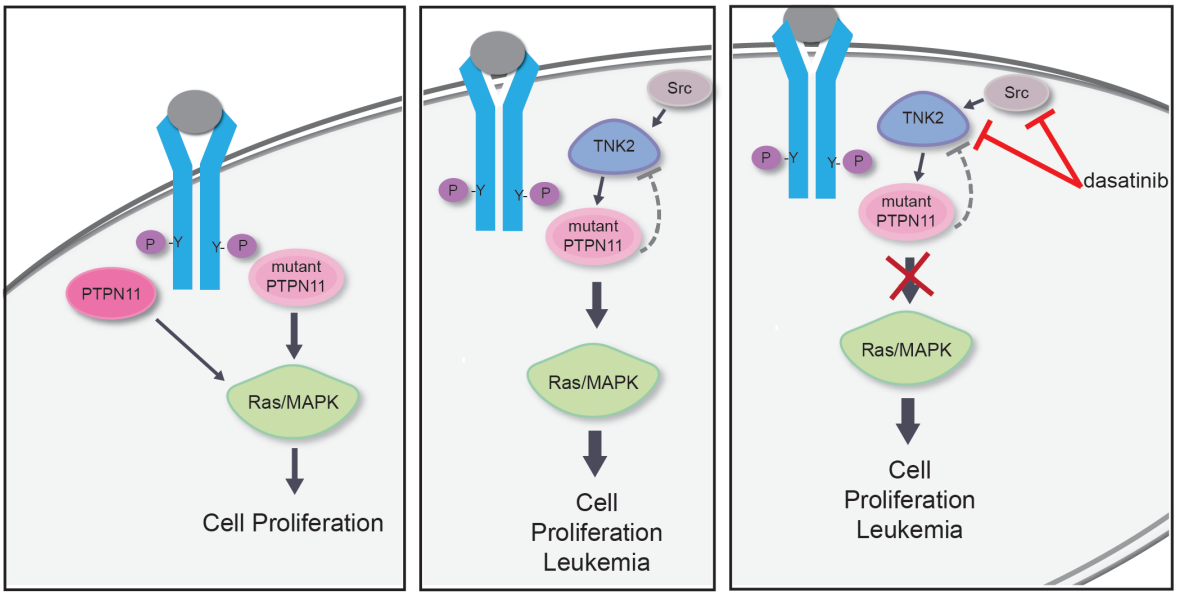

Figure 4-1:Working model.

Left panel: PTPN11 signaling is necessary for sustaining Ras/MAPK activation, with activating mutations of PTPN11 leading to increased Ras/MAPK signaling and cell proliferation. Middle panel: Data presented in this dissertation suggests a new paradigm in which TNK2 activates PTPN11, especially mutant PTPN11, leading to even more Ras/MAPK signaling and leukemogenesis. Inhibition of TNK2 with dasatinib abolishes this Ras/MAPK signaling (right panel).

4-2: Discussion

4-2.1: Synthetic lethality of TNK2 in PTPN11-mutant leukemia.

This dissertation describes the characterization of a novel interaction between PTPN11 and its upstream kinase, TNK2. My data suggest that TNK2 directly interacts with PTPN11 in what seems to be a closely regulated feedback loop. TNK2 expression results in phosphorylated and activated PTPN11, as evidenced by experiments using the dasatinib-resistant gatekeeper mutant TNK2 T205I (Fig. 2-15,16). This phosphorylation is necessary for complete activation of PTPN11, even in the presence of the pathogenic activating mutation E76K, as seen by mutating the C-terminal tyrosine residues of PTPN11 (Figs. 2-12, 13).

PTPN11 activity correlates with dephosphorylation of TNK2. My work evaluating overactive PTPN11 mutants, inactive C-terminal tyrosine mutants of PTPN11, and PTPN11 inhibition experiments support this feedback model (Figs. 2-7,14,18). This relationship has functional implications; co-expression of mutant-PTPN11 and TNK2 results in significantly more Ras/MAPK signaling and GM-CSF hypersensitivity, both hallmarks of JMML [97]. These increases in MAPK signaling and colony

formation are blocked by pharmacological inhibition of TNK2 by dasatinib or AIM-100. More importantly, data from primary JMML and AML patient samples identify PTPN11 mutations as a genetic marker for sensitivity to TNK2 inhibition.

4-2.2: Role of PTPN11 in TNK2 dephosphorylation

The PTPN11-dependent dephosphorylation of TNK2 has yet to be fully elucidated. Co-immunoprecipitation of PTPN11 and TNK2 suggests that PTPN11 and TNK2 interact, but whether there is a phosphate removed from the kinase domain tyrosine residue of TNK2 or a reduction of active phosphorylation of that tyrosine remains unknown. Future experiments to dissect this mechanism would need to identify any additional proteins that may be acting in a complex with PTPN11 and TNK2. Additional *in vitro* protein stability and phosphorylation kinetics assays will be critical to fully elucidate the mechanistic details of the functional relationship between PTPN11 and TNK2.

4-2.3: Synthetic lethality of TNK2 inhibition in Ras-transformed tumors

While AML patient samples with N-Ras or K-Ras mutations presented in this dissertation were not differentially sensitive to dasatinib treatment compared with wild-type samples, some evidence suggested that N-Ras or v-Ras transformed cell lines might be sensitive to TNK2 inhibition [112, 113]. A 2005 study by Nur *et al.* concluded that TNK2 is important for transduction of Ras signaling in v-Ras transformed NIH3T3 cells, and that knockdown of TNK2 by siRNA was cytotoxic to these cells [113]. More recent research from Nonami *et al.* demonstrated that TNK2 (as a promoter of AKT signaling) showed synthetic lethality when inhibited in Ba/F3 cells transformed by mutant N-Ras [112]. This effect suggests a role for TNK2 in rescuing malignant cells by activating alternate proliferative pathways in Ras-transformed cells, including the AKT pathway.

AKT signaling, especially downstream of PI3K subunit p110δ has been shown to be essential in MPN/MDS mouse models and in JMML cells transformed by oncogenic Ras signaling [114-116]. The inhibition of TNK2 may thus have a multi-tiered effect in PTPN11-mutant JMML cells whereby Ras/MAPK and downstream AKT signaling is inhibited. The deconvolution of these interactions is made challenging, however, due to reports that activated

mutant PTPN11 can also increase signaling through the PI3K/Akt pathway [116].

4-2.4: Role of SRC kinase in TNK2/PTPN11 signaling.

SRC has been reported to be both upstream of TNK2 and downstream/concurrent with PTPN11 with regards to p44/42 MAPK signaling, as well as a target of dasatinib [37, 38, 70, 117]. However, the role of SRC kinase in the interplay between PTPN11 and TNK2 and the degree of its involvement is unknown. The efficacy of the TNK2-specific inhibitor AIM-100 in our *in vitro* system suggests that SRC is not the sole activator of TNK2, but SRC's role in TNK2 activation with regards to mutant PTPN11 is still under investigation. siRNA inhibition in cell lines transformed by mutant PTPN11 (and that also express TNK2) has yet to be confirmed, but the use of alternative experimental approaches, such as CRISPR/Cas9, may be more successful. Interestingly, two independent studies found synergistic tumor targeting with the combination of PTPN11 inhibition and dasatinib treatment or SRC knockdown [118, 119]. The efficacy of SRC knockdown in the presence of PTPN11 in non-leukemic cells does not preclude TNK2 as the target of dasatinib in the work described here.

While SRC inhibition may be occurring upstream of TNK2 and contribute to dasatinib-mediated TNK2 inactivation, TNK2 phosphorylation levels were not significantly affected by dasatinib treatment in the work presented in this dissertation. It is likely that SRC is targeted by dasatinib as a downstream effector of Ras/MAPK signaling, but the activity of mutant PTPN11 as an activator of multiple proliferative pathways might render this inhibition event to be less effective. Preliminary data using a TNK2 mutant with reduced SRC interaction ability, TNK2 Y518F [70], suggests that interaction of TNK2 with SRC is not necessary for PTPN11 phosphorylation, and that TNK2 Y518F interacts with PTPN11 at similar levels as TNK2 wild-type (Fig 4-2).

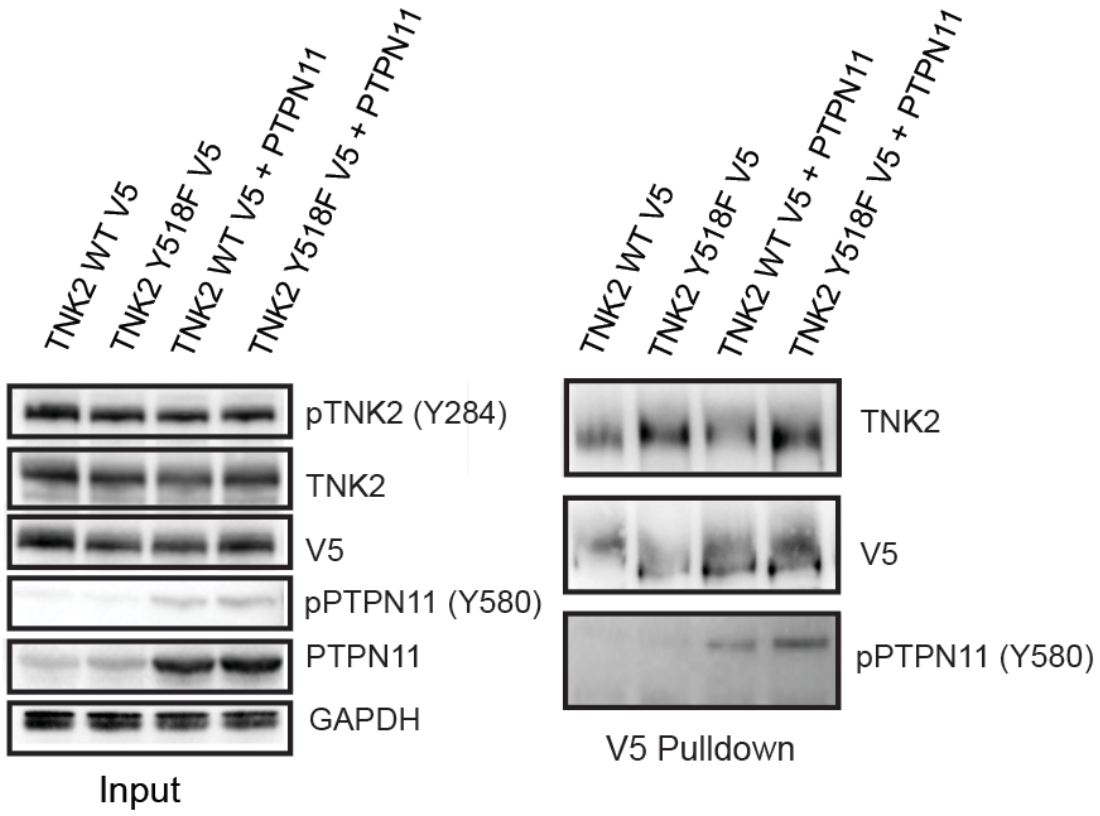

Figure 4-2: SRC activation of TNK2 is not required for PTPN11 interaction with TNK2.

293T17 cells were co-transfected with overexpression constructs containing PTPN11, TNK2 V5, TNK2 Y518F V5, or empty vector controls. Lysates were collected at 48 hours and subjected to V5 immunoprecipitation, followed by immunoblot. Left: input. Right: V5 pulldown.

Ultimately, the best model system for investigating the role of SRC could be patient-derived xenografts from PTPN11-mutant AML and JMML patients. Currently, cells from an AML patient with mutant PTPN11 that showed exquisite sensitivity to dasatinib in our *in vitro* screen have been injected into a cohort of NOD.*Cg-Prkdc*^{scid} *Il2rg*^{tm1Wjl}Tg (CMVIL3,CSF2,KITLG) 1Eav/MloySzJ (NSGS) mice [120]. This is an immunodeficient mouse constitutively expressing human SCF, GM-CSF and IL-3. This mouse has recently been shown to increase efficiency in engrafting AML samples as well as JMML [121]. If these cells demonstrate similar dasatinib sensitivity seen in our *in vitro* screen, cells isolated from untreated mice could be used to perform CRISPR/Cas9 knockdown of key proteins including TNK2 and SRC to further elucidate mechanisms of dasatinib sensitivity in PTPN11-mutant leukemias.

4-2.5: Targeting PTPN11 in patient tumors

While PTPN11 is known to be necessary for sustaining signaling through Ras/MAPK, its involvement as a regulator at several levels of the signaling cascade has made it challenging to fully determine its exact mechanisms of action. PTPN11 has become an attractive therapeutic target, and an exciting

recent development in this area has been the identification of allosteric PTPN11 inhibitors, such as SHP099 [102]. However, the potential clinical efficacy of these molecules may be limited, as SHP099 has limited activity against activated PTPN11 because it binds only the closed conformation of PTPN11 [101, 102, 122]. Inhibition of proteins in the Ras/MAPK pathway downstream of PTPN11 is an option that is being explored by other groups [123, 124], but the ability of mutant PTPN11 to activate alternate pathways like JAK/Stat or PI3K/Akt signaling makes resistance to these drugs a distinct possibility.

4-2.6: TNK2 inhibition for germline PTPN11 mutant patients.

Mutations in PTPN11 drive the pathogenesis of JMML, sometimes even as germline events. Thus, inhibition of TNK2 could be useful for maintenance of remission. Implications for Noonan Syndrome (NS) patients have not been explored in this dissertation, but work by Yi et al described in the introduction to this dissertation suggests that dasatinib may have a bright therapeutic future in patients with NS [125].

While this dissertation has not touched on the contributions of mutant PTPN11 in the stromal compartment of patients with germline mutations,

work from other groups suggests that these cells contribute to leukemogenesis through CCL3 signaling [126]. Mice bearing activating PTPN11 mutations in mesenchymal stem/progenitor cells and osteoprogenitors promoted a myeloproliferative phenotype in normal transplanted cells. This effect was reversible with the administration of CCL3 receptor agonists. Perhaps dasatinib could be used in combination with a CCL3 receptor agonist to abrogate the effects of PTPN11-mutant stromal cells in patients with NS or LEOPARD syndrome.

4-2.7: Functional screening to identify novel targeted and combinatorial therapies

The identification of TNK2 as a functional target originated in an *ex vivo* screen of a primary JMML patient sample. While high-throughput genomic and whole-exome sequencing has become increasingly available, identification of mutations needs to be accompanied by additional functional analysis, especially for poorly characterized mutations. Additionally, effective drugs currently approved by the Food and Drug Administration target only a subset of known mutated tumor driver genes [127]. As we move towards personalized cancer therapy, *ex vivo* functional screening is a promising avenue to identify drug targets that are not directly mutated. This type of

personalized analysis can become even more relevant in the face of resistance to existing therapies [128].

4-2.8: Broader Impact.

Efficacy of TNK2 inhibition would depend upon a tumor's dependence on PTPN11 for transformation and survival. In AML, for instance, PTPN11 mutations may occur later in the evolution of the disease, tempering the probability of success of a single agent therapy. TNK2 inhibitors may prove to be an important component of an eventual molecularly-targeted combinatorial therapy strategy, a recently promising field recently showing efficacy in AML patient samples [128].

Taken together, the data presented in this dissertation suggest that TNK2 plays a pivotal role in activation of the PTPN11/MAPK pathway in leukemia cells, and that targeting TNK2 could provide valuable new therapeutic strategies for patients with activating PTPN11 mutations. As discussed in section 1-9 of this dissertation, PTPN11 mutations have been implicated as a driver in solid tumors. Dasatinib has shown some promise as a therapy in PTPN11-mutant lung tumors and triple-negative breast cancer [54, 87]. It is my hope that the efficacy of TNK2 inhibition might be explored in other

tumor model systems as well, and incorporated into future therapies for a broad range of patients.

Chapter 5 : Appendix

5-1: Preliminary data suggests that dasatinib reduces engraftment of PTPN11-mutant cells in a syngeneic mouse model

In order to determine *in vivo* efficacy of dasatinib treatment to reduce activated PTPN11 mutant driven disease, a syngeneic mouse model was established using Balb/C mice[19]. It has been previously shown that mice transplanted with PTPN11 E76K mutant cells develop a myeloproliferative disease in a time frame of 90 days [130]. Bone marrow from Balb/C donor mice was harvested and retrovirally transduced to express PTPN11-E76K and GFP. These cells were transplanted into lethally irradiated Balb/C mice. At 4 weeks post-transplantation, the mice were treated with daily dasatinib at 40mg/Kg or vehicle control for 8 weeks.

---

[19] A genetically modified conditional mouse model of JMML exists that utilizes a conditional knock-in of a single *Ptpn11*^{D16Y} allele. Expression of *Ptpn11*^{D16Y} results in a fatal and invasive MPD accompanied by anemia. However, the timeline from induction of PTPN11 expression to disease occurrence is about 6 months, with 50% penetrance [129]. Our lab chose not to pursue this model

The data suggest that in this transplant model, PTPN11-mutant cells are sensitive to dasatinib treatment. Overall blood counts were not significantly different between the two arms, and treatment was well tolerated (Fig 6-1). While all mice had enlarged spleens at time of harvest, those in the dasatinib group had significantly smaller spleen size than controls ($p=0.0028$) (Fig 6-2), consistent with percent GFP engraftment (Fig. 6-3). Peripheral blood and bone marrow FACS GFP analyses show higher levels of PTPN11 E76K positive cells in the vehicle control mice, with a significant increase in peripheral blood fold-change GFP compared to pre-treatment values for each mouse ($p=0.0303$) (Figs. 6-4 to 6-6).

To determine *ex vivo* sensitivity of transplanted cells to dasatinib treatment, spleen cells from vehicle control mice were pooled and plated in the presence of dasatinib for 72 hours followed by colorimetric viability assay (Fig. 6-7). The IC_{50} for dasatinib in these spleen cells was in the physiological range, at around 50nM, suggesting that these cells might harbor a susceptibility to dasatinib treatment. These spleen cells were also subjected to 2hr dasatinib or vehicle control treatment

(identical to heterologous 293T17 cell experiments) and cells have been collected for future immunoblot analysis.

These data are preliminary, and full interpretation must be suspended prior to histological confirmation of disease burden in these mice. Additionally, protein expression will be confirmed by PCR and immunoblot. This experiment will be repeated for confirmation, with a possible extension of dasatinib treatment time. These preliminary data are, however, promising: PTPN11 mutant cells show less engraftment in all hematopoietic compartments evaluated, and spleen cells from control mice show sensitivity to dasatinib treatment. If these data are confirmed, this model can be used for future studies to investigate the efficacy of dasatinib treatment and combinatorial therapies in PTPN11-mutant leukemias.

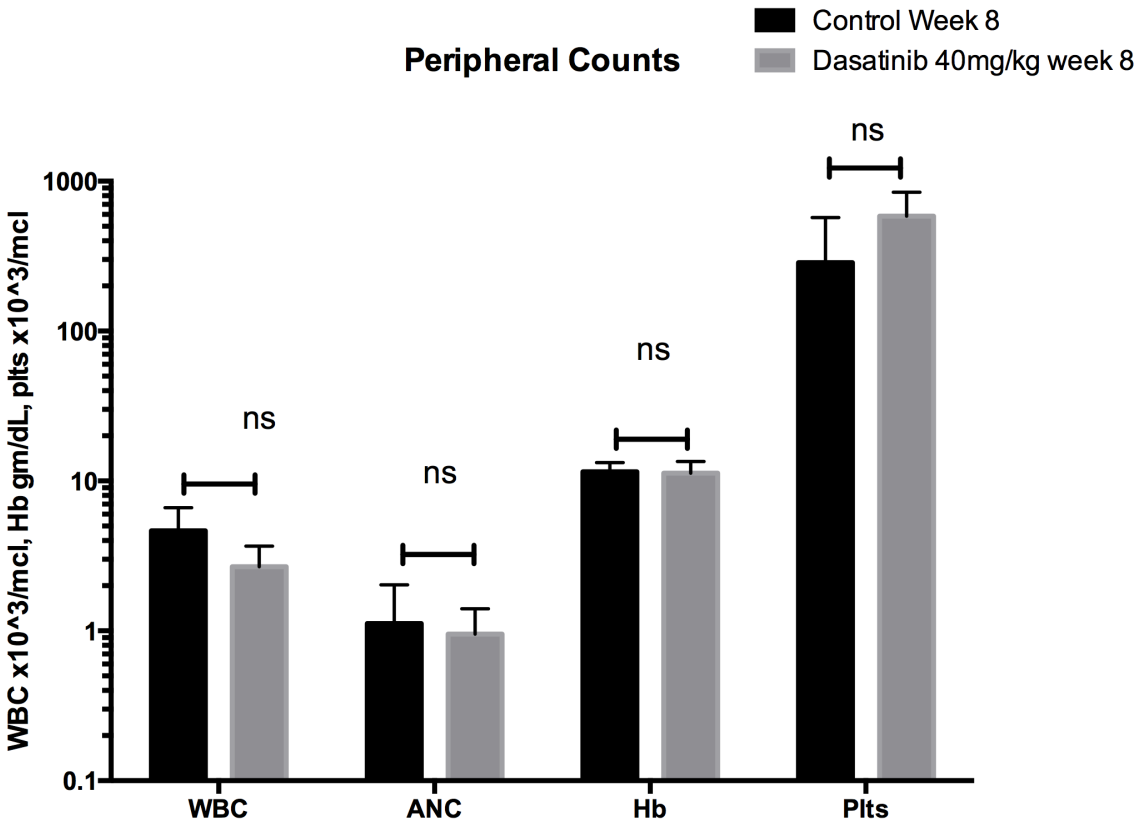

Figure 5-1: Dasatinib has no significant effect on peripheral blood counts.

Peripheral blood counts from week 8 of drug treatment. WBC:White blood counts. ANC: Absolute neutrophil count, Hb: Hemoglobin, Plts: Platelets. n=11. Error bars represent SEM.

i.

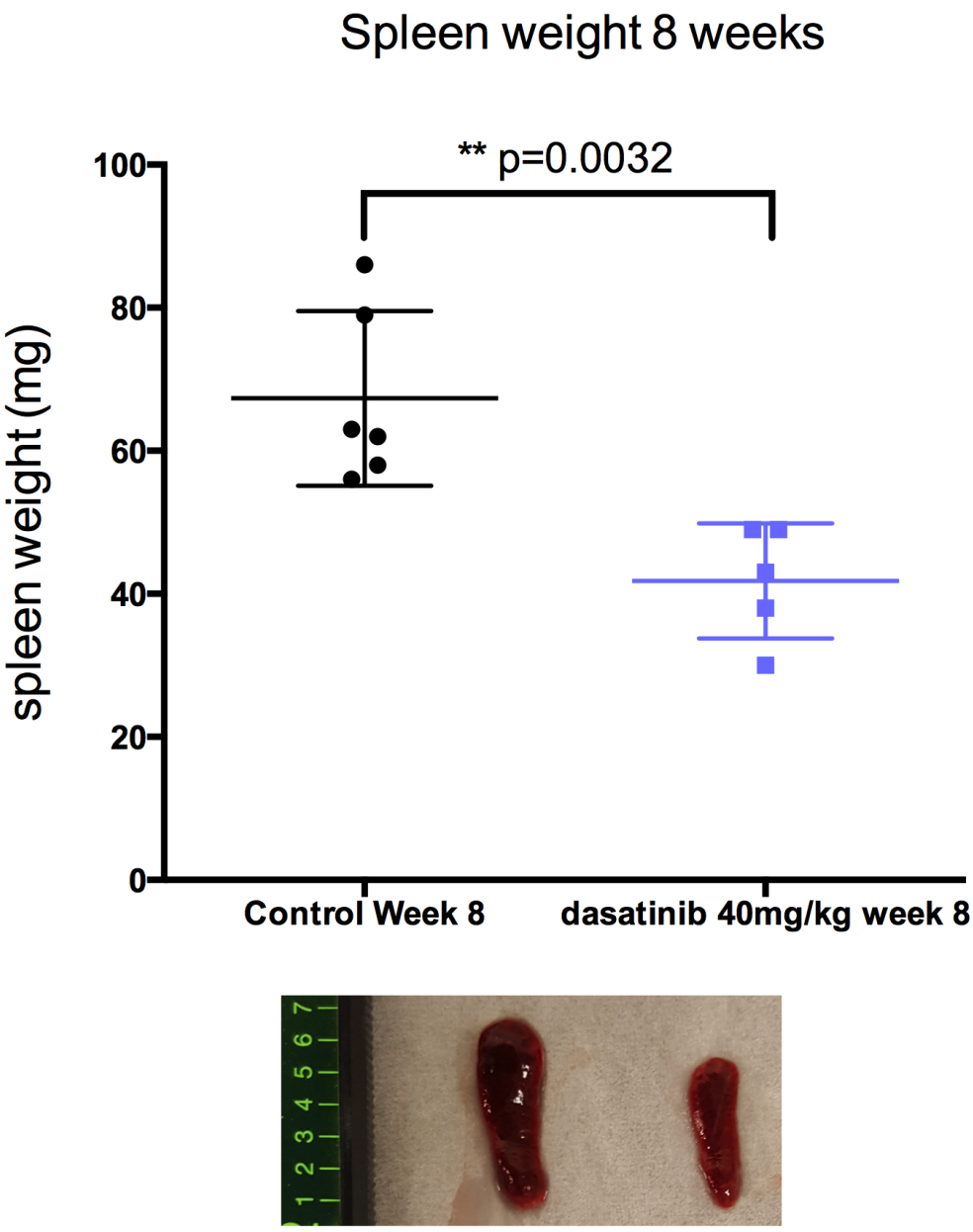

Figure 5-2: Dasatinib significantly reduces spleen size in PTPN11-mutant syngeneic transplant mice.

i. Average spleen weight. Spleen weight was collected at time of sacrifice. p=0.0028 by student's T-Test n=11. Error bars represent SEM. ii. Representative spleens from control and dasatinib mouse, repectively.

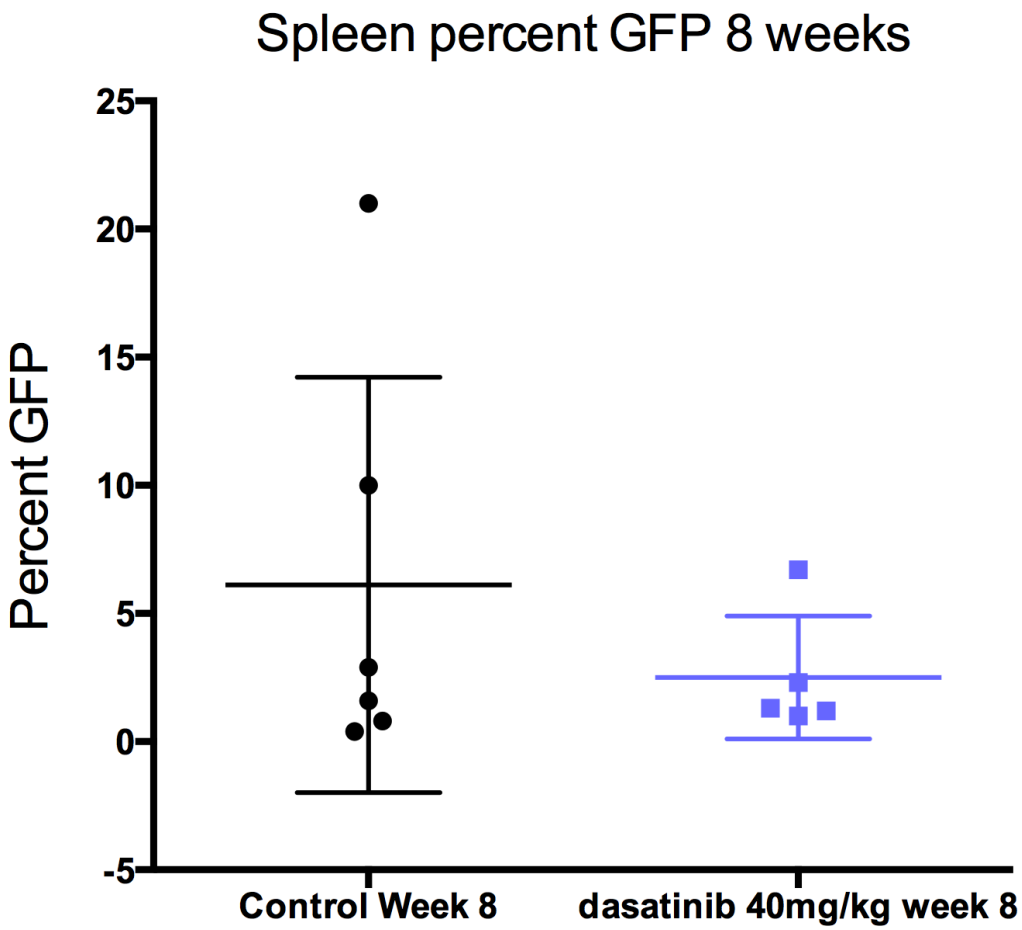

Figure 5-3: Dasatinib reduces PTPN11-mutant cell spleen engraftment.

Spleen percent GFP from week 8 of drug treatment. Samples underwent homogenization through nylon strainer and red blood cell lysis, followed by FACS analysis for GFP+ cells. n=11. Error bars represent SEM.

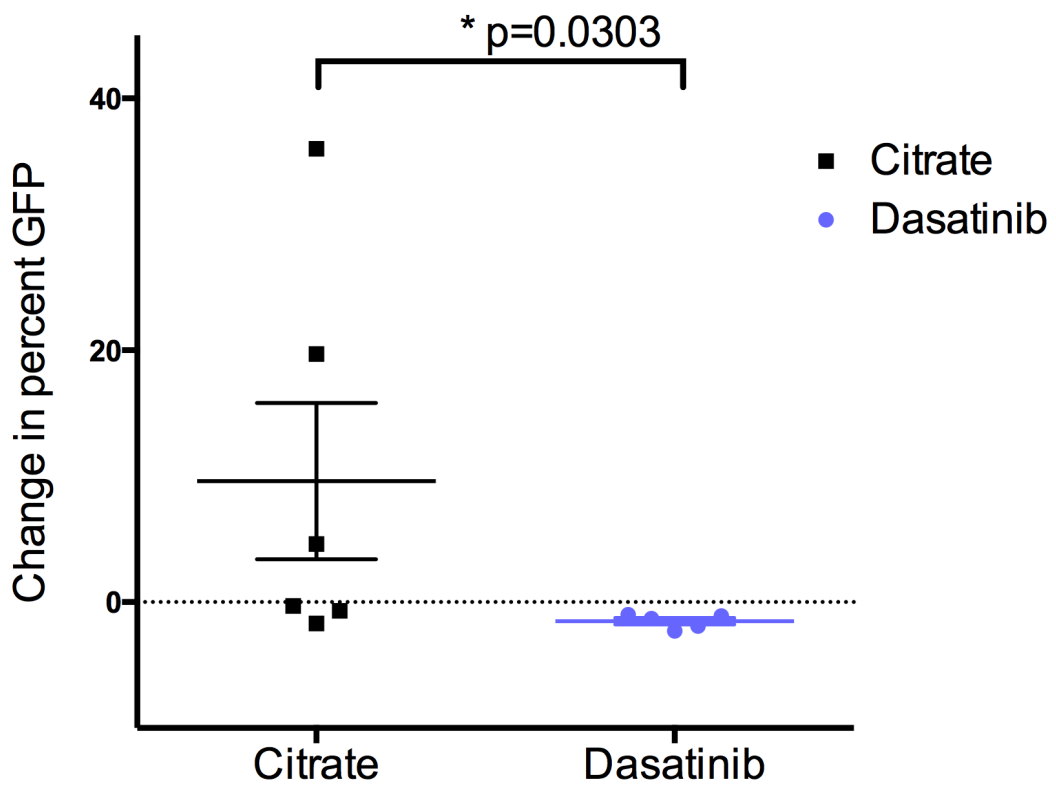

Figure 5-4: Dasatinib significantly reduces peripheral blood PTPN11-mutant cells.

Peripheral blood GFP from week 8 of drug treatment. Samples underwent red blood cell lysis, followed by FACS analysis for GFP+ cells. Fold change comparison to pre-treatment values. n=11 p=0.0303 by student's T-test. Error bars represent SEM.

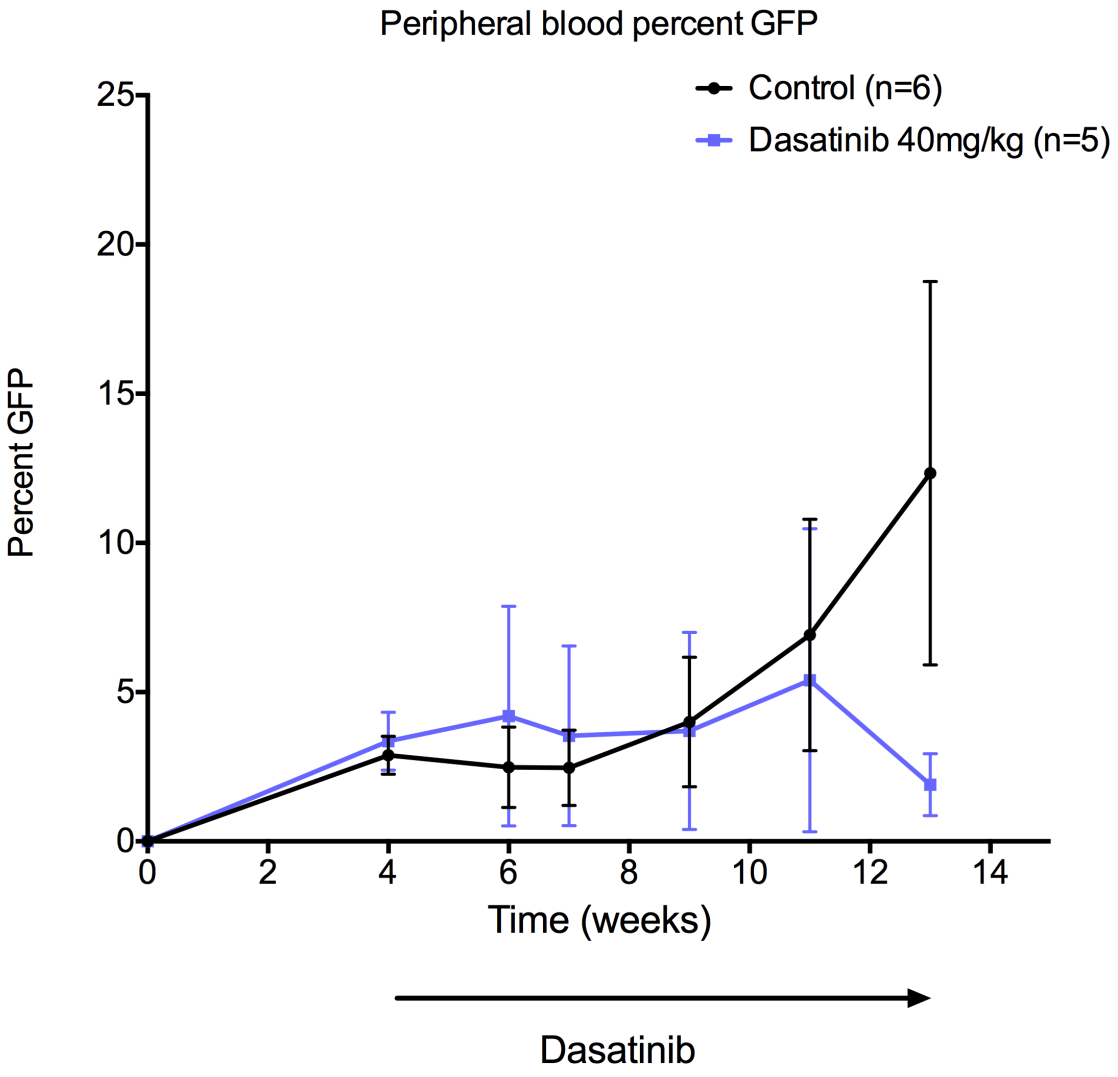

Figure 5-5: Dasatinib reduces engraftment of PTPN11-mutant peripheral blood cells.

Peripheral blood GFP percentage over time. Samples underwent red blood cell lysis, followed by FACS analysis for GFP+ cells. Arrow indicates initiation of drug treatment. Error bars represent SEM.

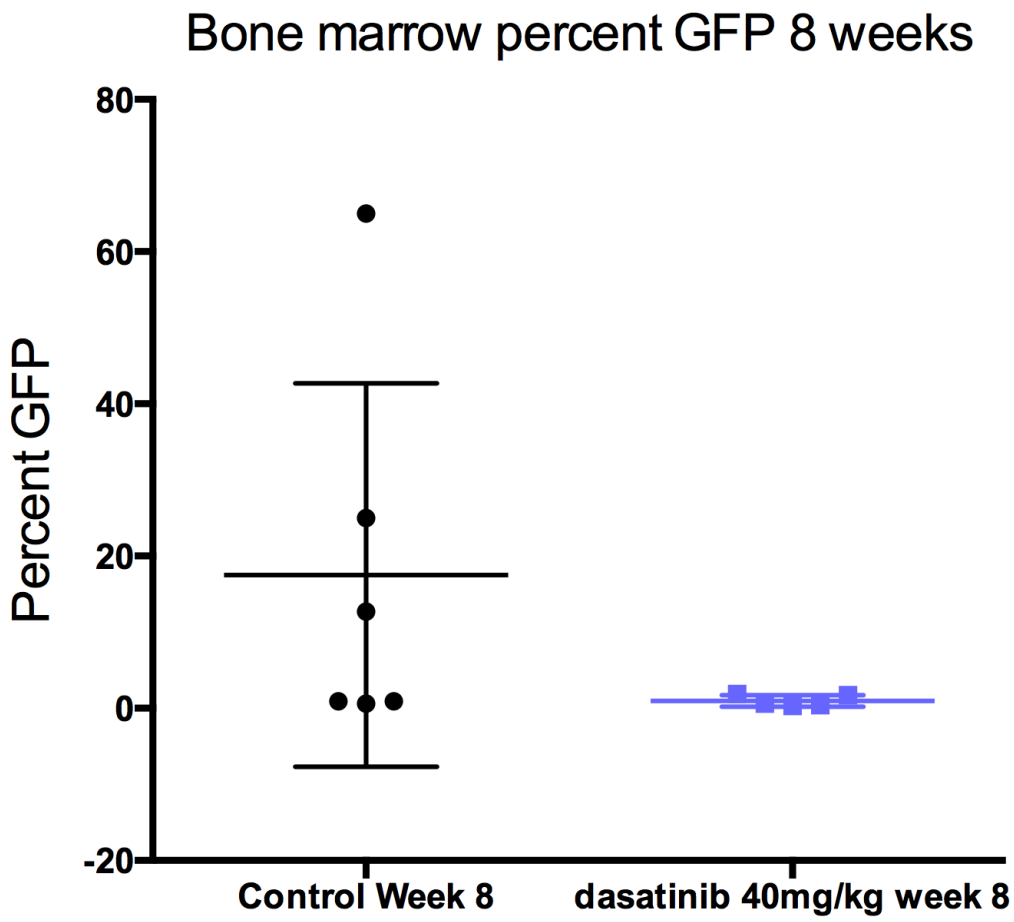

Figure 5-6: Dasatinib reduces PTPN11-mutant bone marrow cell engraftment.

Bone marrow percent GFP at week 8 of drug treatment. Samples underwent homogenization through nylon strainer and red blood cell lysis, followed by FACS analysis for GFP+ cells. Error bars represent SEM.

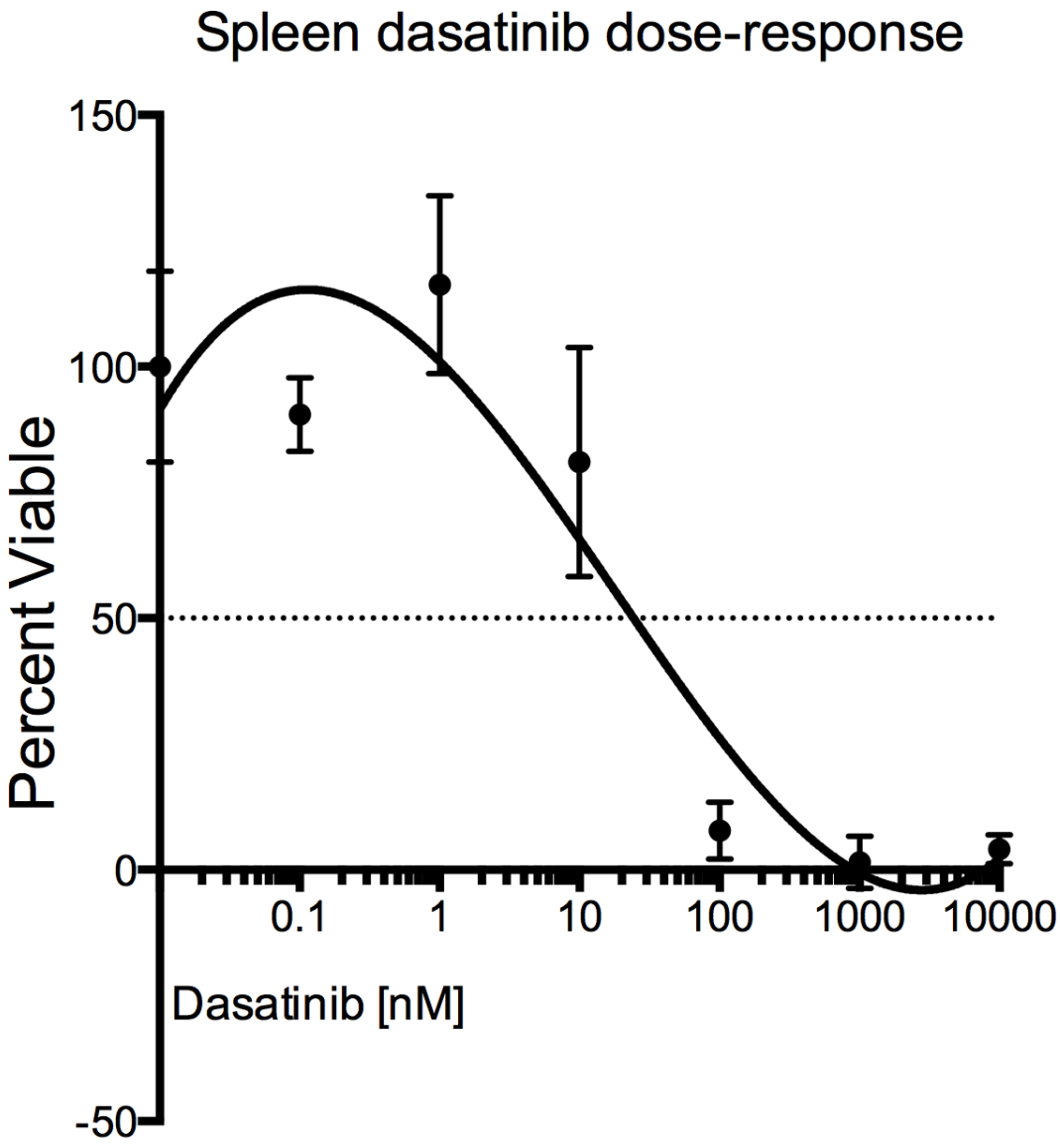

Figure 5-7: Spleen cells from vehicle control mice display *ex vivo* dasatinib sensitivity.

Samples underwent homogenization through nylon strainer and red blood cell lysis, then were plated in media with a dose-gradient of dasatinib for 72 hrs. Viability was determined by MTS assay. n=3. Error bars represent SEM. Line represents non-linear fit.

5-2: Materials and Methods

Murine retrovirus was created by co-transfecting PTPN11 E76K MSCV-IRES-GFP plasmid and the EcoPac plasmid (provided by Dr. Rick Van Etten) into 293T17 cells using FuGENE 6 (ProMega). Supernatants were harvested 72 hours later and snap-frozen. Pooled viral supernatant was thawed on ice and concentrated via ultracentrifugation on a sucrose gradient.

Balb/c (Jackson Laboratories) donor mice (6 weeks old) were primed by retro-orbital injection of 3 mg 5-fluorouracil (5-FU; American Pharmaceutical Partners, Schaumburg, IL). Bone marrow was harvested from Balb/C (6-9 weeks old) mice by flushing the femur and tibia with medium. Cells were cultured at 5×10^5 per mL with concentrated viral supernatant, polybrene (American Bioanalyticals) and HEPES (4-(2-hydroxyethyl)-1-piperazineethanesulfonic acid) buffer by centrifugation at 2500rpm at 30°C for 90 min, then placed back at 37°C. After 24 hours, the medium was replaced with fresh retroviral "cocktail" and cells were centrifuged as above, then placed back at 37°C for additional 24 hours.

Cells were washed twice and suspended in PBS. 6×10^5 cells in 100uL PBS was introduced into lethally irradiated (2 × 450Gy X-Ray exposure) 6 week old Balb/C mice by retro-orbital injection. Mice were given water containing Neomycin (2 mg/mL) and Polymyxin B (1 mg/mL) for two weeks following irradiation.

Mice were monitored for well being, weight and peripheral blood GFP engraftment by flow cytometry on a FACSAria flow cytometer following transplantation. Blood counts were determined using a Vet ABC animal blood counter (Heska, Fort Collins, CO). Beginning at four weeks post-transplantation, mice were divided into control or drug arms (with matched peripheral blood GFP engraftment) and administered 40mg/kg dasatinib in citrate buffer or citrate buffer control daily for 8 weeks by oral gavage followed by sacrifice.

Organs were dissected and WBC from spleen and bone marrow were harvested by passing through a 70-µm nylon cell strainer (BD Biosciences, Bedford, MA) followed by red cell lysis. Peripheral blood at time of sacrifice was harvested by cardiac puncture. GFP engraftment

of peripheral blood, spleen, and liver was analyzed by flow cytometry as above. Spleen cells from control mice were pooled, and plated at 50,000cpw in 100ul R10 media with a tenfold dilution series of dasatinib (n=3). At 72 hours, cells were subjected to the CellTiter 96 AQueous one solution cell proliferation assay (MTS) (Promega). All values were normalized to 3 wells containing media alone.

Chapter 6 : References

1. Kampen, K.R., *The discovery and early understanding of leukemia.* Leuk Res, 2012. **36**(1): p. 6-13.
2. Goodman, L.S., M.M. Wintrobe, and et al., *Nitrogen mustard therapy; use of methyl-bis (beta-chloroethyl) amine hydrochloride and tris (beta-chloroethyl) amine hydrochloride for Hodgkin's disease, lymphosarcoma, leukemia and certain allied and miscellaneous disorders.* J Am Med Assoc, 1946. **132**: p. 126-32.
3. Joensuu, H., *Systemic chemotherapy for cancer: from weapon to treatment.* Lancet Oncol, 2008. **9**(3): p. 304.
4. Hochhaus, A., et al., *Long-Term Outcomes of Imatinib Treatment for Chronic Myeloid Leukemia.* N Engl J Med, 2017. **376**(10): p. 917-927.
5. Tartaglia, M., et al., *Somatic mutations in PTPN11 in juvenile myelomonocytic leukemia, myelodysplastic syndromes and acute myeloid leukemia.* Nat Genet, 2003. **34**(2): p. 148-50.
6. Sun, J., et al., *Antagonism between binding site affinity and conformational dynamics tunes alternative cis-interactions within Shp2.* Nat Commun, 2013. **4**: p. 2037.
7. Van Etten, R.A., *Aberrant cytokine signaling in leukemia.* Oncogene, 2007. **26**(47): p. 6738-49.

8. Johnson, L.N. and D. Barford, *The effects of phosphorylation on the structure and function of proteins.* Annu Rev Biophys Biomol Struct, 1993. **22**: p. 199-232.

9. Audagnotto, M. and M. Dal Peraro, *Protein post-translational modifications: In silico prediction tools and molecular modeling.* Comput Struct Biotechnol J, 2017. **15**: p. 307-319.

10. Tiganis, T. and A.M. Bennett, *Protein tyrosine phosphatase function: the substrate perspective.* Biochem J, 2007. **402**(1): p. 1-15.

11. Drebin, J.A., et al., *Inhibition of tumor growth by a monoclonal antibody reactive with an oncogene-encoded tumor antigen.* Proc Natl Acad Sci U S A, 1986. **83**(23): p. 9129-33.

12. Lambertini, M., et al., *Adjuvant trastuzumab: a 10-year overview of its benefit.* Expert Rev Anticancer Ther, 2017. **17**(1): p. 61-74.

13. Schindler, T., et al., *Structural mechanism for STI-571 inhibition of abelson tyrosine kinase.* Science, 2000. **289**(5486): p. 1938-42.

14. Gibbons, D.L., et al., *The rise and fall of gatekeeper mutations? The BCR-ABL1 T315I paradigm.* Cancer, 2012. **118**(2): p. 293-9.

15. Geest, C.R. and P.J. Coffer, *MAPK signaling pathways in the regulation of hematopoiesis.* J Leukoc Biol, 2009. **86**(2): p. 237-50.

16. Chang, E.H., et al., *Human genome contains four genes homologous to transforming genes of Harvey and Kirsten murine sarcoma viruses.* Proc Natl Acad Sci U S A, 1982. **79**(16): p. 4848-52.

17. Malumbres, M. and M. Barbacid, *RAS oncogenes: the first 30 years.* Nat Rev Cancer, 2003. **3**(6): p. 459-65.

18. Chung, E. and M. Kondo, *Role of Ras/Raf/MEK/ERK signaling in physiological hematopoiesis and leukemia development.* Immunol Res, 2011. **49**(1-3): p. 248-68.

19. Leicht, D.T., et al., *Raf kinases: function, regulation and role in human cancer.* Biochim Biophys Acta, 2007. **1773**(8): p. 1196-212.

20. Fabian, J.R., et al., *A single amino acid change in Raf-1 inhibits Ras binding and alters Raf-1 function.* Proc Natl Acad Sci U S A, 1994. **91**(13): p. 5982-6.

21. Boucher, M.J., et al., *MEK/ERK signaling pathway regulates the expression of Bcl-2, Bcl-X(L), and Mcl-1 and promotes survival of human pancreatic cancer cells.* J Cell Biochem, 2000. **79**(3): p. 355-69.

22. Roberts, P.J. and C.J. Der, *Targeting the Raf-MEK-ERK mitogen-activated protein kinase cascade for the treatment of cancer.* Oncogene, 2007. **26**(22): p. 3291-310.

23. Bos, J.L., *ras oncogenes in human cancer: a review.* Cancer Res, 1989. **49**(17): p. 4682-9.

24. Rodenhuis, S., *ras and human tumors.* Semin Cancer Biol, 1992. **3**(4): p. 241-7.

25. Davies, H., et al., *Mutations of the BRAF gene in human cancer.* Nature, 2002. **417**(6892): p. 949-54.

26. Mattingly, R.R., *Activated Ras as a Therapeutic Target: Constraints on Directly Targeting Ras Isoforms and Wild-Type versus Mutated Proteins.* ISRN Oncol, 2013. **2013**: p. 536529.

27. Freeman, R.M., Jr., J. Plutzky, and B.G. Neel, *Identification of a human src homology 2-containing protein-tyrosine-phosphatase: a putative homolog of Drosophila corkscrew.* Proc Natl Acad Sci U S A, 1992. **89**(23): p. 11239-43.

28. Bennett, A.M., et al., *Protein-tyrosine-phosphatase SHPTP2 couples platelet-derived growth factor receptor beta to Ras.* Proc Natl Acad Sci U S A, 1994. **91**(15): p. 7335-9.

29. Heiss, E., et al., *Identification of Y589 and Y599 in the juxtamembrane domain of Flt3 as ligand-induced autophosphorylation sites involved in binding of Src family kinases and the protein tyrosine phosphatase SHP2.* Blood, 2006. **108**(5): p. 1542-50.

30. Furcht, C.M., J.M. Buonato, and M.J. Lazzara, *EGFR-activated Src family kinases maintain GAB1-SHP2 complexes distal from EGFR.* Sci Signal, 2015. **8**(376): p. ra46.

31. Araki, T., H. Nawa, and B.G. Neel, *Tyrosyl phosphorylation of Shp2 is required for normal ERK activation in response to some, but not all, growth factors.* J Biol Chem, 2003. **278**(43): p. 41677-84.

32. Chan, G., et al., *Essential role for Ptpn11 in survival of hematopoietic stem and progenitor cells.* Blood, 2011. **117**(16): p. 4253-61.

33. Chan, G., D. Kalaitzidis, and B.G. Neel, *The tyrosine phosphatase Shp2 (PTPN11) in cancer.* Cancer Metastasis Rev, 2008. **27**(2): p. 179-92.

34. Flotho, C., C.P. Kratz, and C.M. Niemeyer, *How a rare pediatric neoplasia can give important insights into biological concepts: a perspective on juvenile myelomonocytic leukemia.* Haematologica, 2007. **92**(11): p. 1441-6.

35. Agazie, Y.M. and M.J. Hayman, *Molecular mechanism for a role of SHP2 in epidermal growth factor receptor signaling.* Mol Cell Biol, 2003. **23**(21): p. 7875-86.

36. Hanafusa, H., et al., *Shp2, an SH2-containing protein-tyrosine phosphatase, positively regulates receptor tyrosine kinase signaling by dephosphorylating and inactivating the inhibitor Sprouty.* J Biol Chem, 2004. **279**(22): p. 22992-5.

37. Bunda, S., et al., *Src promotes GTPase activity of Ras via tyrosine 32 phosphorylation.* Proc Natl Acad Sci U S A, 2014. **111**(36): p. E3785-94.

38. Bunda, S., et al., *Inhibition of SHP2-mediated dephosphorylation of Ras suppresses oncogenesis.* Nat Commun, 2015. **6**: p. 8859.

39. Qu, C.K., et al., *Biased suppression of hematopoiesis and multiple developmental defects in chimeric mice containing Shp-2 mutant cells.* Mol Cell Biol, 1998. **18**(10): p. 6075-82.

40. Zhu, H.H., et al., *Kit-Shp2-Kit signaling acts to maintain a functional hematopoietic stem and progenitor cell pool.* Blood, 2011. **117**(20): p. 5350-61.

41. Keilhack, H., et al., *Diverse biochemical properties of Shp2 mutants. Implications for disease phenotypes.* J Biol Chem, 2005. **280**(35): p. 30984-93.

42. Kratz, C.P., et al., *The mutational spectrum of PTPN11 in juvenile myelomonocytic leukemia and Noonan syndrome/myeloproliferative disease.* Blood, 2005. **106**(6): p. 2183-5.

43. Stieglitz, E., et al., *The genomic landscape of juvenile myelomonocytic leukemia.* Nat Genet, 2015. **47**(11): p. 1326-33.

44. Sakaguchi, H., et al., *Exome sequencing identifies secondary mutations of SETBP1 and JAK3 in juvenile myelomonocytic leukemia.* Nat Genet, 2013. **45**(8): p. 937-41.

45. Papaemmanuil, E., H. Dohner, and P.J. Campbell, *Genomic Classification in Acute Myeloid Leukemia.* N Engl J Med, 2016. **375**(9): p. 900-1.

46. Haggstrom, M.f.o.b.A.R.-I.H.h.d.p., *Simplified Hematopoiesis.* CC BY-SA 3.0, 2011.

47. Doulatov, S., et al., *Hematopoiesis: a human perspective.* Cell Stem Cell, 2012. **10**(2): p. 120-36.

48. Emanuel, P.D., *Juvenile myelomonocytic leukemia.* Curr Hematol Rep, 2004. **3**(3): p. 203-9.

49. Arico, M., A. Biondi, and C.H. Pui, *Juvenile myelomonocytic leukemia.* Blood, 1997. **90**(2): p. 479-88.

50. Passmore, S.J., et al., *Paediatric myelodysplastic syndromes and juvenile myelomonocytic leukaemia in the UK: a population-based study of incidence and survival.* Br J Haematol, 2003. **121**(5): p. 758-67.

51. Hasle, H., et al., *Myelodysplastic syndrome, juvenile myelomonocytic leukemia, and acute myeloid leukemia associated with complete or*

partial monosomy 7. European Working Group on MDS in Childhood (EWOG-MDS). Leukemia, 1999. **13**(3): p. 376-85.

52. Locatelli, F., et al., *Hematopoietic stem cell transplantation (HSCT) in children with juvenile myelomonocytic leukemia (JMML): results of the EWOG-MDS/EBMT trial.* Blood, 2005. **105**(1): p. 410-9.

53. Roberts, A.E., et al., *Noonan syndrome.* Lancet, 2013. **381**(9863): p. 333-42.

54. Schneeberger, V.E., et al., *SHP2E76K mutant promotes lung tumorigenesis in transgenic mice.* Carcinogenesis, 2014. **35**(8): p. 1717-25.

55. Chen, L., et al., *Mutated Ptpn11 alters leukemic stem cell frequency and reduces the sensitivity of acute myeloid leukemia cells to Mcl1 inhibition.* Leukemia, 2015. **29**(6): p. 1290-300.

56. Cancer Genome Atlas Research, N., *Genomic and epigenomic landscapes of adult de novo acute myeloid leukemia.* N Engl J Med, 2013. **368**(22): p. 2059-74.

57. Tartaglia, M., et al., *Genetic evidence for lineage-related and differentiation stage-related contribution of somatic PTPN11 mutations to leukemogenesis in childhood acute leukemia.* Blood, 2004. **104**(2): p. 307-13.

58. Gilliland, D.G. and J.D. Griffin, *The roles of FLT3 in hematopoiesis and leukemia.* Blood, 2002. **100**(5): p. 1532-42.

59. Shelton, J., et al., *Metabolism, Biochemical Actions, and Chemical Synthesis of Anticancer Nucleosides, Nucleotides, and Base Analogs.* Chem Rev, 2016. **116**(23): p. 14379-14455.

60. Wang, A.H., et al., *Interactions between an anthracycline antibiotic and DNA: molecular structure of daunomycin complexed to d(CpGpTpApCpG) at 1.2-A resolution.* Biochemistry, 1987. **26**(4): p. 1152-63.

61. Hou, H.A., et al., *Characterization of acute myeloid leukemia with PTPN11 mutation: the mutation is closely associated with NPM1 mutation but inversely related to FLT3/ITD.* Leukemia, 2008. **22**(5): p. 1075-8.

62. Manser, E., et al., *A non-receptor tyrosine kinase that inhibits the GTPase activity of p21cdc42.* Nature, 1993. **363**(6427): p. 364-7.

63. Shinmura, K., et al., *TNK2 gene amplification is a novel predictor of a poor prognosis in patients with gastric cancer.* J Surg Oncol, 2014. **109**(3): p. 189-97.

64. Howlin, J., J. Rosenkvist, and T. Andersson, *TNK2 preserves epidermal growth factor receptor expression on the cell surface and*

enhances migration and invasion of human breast cancer cells. Breast Cancer Res, 2008. **10**(2): p. R36.

65. Prieto-Echague, V., et al., *Cancer-associated mutations activate the nonreceptor tyrosine kinase Ack1.* J Biol Chem, 2010. **285**(14): p. 10605-15.

66. Felschow, D.M., C.I. Civin, and G.T. Hoehn, *Characterization of the tyrosine kinase Tnk1 and its binding with phospholipase C-gamma1.* Biochem Biophys Res Commun, 2000. **273**(1): p. 294-301.

67. Modzelewska, K., et al., *Ack1 mediates Cdc42-dependent cell migration and signaling to p130Cas.* J Biol Chem, 2006. **281**(49): p. 37527-35.

68. Mahajan, K. and N.P. Mahajan, *ACK1/TNK2 tyrosine kinase: molecular signaling and evolving role in cancers.* Oncogene, 2015. **34**(32): p. 4162-7.

69. Yokoyama, N. and W.T. Miller, *Biochemical properties of the Cdc42-associated tyrosine kinase ACK1. Substrate specificity, authphosphorylation, and interaction with Hck.* J Biol Chem, 2003. **278**(48): p. 47713-23.

70. Chan, W., S.T. Sit, and E. Manser, *The Cdc42-associated kinase ACK1 is not autoinhibited but requires Src for activation.* Biochem J, 2011. **435**(2): p. 355-64.

71. Lin, Q., et al., *HECT E3 ubiquitin ligase Nedd4-1 ubiquitinates ACK and regulates epidermal growth factor (EGF)-induced degradation of EGF receptor and ACK.* Mol Cell Biol, 2010. **30**(6): p. 1541-54.

72. Xie, B., et al., *ACK1 promotes hepatocellular carcinoma progression via downregulating WWOX and activating AKT signaling.* Int J Oncol, 2015. **46**(5): p. 2057-66.

73. Mahajan, N.P., et al., *Activated Cdc42-associated kinase Ack1 promotes prostate cancer progression via androgen receptor tyrosine phosphorylation.* Proc Natl Acad Sci U S A, 2007. **104**(20): p. 8438-43.

74. Buchwald, M., et al., *SIAH ubiquitin ligases target the nonreceptor tyrosine kinase ACK1 for ubiquitinylation and proteasomal degradation.* Oncogene, 2013. **32**(41): p. 4913-20.

75. Chan, W., et al., *Down-regulation of active ACK1 is mediated by association with the E3 ubiquitin ligase Nedd4-2.* J Biol Chem, 2009. **284**(12): p. 8185-94.

76. Chua, B.T., et al., *Somatic mutation in the ACK1 ubiquitin association domain enhances oncogenic signaling through EGFR regulation in renal cancer derived cells.* Mol Oncol, 2010. **4**(4): p. 323-34.

77. van der Horst, E.H., et al., *Metastatic properties and genomic amplification of the tyrosine kinase gene ACK1.* Proc Natl Acad Sci U S A, 2005. **102**(44): p. 15901-6.

78. Thelemann, A., et al., *Phosphotyrosine signaling networks in epidermal growth factor receptor overexpressing squamous carcinoma cells.* Mol Cell Proteomics, 2005. **4**(4): p. 356-76.

79. Furlow, B., *Tyrosine kinase ACK1 promotes prostate tumorigenesis.* Lancet Oncol, 2006. **7**(1): p. 17.

80. Liu, Y., et al., *Dasatinib inhibits site-specific tyrosine phosphorylation of androgen receptor by Ack1 and Src kinases.* Oncogene, 2010. **29**(22): p. 3208-16.

81. Mahajan, N.P., et al., *Activated tyrosine kinase Ack1 promotes prostate tumorigenesis: role of Ack1 in polyubiquitination of tumor suppressor Wwox.* Cancer Res, 2005. **65**(22): p. 10514-23.

82. Grovdal, L.M., et al., *Dysregulation of Ack1 inhibits down-regulation of the EGF receptor.* Exp Cell Res, 2008. **314**(6): p. 1292-300.

83. Wang, L., et al., *Comparison of gene expression profiles between primary tumor and metastatic lesions in gastric cancer patients using laser microdissection and cDNA microarray.* World J Gastroenterol, 2006. **12**(43): p. 6949-54.

84. Mahajan, K., et al., *Ack1-mediated androgen receptor phosphorylation modulates radiation resistance in castration-resistant prostate cancer.* J Biol Chem, 2012. **287**(26): p. 22112-22.

85. Shen, F., et al., *Activated Cdc42-associated kinase 1 is a component of EGF receptor signaling complex and regulates EGF receptor degradation.* Mol Biol Cell, 2007. **18**(3): p. 732-42.

86. Maxson, J.E., et al., *Oncogenic CSF3R mutations in chronic neutrophilic leukemia and atypical CML.* N Engl J Med, 2013. **368**(19): p. 1781-90.

87. Wu, X., et al., *The non-receptor tyrosine kinase TNK2/ACK1 is a novel therapeutic target in triple negative breast cancer.* Oncotarget, 2017. **8**(2): p. 2971-2983.

88. Davis, M.I., et al., *Comprehensive analysis of kinase inhibitor selectivity.* Nat Biotechnol, 2011. **29**(11): p. 1046-51.

89. Reddy, R.J., et al., *Early signaling dynamics of the epidermal growth factor receptor.* Proc Natl Acad Sci U S A, 2016. **113**(11): p. 3114-9.

90. Bunda, S., et al., *Inhibition of SRC corrects GM-CSF hypersensitivity that underlies juvenile myelomonocytic leukemia.* Cancer Res, 2013. **73**(8): p. 2540-50.

91. Bridges, C.B., *The origin of variation.* Amer. Nat., 1922.

92. Iglehart, J.D. and D.P. Silver, *Synthetic lethality--a new direction in cancer-drug development.* N Engl J Med, 2009. **361**(2): p. 189-91.

93. Nijman, S.M., *Synthetic lethality: general principles, utility and detection using genetic screens in human cells.* FEBS Lett, 2011. **585**(1): p. 1-6.

94. Tyner, J.W., et al., *RNAi screen for rapid therapeutic target identification in leukemia patients.* Proc Natl Acad Sci U S A, 2009. **106**(21): p. 8695-700.

95. Siegel, R.L., K.D. Miller, and A. Jemal, *Cancer statistics, 2015.* CA Cancer J Clin, 2015. **65**(1): p. 5-29.

96. Tyner, J.W., et al., *Kinase pathway dependence in primary human leukemias determined by rapid inhibitor screening.* Cancer Res, 2013. **73**(1): p. 285-96.

97. Emanuel, P.D., et al., *Selective hypersensitivity to granulocyte-macrophage colony-stimulating factor by juvenile chronic myeloid leukemia hematopoietic progenitors.* Blood, 1991. **77**(5): p. 925-9.

98. Maxson, J.E., et al., *Identification and Characterization of Tyrosine Kinase Nonreceptor 2 Mutations in Leukemia through Integration of Kinase Inhibitor Screening and Genomic Analysis.* Cancer Res, 2016. **76**(1): p. 127-38.

99. Azam, M., et al., *Activation of tyrosine kinases by mutation of the gatekeeper threonine.* Nat Struct Mol Biol, 2008. **15**(10): p. 1109-18.

100. Mahajan, K., et al., *Effect of Ack1 tyrosine kinase inhibitor on ligand-independent androgen receptor activity.* Prostate, 2010. **70**(12): p. 1274-85.

101. Chen, Y.N., et al., *Allosteric inhibition of SHP2 phosphatase inhibits cancers driven by receptor tyrosine kinases.* Nature, 2016. **535**(7610): p. 148-52.

102. Garcia Fortanet, J., et al., *Allosteric Inhibition of SHP2: Identification of a Potent, Selective, and Orally Efficacious Phosphatase Inhibitor.* J Med Chem, 2016. **59**(17): p. 7773-82.

103. Tyner, J. and B.J. Druker, *RNAi screen for therapeutic target in leukemia.* Cell Cycle, 2009. **8**(14): p. 2144.

104. Li, H. and R. Durbin, *Fast and accurate short read alignment with Burrows-Wheeler transform.* Bioinformatics, 2009. **25**(14): p. 1754-60.

105. McKenna, A., et al., *The Genome Analysis Toolkit: a MapReduce framework for analyzing next-generation DNA sequencing data.* Genome Res, 2010. **20**(9): p. 1297-303.

106. Cibulskis, K., et al., *Sensitive detection of somatic point mutations in impure and heterogeneous cancer samples.* Nat Biotechnol, 2013. **31**(3): p. 213-9.

107. Koboldt, D.C., et al., *VarScan 2: somatic mutation and copy number alteration discovery in cancer by exome sequencing.* Genome Res, 2012. **22**(3): p. 568-76.

108. McLaren, W., et al., *Deriving the consequences of genomic variants with the Ensembl API and SNP Effect Predictor.* Bioinformatics, 2010. **26**(16): p. 2069-70.

109. Kandoth, C., *vcf2maf.* Github, 2016.

110. Liao, Y., G.K. Smyth, and W. Shi, *The Subread aligner: fast, accurate and scalable read mapping by seed-and-vote.* Nucleic Acids Res, 2013. **41**(10): p. e108.

111. Liao, Y., G.K. Smyth, and W. Shi, *featureCounts: an efficient general purpose program for assigning sequence reads to genomic features.* Bioinformatics, 2014. **30**(7): p. 923-30.

112. Nonami, A., et al., *Identification of novel therapeutic targets in acute leukemias with NRAS mutations using a pharmacologic approach.* Blood, 2015. **125**(20): p. 3133-43.

113. Nur, E.K.A., et al., *Requirement of activated Cdc42-associated kinase for survival of v-Ras-transformed mammalian cells.* Mol Cancer Res, 2005. **3**(5): p. 297-305.

114. Gritsman, K., et al., *Hematopoiesis and RAS-driven myeloid leukemia differentially require PI3K isoform p110alpha.* J Clin Invest, 2014. **124**(4): p. 1794-809.

115. Akutagawa, J., et al., *Targeting the PI3K/Akt pathway in murine MDS/MPN driven by hyperactive Ras.* Leukemia, 2016. **30**(6): p. 1335-43.

116. Goodwin, C.B., et al., *PI3K p110delta uniquely promotes gain-of-function Shp2-induced GM-CSF hypersensitivity in a model of JMML.* Blood, 2014. **123**(18): p. 2838-42.

117. Zhang, S.Q., et al., *Shp2 regulates SRC family kinase activity and Ras/Erk activation by controlling Csk recruitment.* Mol Cell, 2004. **13**(3): p. 341-55.

118. Gomes, E.G., S.F. Connelly, and J.M. Summy, *Targeting the yin and the yang: combined inhibition of the tyrosine kinase c-Src and the tyrosine phosphatase SHP-2 disrupts pancreatic cancer signaling and biology in vitro and tumor formation in vivo.* Pancreas, 2013. **42**(5): p. 795-806.

119. Sharma, N., et al., *Oncogenic KIT-induced aggressive systemic mastocytosis requires SHP2/PTPN11 phosphatase for disease progression in mice.* Oncotarget, 2014. **5**(15): p. 6130-41.

120. Wunderlich, M., et al., *AML xenograft efficiency is significantly improved in NOD/SCID-IL2RG mice constitutively expressing human SCF, GM-CSF and IL-3.* Leukemia, 2010. **24**(10): p. 1785-8.

121. Yoshimi, A., et al., *Robust patient-derived xenografts of MDS/MPN overlap syndromes capture the unique characteristics of CMML and JMML.* Blood, 2017. **130**(4): p. 397-407.

122. He, R.J., et al., *Protein tyrosine phosphatases as potential therapeutic targets.* Acta Pharmacol Sin, 2014. **35**(10): p. 1227-46.

123. Loh, M. 2017; Available from: https://www.lohlab.com/projects-images.

124. Chang, T., et al., *Sustained MEK inhibition abrogates myeloproliferative disease in Nf1 mutant mice.* J Clin Invest, 2013. **123**(1): p. 335-9.

125. Yi, J.S., et al., *Low-dose dasatinib rescues cardiac function in Noonan syndrome.* JCI Insight, 2016. **1**(20): p. e90220.

126. Dong, L., et al., *Leukaemogenic effects of Ptpn11 activating mutations in the stem cell microenvironment.* Nature, 2016. **539**(7628): p. 304-308.

127. Dienstmann, R., et al., *Database of genomic biomarkers for cancer drugs and clinical targetability in solid tumors.* Cancer Discov, 2015. **5**(2): p. 118-23.

128. Kurtz, S.E., et al., *Molecularly targeted drug combinations demonstrate selective effectiveness for myeloid- and lymphoid-derived hematologic malignancies.* Proc Natl Acad Sci U S A, 2017.

129. Chan, G., et al., *Leukemogenic Ptpn11 causes fatal myeloproliferative disorder via cell-autonomous effects on multiple stages of hematopoiesis.* Blood, 2009. **113**(18): p. 4414-24.

130. Mohi, M.G., et al., *Prognostic, therapeutic, and mechanistic implications of a mouse model of leukemia evoked by Shp2 (PTPN11) mutations.* Cancer Cell, 2005. **7**(2): p. 179-91.